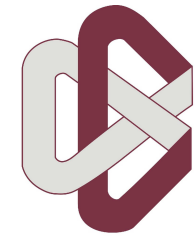

CIMAT

CENTRO DE INVESTIGACIÓN EN MATEMÁTICAS.

DOCTORADO EN CIENCIAS CON ORIENTACIÓN EN MATEMÁTICAS APLICADAS.

MATHEMATICAL MODELING APPROACHES IN EPIDEMIOLOGY: WITHIN HOST-DYNAMICS, CONTROL STRATEGIES AND COST-EFFECTIVENESS ANALYSIS

TESIS

QUE PARA OPTAR POR EL GRADO DE:

DOCTOR EN CIENCIAS

CON ORIENTACIÓN EN
MATEMÁTICAS APLICADAS

P R E S E N T A:

FERNANDO SALDAÑA GARCIA

DIRECTOR DE TESIS:
DR. IGNACIO BARRADAS BRIBIESCA.

Guanajuato, Gto. México. Agosto 2020

CIMAT
Centro de Investigación en Matemáticas, A.C.

MATHEMATICAL MODELING APPROACHES IN EPIDEMIOLOGY: WITHIN-HOST DYNAMICS, CONTROL STRATEGIES AND COST-EFFECTIVENESS ANALYSIS

T E S I S

Que para obtener el grado de

Doctor en Ciencias

con Orientación en

Matemáticas Aplicadas

Presenta

Fernando Saldaña García

Director de Tesis:

Dr. José Ignacio Barradas

Autorización de la versión final

Guanajuato, Gto., Diciembre 2020

¿No son las montañas, las olas, los cielos, una parte de mí mismo y de mi alma, así como yo soy parte de todo esto?

Acknowledgements

La travesía que representa completar los estudios doctorales es una aventura larga y complicada. El camino que hay que recorrer a veces no es claro y por ende es de gran ayuda tener amigos cuya compañía y consejo te impidan caer en el vacío. Son muchas las personas con las que he coincidido durante este viaje doctoral y quiero agradecer tanto a los que me aportaron en algún aspecto académico como a los que simplemente me ayudaron a vivir la vida. En especial, agradezco a mi asesor el Dr. Ignacio Barradas por guiarme en mis estudios doctorales y por compartir su sabiduría de vida. Finalmente quiero agradecer al Consejo Nacional de Ciencia y Tecnología (CONACyT), México, porque aunque no solo de pan vive el hombre, sin pan ningún hombre vive.

Abstract

This thesis is devoted to the mathematical modeling of infectious diseases and public health giving particular attention to the study of the infection by the human papillomavirus (HPV). We propose several mathematical models to understand and explain health behavior and to guide the identification, development, and implementation of disease prevention programs.

The majority of the mathematical models constructed in this work are based on ordinary differential equations describing the average dynamics underlying the infectious disease under study. The mathematical tools that we have used to analyze such models include global stability analysis of equilibria via Lyapunov's direct method, numerical bifurcation analysis, global sensitivity analysis using the method of Sobol, and optimal control theory. The mathematical models proposed here cover two of the dominant sub-disciplinary fields that address the study of infectious diseases: (i) modeling of between-host dynamics of infectious disease transmission and (ii) modeling within-host dynamics of infectious diseases, that is, modeling pathogen-immune interactions. Between-host models have been widely used to aid public health officers to make optimal decisions about disease control. Within-host models commonly study the interactions of the pathogen and the host defense mechanisms throughout an infection.

The main goal of this work is to use mathematical modeling to better understand the causes of a disease, the complexity in the disease transmission mechanism and to evaluate and optimatize various detection, prevention, and vaccination programs aiming to control the spread of the infection.

Introduction

Mathematical modeling is a tool which has been successfully used to study the mechanisms by which diseases spread, to predict the future course of an outbreak, and to evaluate strategies to control an epidemic. In 1662, John Graunt published his book *Natural and Political Observations made upon the Bills of Mortality* which was the first study that systematically tried to quantify the causes of death. However, the very first publication addressing the mathematical modeling of epidemics *Essai d'une nouvelle analyze de la mortalité causée par la petite vérole* by Daniel Bernoulli dates back in 1766. In this work, Bernoulli developed a mathematical model to analyze the mortality due to smallpox in England, which at that time was one in 14 of the total mortality. Bernoulli used his model to show that inoculation against the virus would increase the life expectancy at birth by about three years.

In the early 20th century, Ronald Ross published his paper *The prevention of malaria* which establishes modern mathematical epidemiology. In this work, Ross addressed the mechanistic a priori modeling approach using a set of equations to approximate the discrete-time dynamics of malaria through the mosquito-borne pathogen transmission. Ross showed that reduction of the mosquito population below a critical level would be sufficient to control the spread of the infection. This result is the first appearance of the concept of the basic reproduction number which later becomes one of the most important ideas for the theory of mathematical epidemiology.

Following up on the work of Ross, Kermack and McKendrick published a sequence of three seminal papers which founded the deterministic compartmental epidemic modeling (Kermack and McKendrick, 1927, 1932, 1933). In these papers, Kermack and McKendrick addressed the mass–action incidence in disease transmission cycle, suggesting that the probability of infection of a susceptible is analogous to the number of its contacts with infected individuals. Kermack and McKendrick formulated for the first time a deterministic epidemic model that includes susceptible, infected, and removed individuals, this corresponds to the so-called compartmental SIR epidemic model. In compartmental epidemic models, the population is divided into compartments, with the assumption that every individual in the same compartment has the same characteristics.

Mathematical modeling of infectious diseases gained importance in the 1980s with the appearance of the HIV epidemics (Martcheva, 2015). Since then, epidemic models are being increasingly used to investigate the transmission dynamics of several infectious diseases. Although these models may be rather simple, their study is important to gain insight into the underlying aspects of disease spread and control. As remarked by professor Brauer (Brauer, 2017), there is always a trade-off between simple or strategic models, which omit most details and are designed only to highlight general qualitative behavior and detailed model designed for specific situations including short-term quantitative predictions.

The fundamental goal of this thesis is to develop epidemic models and evaluate realistic health-care interventions to prevent and control epidemics in such a way that the results are useful for public health professionals. We give particular attention to the study of the dynamics of the infection by the human papillomavirus but we also investigate other topics related to the theory of mathematical epidemiology.

This dissertation is subdivided into four related but also independent chapters. In Chapter 1, we explore control strategies for multigroup epidemic models. We develop compartmental *SIRS* models to study the dynamics of n host groups sharing the same source of infection in addition to the transmission among members of the same group. In particular, we consider a model for infectious diseases with free-living pathogens in the environment and a metapopulation model with a central patch. We give the detailed derivation of the target reproduction number under three public health interventions and provide the corresponding biological insights. Moreover, using the next-generation approach, we calculate the basic reproduction numbers associated with the subsystems of our models and determine algebraic connections to the target reproduction number of the complete model. The main result of this chapter illustrates that understanding the topological structure of the infection process and partitioning it in simple cycles is useful to design and evaluate control strategies. The results of this chapter were published by the *Bulletin of Mathematical Biology*, see (Saldaña and Barradas, 2018).

In Chapter 2, we propose a within-host metapopulation model to study the possibility of vaccine-induced type replacement for oncogenic HPV types. Vaccine-induced strain replacement is a phenomenon in which vaccination leads to the emergence and dominance of non-vaccine pathogen strains. This replacement is due to a decreased fitness of the vaccine types after a vaccination scheme and the fact that non-vaccine types can still infect vaccinated individuals. Given the vast diversity of HPV types, there have been speculations over whether vaccine targeted-types will be replaced by other types not targeted by the vaccine. It is generally believed that the theoretical possibility of type replacement strongly depends on the existence of natural type competition mechanisms. Nevertheless, our results suggest that

type replacement is viable at the within-host level if the degree of cross-protection induced by the vaccine is low, even if there is no underlying competition among HPV types. The results of this chapter were published by *Mathematical Methods in the Applied Sciences*, see (Saldaña and Barradas, 2020).

In Chapter 3, we investigate what is the best combination of vaccination and screening to minimize human papillomavirus (HPV) associated morbidity but also the cost of the health-care interventions. Since HPV-associated morbidity and mortality are usually higher in females than in males, in the majority of countries the primary target group of HPV vaccination programs in adolescent girls aged 9-14. However, considering that recent HPV vaccines have been licensed for a broader age range in both males and females, we analyze the potential health benefits of extending vaccination to males, as well as older individuals, versus a higher economic cost of such programs. Our main goal in this chapter is to use optimal control theory to gain insight into the best combination of vaccination and screening to reduce the spread of HPV infection, as well as the cost of the intervention strategies. Some results of Chapter 3 can be found in (Saldaña et al., 2019) published by *Abstract and Applied Analysis*.

Finally, in Chapter 4 we investigate the role of reproductive social behavior and prompt disease treatment in the control of sexually transmitted infections. In mathematical terms, we study general recovery functions and treatment in the dynamics of an *SIS* model for sexually transmitted infections with nonzero partnership length. It is shown how partnership dynamics influence the predicted prevalence at the steady-state and the basic reproduction number. Sobol's indices are used to evaluate the contribution of model parameters to the overall variance of $\mathscr{R}_0$. The recovery functions studied here take into account that society's capacity to provide treatment is limited when the number of infected individuals is large. Bifurcation analysis is used to establish a relationship between an alert level of prevalence and the minimum recovery time that guarantees the eradication of the disease. We also show that a backward bifurcation can occur when there are delays in the treatment of infected individuals. The results of Chapter 4 were published by *Infectious Disease Modeling*, see (Saldaña and Barradas, 2019).

Table of contents

List of figures

List of tables

Chapter 1

Control Strategies in Multigroup Models: The Case of the Star Network Topology

1.1 Introduction

[1]

An omnipresent quantity in the modeling of infectious diseases is the basic reproduction number $\mathscr{R}_0$ (Heesterbeek, 2002). This quantity is usually defined as the average number of secondary cases of an infection caused by a *typical* infected individual over the course of its infectious period in a population consisting of susceptibles only. In the case of the simplest compartmental epidemic models of the *SIS* (susceptible-infectious-susceptible) and *SIR* (susceptible-infectious-recovered) types, and a considerable number of generalizations (Lajmanovich and Yorke, 1976), the famous threshold property: *the disease can invade if* $\mathscr{R}_0 > 1$, *whereas it cannot if* $\mathscr{R}_0 < 1$ is valid.

The roots of the basic reproduction concept can be traced through the work of Alfred Lotka, Ronald Ross, and others, but its first modern application in epidemiology was by George MacDonald in 1952, who constructed population models of the spread of malaria. In the context of epidemic modeling, $\mathscr{R}_0$ is often found through the analysis of the eigenvalues of the Jacobian matrix at the disease-free equilibrium. Nevertheless, this approach may fail (Martcheva, 2015) in populations with various degrees of host and pathogen heterogeneity. In these cases, the mathematical description of what is a *typical* infected individual is difficult to quantify. In order to overcome this problem, Diekmann and his collaborators (Diekmann et al., 1990) introduced the next-generation matrix $\mathbf{K} = \left[k_{ij}\right]$ to derive the the basic reproduction number. In populations with n host types, $\mathbf{K}$ is an $n \times n$ matrix whose

[1] This Chapter is based on (Saldaña and Barradas, 2018)

entry k_{ij} gives the expected number of new infections among susceptible individuals of type i, generated by an infected individual of type j. In this work, $\mathscr{R}_0$ is defined as the spectral radius of the next-generation matrix, that is, $\mathscr{R}_0 = \rho(\mathbf{K})$.

The value of $\mathscr{R}_0$ not only is an indicator of the severity of an epidemic, generally, the larger the value of $\mathscr{R}_0$, the harder it is to control the epidemic. $\mathscr{R}_0$ is also a powerful tool to estimate the control effort needed to eradicate a disease when treating homogeneous populations. In fact, for homogeneous populations, it is known (Keeling et al., 2013) that an infection can be eliminated provided that a proportion of individuals greater than $1-1/\mathscr{R}_0$ have been afforded lifelong protection.

However, for a large number of infectious diseases, the host population is not homogeneous (Roberts and Heesterbeek, 2003). Furthermore, in real situations, there are multiple constraints (economic and geographical considerations among others) that may significantly affect the design of control policies. Therefore, it is common that control strategies are not aimed at all host individuals; instead, they treat a particular group of individuals or interactions among them.

When designing control measures that target specific types of individuals in heterogeneous populations, the concept of the target reproduction number proposed in (Shuai et al., 2013) arises naturally to quantify the effort needed to control epidemic outbreaks. The basic idea behind the method of (Shuai et al., 2015) is that it is possible to reduce the value of $\mathscr{R}_0$ by controlling a specific set S of entries of the next-generation matrix $\mathbf{K} = \left[k_{ij}\right]$. Let $\mathbf{K}_S$ be the target matrix corresponding to the target set S defined by

$$[\mathbf{K}_S]_{ij} = \begin{cases} k_{ij}, & \text{if } (i,j) \in S \\ 0, & \text{otherwise.} \end{cases}$$

The target reproduction number $\mathscr{T}_S$ for the target set S is defined as the spectral radius of the matrix $\mathbf{K}_S \cdot (\mathbf{I} - \mathbf{K} + \mathbf{K}_S)^{-1}$, provided that $\rho(\mathbf{K} - \mathbf{K}_S) < 1$, where $\mathbf{I}$ is the identity matrix and ρ denotes the spectral radius. This last condition had been called the controllability condition (Knipl, 2016), since whenever $\rho(\mathbf{K} - \mathbf{K}_S) > 1$ the disease cannot be eradicated by targeting only S (Shuai et al., 2013). However, since the term controllability evokes formal control theory, we will not use this terminology.

Analogously to $\mathscr{R}_0$, the target reproduction number has the property that if a proportion bigger than $1-1/\mathscr{T}_S$ of the S entries in $\mathbf{K}$ can be reduced, then the disease can be eradicated. Moreover, when the next-generation matrix is irreducible, then $\mathscr{R}_0 < 1$ if and only if $\mathscr{T}_S < 1$ for a general target set S, as long as the target reproduction number is well defined.

On the other hand, for many diseases the structure of the infection process can be subdivided as a combination of different cycles of infection (Olmos et al., 2015) and it is

logical to speculate if there is a relationship between the topological structure of the cycles of infection and the optimal design of public health interventions. Therefore, we propose to examine and control the local dynamics of an infection with a heterogeneous host population to prevent a major outbreak at the global level. In particular, our focus will be models with multiple host types whose infection process follows the star network topology (Edwards et al., 2010), i.e., models with a common source of infection for all the groups but not direct transmission among them.

Using these ideas, in this chapter we establish connections among the target reproduction number for the whole model and $\mathscr{R}_0$'s of submodels that facilitate the design and evaluation of control strategies. In section 1.2, we illustrate our method with an epidemiological model for leptospirosis in humans and animals. Different control strategies are proposed and the target reproduction number is computed in each case. General models with n hosts types are studied in section 1.3. In particular, we consider a compartmental model for infections with free-living pathogens in the environment and a metapopulation model with a central patch. In the last section, we summarize and interpret our results.

1.2 Leptospirosis as an Example of an Environmentally Driven Disease

Leptospirosis is a widespread bacterial zoonosis with highest burden in low-income populations living in tropical and subtropical regions, both in urban and in rural environments. Except for Antarctica, leptospirosis is present in all continents (Adler and de la Peña Moctezuma, 2010) with more than $500,000$ cases per year reported globally (Ullmann and Langoni, 2011). Although rodents have been recognized as the most important reservoirs of leptospiral infection, humans, domestic pets, cattle and almost every mammal can also contract this infection (Evangelista and Coburn, 2010).

Environmental conditions play an important role in the transmission of leptospirosis. In fact, leptospires can survive in moist soil and freshwater for a few weeks up to several months (Ko et al., 1999). Moreover, both humans and animals become infected with leptospires through close contact with water, food or soil contaminated mainly with the urine of reservoir animals (Ganoza et al., 2006). Human to human transmission is also possible by sexual intercourse, transplacentally from mother to fetus and via breast milk to a child. Urine from a patient suffering from leptospirosis should be considered infectious (Terpstra, 2003).

In humans, leptospirosis first presents as an acute fever with headache and myalgia and accounts for one of the numerous possible etiologies of acute fevers in medical settings. If

left untreated, it can degenerate into severe forms, with kidney and/or liver damage as well as severe pulmonary hemorrhage. Case fatality rates range from less than 5% to more than 30% depending on the clinical presentation and the case management. In developing countries, leptospirosis poses a number of challenges not only in the fields of public health (prevention and education, preparedness, intervention) but also in the fields of medical and biological diagnosis and case management.

Several mathematical models have been proposed to study the transmission of leptospirosis in a population over time. In (Holt et al., 2006) the authors proposed a model to study the spread and maintenance of leptospirosis in rodents. One of the first compartmental models for leptospirosis that considered both human and animals was proposed in (Triampo et al., 2007). In their work, they proposed a deterministic epidemic model under the *SIRS* (susceptible-infectious-recovered-susceptible) structure and considered real data of leptospirosis in Thailand. Recently, in (Baca-Carrasco et al., 2015) an epidemiological model that included explicitly a variable for the leptospires in the environment was proposed. This model considers the indirect infections caused by the bacteria present in the environment; however, it did not include possible direct transmissions between humans.

Here, we present a two-group epidemiological *SIRS* model for the dynamics of leptospiral infection in humans and animals. Given the importance of the indirect infections caused by contact with a contaminated environment, we consider an equation for the free-living leptospira in the environment as in (Baca-Carrasco et al., 2015) but we also allow direct transmissions among humans. To derive our model, let $S_i(t)$, $I_i(t)$ and $R_i(t)$ denote the number of susceptible, infectious and recovered individuals of host type $i \in \{1,2\}$ at time t, with $i = 1$ representing humans and $i = 2$ representing animals. Therefore, the total population size of host type i at time t is given by

$$N_i(t) = S_i(t) + I_i(t) + R_i(t) \quad \text{for} \quad i \in \{1,2\}.$$

The variable $P(t)$ represents the amount of leptospira present in the environment.

We assume that individuals enter to the population as susceptibles at a constant rate Λ_i and die at a per capita death rate μ_i, $i = 1,2$. No additional death due to the disease is considered. Susceptible humans can be infected by direct (sexual) contact with other humans at a rate β_{11} and indirectly via the external environment at a rate β_{1p}. New infections in animals are also due to direct contact with infected animals at a rate β_{22} and through indirect exposure with a contaminated environment at a rate β_{2p}. Infectious individuals of host type $i \in \{1,2\}$ recover at a constant rate γ_i proportional to the size of their class, and the loss of immunity occurs at an average time of $1/\nu_i$. The presence of leptospira in the environment

increases due to the shedding of infected humans and animals at rates c_1 and c_2, respectively. The bacteria survive in the environment for a mean time of $1/\mu_p$.

Under these hypotheses, our model is given by the following system of differential equations:

$$\begin{aligned}
\dot{S}_i &= \Lambda_i - (\beta_{ii} I_i/N_i + \beta_{ip} P) S_i - \mu_i S_i + \nu_i R_i, \\
\dot{I}_i &= (\beta_{ii} I_i/N_i + \beta_{ip} P) S_i - (\mu_i + \gamma_i) I_i, \qquad i \in \{1,2\} \\
\dot{R}_i &= \gamma_i I_i - (\nu_i + \mu_i) R_i, \\
\dot{P} &= c_1 I_1 + c_2 I_2 - \mu_p P.
\end{aligned} \tag{1.1}$$

All the parameters are considered nonnegative. Note that we assumed mass action incidence for the indirect (environment-to-host) transmission and standard incidence for the direct (host-to-host) transmission.

It is easy to see that the total population size for any host type is asymptotically constant since

$$\dot{N}_i = \Lambda_i - \mu_i N_i, \quad i \in \{1,2\}.$$

The unique disease-free equilibrium of system (1.1) is given by

$$\varepsilon_0 = (N_1^*, 0, 0, N_2^*, 0, 0, 0) \tag{1.2}$$

with $N_i^* = \Lambda_i/\mu_i$ for $i \in \{1,2\}$.

Disregarding the infections caused by the contaminated environment, it is easy to calculate the basic reproduction number associated with the direct transmission of the disease for any host type,

$$\mathscr{R}_i = \frac{\beta_{ii}}{\mu_i + \gamma_i}, \qquad i \in \{1,2\} \tag{1.3}$$

and $\mathscr{R}_i$ gives the average number of secondary infectious corresponding to the direct transmission cycle for the i th host-type. The dynamics of the infection process for system (1.1) is shown in Fig. 1.1.

Fig. 1.1 Topological structure of the infection process for model (1.1). In this case, there are two infection cycles, for both, the indirect transmission ($\mathscr{R}_{1p}$ and $\mathscr{R}_{2p}$) and the direct transmission ($\mathscr{R}_1$ and $\mathscr{R}_2$).

As many examples in the literature show (Baca-Carrasco and Velasco-Hernández, 2016; Chen et al., 2009; Martcheva, 2015; Olmos et al., 2015), the expressions for $\mathscr{R}_0$ in multigroup models can be very complex, so it would be very useful when evaluating public health interventions to have an expression of $\mathscr{R}_0$ in terms of $\mathscr{R}_0$'s of submodels of the whole system. This will allow the design of local strategies such as control of specific types of individuals or even interactions between them to control the disease at the global level. As previously mentioned, when targeting specific types of individuals or interactions, it is easier to work with the target reproduction number $\mathscr{T}_S$ than with $\mathscr{R}_0$. Moreover, we know $\mathscr{T}_S$ and $\mathscr{R}_0$ are directly related. In fact, if the next-generation matrix $\mathbf{K} = \left[k_{ij}\right]$ is irreducible then $\mathscr{R}_0 < 1$ if and only if $\mathscr{T}_S < 1$ when the target reproduction number is well defined for the target set S (Shuai et al., 2013, 2015).

In general terms, to compute the next-generation matrix, it is necessary to determine the subsystem that describes the production of new infections and changes in state among infected individuals. The Jacobian matrix $\mathbf{J}$ corresponding to the linearization of this subsystem at the infection-free equilibrium is decomposed as $\mathbf{F} - \mathbf{V}$. The matrix $\mathbf{F}$ is the transmission part, describing the production of new infections, and $\mathbf{V}$ describes changes in status, such as recovery or death (Knipl, 2016; Martcheva, 2015; Van den Driessche and Watmough, 2002).

However, different interpretations of the disease process can lead to different decompositions into matrices $\mathbf{F}$ and $\mathbf{V}$. Consequently, different next-generation matrices can be obtained for a compartmental model. This problem is of particular relevance for infections that can be caused by contact with a contaminated environment since the role of the environment can be interpreted in multiple ways (Bani-Yaghoub et al., 2012). In this work, we assume that the environment acts as a reservoir of the infection. Therefore, the pathogen shedding by infectious hosts is placed in the matrix $\mathbf{F}$.

These assumptions give the following matrices $\mathbf{F}$ and $\mathbf{V}$ for model (1.1), computed at the disease-free equilibrium (1.2):

$$\mathbf{F} = \begin{pmatrix} \beta_{11} & 0 & \beta_{1p}N_1^* \\ 0 & \beta_{22} & \beta_{2p}N_2^* \\ c_1 & c_2 & 0 \end{pmatrix} \quad \text{and} \quad \mathbf{V} = \begin{pmatrix} \mu_1+\gamma_1 & 0 & 0 \\ 0 & \mu_2+\gamma_2 & 0 \\ 0 & 0 & \mu_p \end{pmatrix}$$

The product $\mathbf{FV}^{-1}$ gives the following next-generation matrix

$$\mathbf{K} = \begin{pmatrix} \mathscr{R}_1 & 0 & \dfrac{\beta_{1p}N_1^*}{\mu_p} \\ 0 & \mathscr{R}_2 & \dfrac{\beta_{2p}N_2^*}{\mu_p} \\ \dfrac{c_1}{\mu_1+\gamma_1} & \dfrac{c_2}{\mu_2+\gamma_2} & 0 \end{pmatrix}, \tag{1.4}$$

which is clearly an irreducible matrix. Using (1.4), it is not difficult to show that the basic reproduction numbers for the indirect transmission cycle (see figure 1.1) are given by the following formula

$$\mathscr{R}_{ip} = \sqrt{\frac{c_i\beta_{ip}N_i^*}{\mu_p(\mu_i+\gamma_i)}}, \quad i \in \{1,2\}. \tag{1.5}$$

Indeed, the characteristic polynomial of the next-generation matrix (1.4) is

$$\begin{aligned} P(\lambda) &= \lambda^3 - (\mathscr{R}_1+\mathscr{R}_2)\lambda^2 + \left(\mathscr{R}_1\mathscr{R}_2 - \sum_{i=1}^{2}\frac{c_i\beta_{ip}N_i^*}{\mu_p(\mu_i+\gamma_i)}\right)\lambda \\ &+ \left((\mathscr{R}_1+\mathscr{R}_2)\sum_{i=1}^{2}\frac{c_i\beta_{ip}N_i^*}{\mu_p(\mu_i+\gamma_i)} - \sum_{i=1}^{2}\frac{c_i\beta_{ip}N_i^*\mathscr{R}_i}{\mu_p(\mu_i+\gamma_i)}\right). \end{aligned}$$

If we set the reproduction numbers associated with the direct transmission of the disease equal to zero, we get

$$\tilde{P}(\lambda) = \lambda^3 - \left(\sum_{i=1}^{2}\frac{c_i\beta_{ip}N_i^*}{\mu_p(\mu_i+\gamma_i)}\right)\lambda.$$

In order to obtain, for example, $\mathscr{R}_{1p}$, we only need to compute the root of maximum modulus of $\tilde{P}(\lambda)$ when the transmission parameters between host type 2 and the contaminated environment are zero, i.e., $\beta_{2p} = c_2 = 0$. Hence, $\mathscr{R}_{ip}$ satisfies (1.5).

The expression for the $\mathscr{R}_0$ of the complete model is quite complicated, and we are not going to show it here. Instead, we are going to work with the target reproduction number since we know that reducing this quantity below 1 ensures the elimination of the disease; see Theorem 1.3.1.

A wide variety of public health interventions can be of help to reduce the spread of leptospirosis. We analyze some of them in the following section.

1.2.1 Control Strategies in the Two-group Model for Leptospirosis

Leptospirosis can be considered an environmentally driven disease because of the important role of environmental conditions in the transmission of the disease. Different control strategies could be applied to reduce the prevalence of environmentally driven diseases in general and leptospirosis in particular.

(A) Minimizing Exposures to Environmental Risk Factors. The vast majority of human and animal infections with leptospira arise from contact with contaminated water (Terpstra, 2003). Therefore, one effective way to minimize the chances of infection is to avoid contact with contaminated water. In humans, factors related to occupational and recreational activities can represent an increased risk of infection. For example, farmers may be exposed to water contaminated by the urine of rodents or other animals when irrigating fields (Terpstra, 2003). Hence, where appropriate, protective clothing should be worn to reduce the risk of infection.

When preventive measures aim to reduce exposure to environmental risk factors, the target set is $S = \{(1,3),(2,3)\}$. Following the notation in (Shuai et al., 2013) the target matrix $\mathbf{K}_S$ is defined by,

$$[\mathbf{K}_S]_{ij} = \begin{cases} k_{ij}, & \text{if } (i,j) \in S \\ 0, & \text{otherwise;} \end{cases}$$

hence the condition $\rho(\mathbf{K} - \mathbf{K}_S) < 1$ becomes

$$\max\{\mathscr{R}_1, \mathscr{R}_2\} < 1. \tag{1.6}$$

This condition is logical since we cannot expect to eradicate a disease by just reducing the indirect infections caused by environmental factors when any of the basic reproduction numbers associated with the host-to-host transmission cycle has a value above 1. Provided that condition (1.6) is fulfilled, the target reproduction number is defined as the spectral radius of the matrix $\mathbf{K}_S \cdot (\mathbf{I} - \mathbf{K} + \mathbf{K}_S)^{-1}$ given by

$$\begin{pmatrix} \dfrac{\mathscr{R}_{1p}^2}{1-\mathscr{R}_1} & \dfrac{c_2\beta_{1p}N_1^*}{\mu_p(\mu_2+\gamma_2)(1-\mathscr{R}_2)} & \dfrac{\beta_{1p}N_1^*}{\mu_p} \\ \dfrac{c_1\beta_{2p}N_2^*}{\mu_p(\mu_1+\gamma_1)(1-\mathscr{R}_1)} & \dfrac{\mathscr{R}_{2p}^2}{1-\mathscr{R}_2} & \dfrac{\beta_{2p}N_2^*}{\mu_p} \\ 0 & 0 & 0 \end{pmatrix}.$$

Therefore

$$\mathscr{T}_S = \frac{\mathscr{R}_{1p}^2}{1-\mathscr{R}_1} + \frac{\mathscr{R}_{2p}^2}{1-\mathscr{R}_2}. \tag{1.7}$$

Hence, $\mathscr{T}_S$ is an increasing function of each of the local basic reproduction numbers when it is well defined.

(B) Reducing the Shedding Rate. The reduction of certain animal reservoirs such as rodents, immunization of dogs and livestock and prompt treatment after symptoms in humans are all valid ways to reduce the replenishing of pathogen load in the environment due to the excretion of leptospira by infected hosts.

For control strategies that focus on the reduction of the pathogen shedding rate, the target set is $U = \{(3,1),(3,2)\}$. Thus, the target matrix is:

$$\mathbf{K}_U = \begin{pmatrix} 0 & 0 & 0 \\ 0 & 0 & 0 \\ \dfrac{c_1}{\mu_1+\gamma_1} & \dfrac{c_2}{\mu_2+\gamma_2} & 0 \end{pmatrix}.$$

Similar to the case *(A)*, we have

$$\rho(\mathbf{K}-\mathbf{K}_U) < 1 \iff \max\{\mathscr{R}_1,\mathscr{R}_2\} < 1. \tag{1.8}$$

Moreover, given that

$$(\mathbf{I}-\mathbf{K}+\mathbf{K}_U)^{-1} = \begin{pmatrix} \dfrac{1}{1-\mathscr{R}_1} & 0 & \dfrac{\beta_{1p}N_1^*}{\mu_p(1-\mathscr{R}_1)} \\ 0 & \dfrac{1}{1-\mathscr{R}_2} & \dfrac{\beta_{2p}N_2^*}{\mu_p(1-\mathscr{R}_2)} \\ 0 & 0 & 1 \end{pmatrix}$$

as long as condition (1.8) is fulfilled the target reproduction number for the set U is given by

$$\mathscr{T}_U = \frac{\mathscr{R}_{1p}^2}{1-\mathscr{R}_1} + \frac{\mathscr{R}_{2p}^2}{1-\mathscr{R}_2}, \tag{1.9}$$

which coincides with formula (1.7). This reflects the fact that there is a reciprocal feedback between strategies *(A)* and *(B)*. In other words, when the shedding rate is reduced, the risk of getting infected through contact with a contaminated environment also decreases and vice versa.

(C) Combination of approaches (A) and (B). In this case the target set is $W = \{(1,3),(2,3),(3,1),(3,2)\}$. Therefore, the condition $\rho(\mathbf{K}-\mathbf{K}_W) < 1$ is equivalent to $\max\{\mathscr{R}_1,\mathscr{R}_2\} < 1$.

The characteristic polynomial of the matrix $\mathbf{K}_W \cdot (\mathbf{I} - \mathbf{K} + \mathbf{K}_W)^{-1}$ is

$$P(\lambda) = -\lambda^3 + \left(\frac{\mathscr{R}_{1p}^2}{1-\mathscr{R}_1} + \frac{\mathscr{R}_{2p}^2}{1-\mathscr{R}_2} \right) \lambda.$$

Therefore, when it is well defined, the target reproduction number is given by

$$\mathscr{T}_W = \sqrt{\frac{\mathscr{R}_{1p}^2}{1-\mathscr{R}_1} + \frac{\mathscr{R}_{2p}^2}{1-\mathscr{R}_2}}. \tag{1.10}$$

From the formulas for $\mathscr{T}_S$, $\mathscr{T}_U$ and $\mathscr{T}_W$, it is easy to note that

$$1 < \mathscr{T}_W < \mathscr{T}_S = \mathscr{T}_U, \quad \mathscr{T}_S = \mathscr{T}_U < \mathscr{T}_W < 1, \quad or \quad \mathscr{T}_S = \mathscr{T}_U = \mathscr{T}_W = 1$$

which is not surprising since the intervention strategy defined by the set W is stronger than the ones defined by S and U (Shuai et al., 2013).

1.2.2 Numerical Simulations

In this section, we explore numerically model (1.1). We retrieved some parameters from the literature (Baca-Carrasco et al., 2015; Holt et al., 2006; Leirs et al., 1997), and we gathered them in Table 1.1.

In compartmental epidemic models, a classical procedure to reduce disease spread is to choose a feasible set of model parameters

$$\theta = \{\theta_1, \theta_2, \ldots, \theta_n\}.$$

and determine how these parameters should be changed to prevent an epidemic. In our context, this procedure let us to define the target set S as the set of indices

$$S = \{(i_1, j_1), \ldots, (i_m, j_m)\},$$

with the property that if $(i, j) \in S$ then the entry k_{ij} of $\mathbf{K}$ depends at least on one of the parameters in the set θ. On the other hand, if $(i, j) \notin S$ then k_{ij} is independent of the parameters in the set θ.

If a proportion bigger than $1 - 1/\mathscr{T}_S$ of the entries S in $\mathbf{K}$ can be reduced, then the disease can be eradicated. In particular, replacing the entry k_{ij} in $\mathbf{K}$ by $k_{ij}/\mathscr{T}_S$ whenever $(i, j) \in S$, a

Parameter	Range	Units
Λ_1	$[6.0, 29.0]$	person day^{-1}
β_{11}	$[1\times10^{-3}, 5\times10^{-2}]$	day^{-1}
β_{1p}	$[3\times10^{-3}, 6\times10^{-3}]$	leptospires^{-1} day^{-1}
μ_1	$[1/29, 200, 1/14600]$	day^{-1}
γ_1	$[1/20, 1/7]$	day^{-1}
ν_1	$[1/365, 1/10]$	day^{-1}
Λ_2	$[0.5, 4.0]$	animal day^{-1}
β_{22}	$[1\times10^{-3}, 7\times10^{-2}]$	day^{-1}
β_{2p}	$[1\times10^{-3}, 9\times10^{-3}]$	leptospires^{-1} day^{-1}
μ_2	$[1/10, 950, 1/365]$	day^{-1}
γ_2	$[1/30, 1/10]$	day^{-1}
ν_2	$[1/90, 1/30]$	day^{-1}
c_1	$[8.4\times10^{-8}, 2.1\times10^{-7}]$	leptospires person^{-1} day^{-1}
c_2	$[2\times10^{-4}, 2\times10^{-2}]$	leptospires animal^{-1} day^{-1}
μ_p	$[1/180, 1/4]$	day^{-1}

Table 1.1 Estimation of parameters for the two-group model of leptospiral infection in humans and animals (1.1).

controlled next-generation matrix $\mathbf{K}_c$ is formulated

$$[\mathbf{K}_c]_{ij} = \begin{cases} k_{ij}/\mathscr{T}_S, & \text{if } (i,j) \in S \\ k_{ij}, & \text{otherwise} \end{cases}$$

and $\rho(\mathbf{K}_c) = 1$ (Shuai et al., 2013). Therefore, the goal is to change the set of parameters θ in such a way that $\mathbf{K}$ is transformed into $\mathbf{K}_c$.

Let us now analyze the case in which the intervention targets both the shedding rates c_i and the transmission rates via the environment β_{ip}, with $i = 1, 2$. Thus,

$$\theta = \{c_1, c_2, \beta_{1p}, \beta_{2p}\} \tag{1.11}$$

Model parameters (1.11) involve the set of indices $W = \{(1,3),(2,3),(3,1),(3,2)\}$. Therefore, according to (C) above, the target reproduction number is

$$\mathscr{T}_W = \sqrt{\frac{\mathscr{R}_{1p}^2}{1-\mathscr{R}_1} + \frac{\mathscr{R}_{2p}^2}{1-\mathscr{R}_2}}.$$

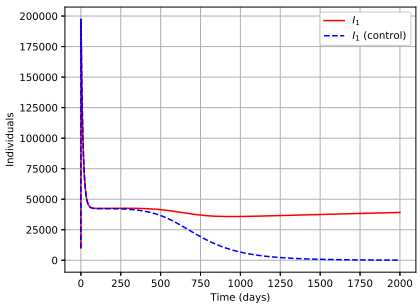

(a)

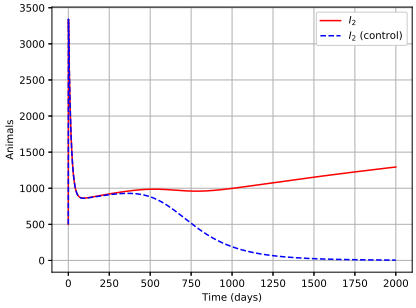

(b)

Fig. 1.2 Prevalence as function of time of humans I_1 (a) and animals I_2 (b), without control (solid curves) and with control (dashed curves). The parameters are as described in the text. In the case with control, we replaced the parameters in the set (1.11), that is, c_1, c_2, β_{1p} and β_{2p} by the controlled parameters $\tilde{c}_1 = c_1/\mathscr{T}_W$, $\tilde{c}_2 = c_2/\mathscr{T}_W$, $\tilde{\beta}_{1p} = \beta_{1p}/\mathscr{T}_W$ and $\tilde{\beta}_{2p} = \beta_{2p}/\mathscr{T}_W$, respectively.

In order to illustrate the dynamics of the model, we check numerically the prevalence on humans and animals as functions of time. We will fix the parameters with the following baseline values (see Table 1.1) consistent with the literature: $\Lambda_1 = 20$, $\beta_{11} = 0.02$, $\beta_{1p} = 0.005$, $\mu_1 = 1/25{,}550$, $\gamma_1 = 1/15$, $\nu_1 = 1/60$, $\Lambda_2 = 3$, $\beta_{22} = 0.01$, $\beta_{2p} = 0.005$, $\mu_2 = 1/3650$, $\gamma_2 = 1/20$, $\nu_2 = 1/70$, $c_1 = 1 \times 10^{-7}$, $c_2 = 1 \times 10^{-4}$, $\mu_p = 1/100$.

For the baseline parameters values, the local reproduction numbers take the values $\mathscr{R}_1 = 0.2998$, $\mathscr{R}_2 = 0.1989$, $\mathscr{R}_{1p} = 0.6188$, and $\mathscr{R}_{2p} = 3.3001$. Correspondingly, $\mathscr{T}_W = 3.7610$. The target reproduction number $\mathscr{T}_W$ is larger than 1 and thus $\mathscr{R}_0 > 1$ (in fact $\mathscr{R}_0 = 3.4603$). Therefore, the disease-free equilibrium is unstable (see Theorem 1.3.1) and we need to apply the intervention. The eradication of the disease is achieved replacing the entry $k_{ij} \in \mathbf{K}$ with $(i,j) \in W$ by $k_{ij}/\mathscr{T}_W$. This transformation can be easily done by dividing the parameters in (1.11) by $\mathscr{T}_W$.

The results of the simulations are shown in Fig. 1.2. In part (a), we plotted the prevalence in humans I_1 and in part (b) the prevalence in animals I_2. For both (a) and (b), the prevalence as function of time is represented by solid curves in the case without control and represented by dashed curves in the case with control, i.e., when $k_{ij} \in \mathbf{K}$ with $(i,j) \in W$ is replaced by $k_{ij}/\mathscr{T}_W$. As we can see in Fig. 1.2, in the case without control the disease is endemic in the population; however, applying the intervention, the prevalence converges to zero and the epidemic is prevented.

1.3 General Models

In the work that follows, we further explore the ideas of the previous section in compartmental models with n host groups sharing a common source of infection besides a possible infection among members of the same group.

This kind of dynamics can be observed in a wide variety of scenarios. For example, it may model a shopping center that is visited by people from different locations. It also can be applied to sexually transmitted diseases with a core group capable of infecting all other groups, but with no direct transmission among the rest of the groups as illustrated in (Edwards et al., 2010).

1.3.1 A Model for Environmentally Driven Infectious Diseases with n Host Types.

In accordance with the World Health Organization (WHO) more than 20% of the burden of global diseases can be attributed to environmental factors (Prüss-Üstün and Corvalán, 2006). Particularly, in developing countries, because of the lack of health-care access, environmental conditions play an important role in the possible outbreak of a significant number of diseases. Naturally, this is the case for infections caused by pathogens with the ability to survive in the environment (soil, water, air, food, contact surfaces, etc). Therefore, when attacking infections with free-living pathogens in the environment, it is vital to minimize exposure to environmental risk factors such as unsafe drinking water, air pollution and other sanitation problems.

In this section, we study a model for infections caused by a pathogen that can survive in the environment for a period of time. Examples of infections of this kind are leptospirosis, cholera, schistosomiasis, hepatitis A, toxoplasmosis, among many others. For this group of infectious, the presence of pathogen in the environment is replenished by infectious hosts that excrete the pathogen into the environment, see (Bani-Yaghoub et al., 2012; Garira et al., 2014; Tien and Earn, 2010) and the references therein.

The model presented here is a classical *SIRS* model that generalizes system (1.1) to include n different host types since given the broad scope of environmental factors it is usual that these diseases affect a large range of individuals that can be subdivided according to different criteria, for example, spatial location, high-risk and low-risk groups, age, species, among others. We also included an equation for the pathogen dynamics.

The construction of our model rests on the following assumptions:

(i) The total population for each host type is divided into susceptible, infectious and recovered individuals, denoted S_i, I_i and R_i, respectively. Hence, the total population size for each type at time t is $N_i(t) = S_i(t) + I_i(t) + R_i(t)$, $i \in \{1,2,\ldots,n\}$. Individuals enter to the population as susceptible at a constant rate Λ_i and die at a per capita rate μ_i, $i \in \{1,2,\ldots,n\}$.

(ii) We assume that there is direct transmission within individuals of the same host type and indirect transmission through contact with a contaminated environment but there are no contacts among the different host types. Host-to-host transmission is modeled with standard incidence and has transmission rate β_{ii}, $i \in \{1,2,\ldots,n\}$. Environment-to-host transmission is modeled with mass action incidence and has transmission rate β_{ip}, $i \in \{1,2,\ldots,n\}$.

(iii) Infected individuals of host type $i \in \{1,2,\ldots,n\}$ recover at a constant rate γ_i proportional to the size of their class and the loss of immunity occurs at an average time of $1/\nu_i$.

(iv) Infected hosts excrete pathogen into the environment at a rate c_i, $i \in \{1,2,\ldots,n\}$, and μ_p is the pathogen clearance rate from the environment.

These assumptions give the following system of differential equations:

$$\begin{aligned}
\dot{S}_i &= \Lambda_i - (\beta_{ii} I_i/N_i + \beta_{ip} P) S_i - \mu_i S_i + \nu_i R_i, \\
\dot{I}_i &= (\beta_{ii} I_i/N_i + \beta_{ip} P) S_i - (\mu_i + \gamma_i) I_i, \qquad i \in \{1,2,\ldots,n\} \\
\dot{R}_i &= \gamma_i I_i - (\nu_i + \mu_i) R_i, \\
\dot{P} &= \sum_{i=1}^{n} c_i I_i - \mu_p P,
\end{aligned} \tag{1.12}$$

where all the parameters are assumed nonnegative.

Global Stability of the Disease-free Equilibrium

Until now, we have assumed that the disease can be eradicated when the target reproduction number is less than 1. However, for that to be true, we need to prove that the disease-free equilibrium is globally asymptotically stable if and only if $\mathscr{R}_0 < 1$. In order to prove the global stability of the disease-free equilibrium, we will construct a suitable Lyapunov function using the methods presented in (Arino and Portet, 2015; Vargas-De-León, 2011).

To determine the disease-free equilibrium of model (1.12), we set the derivatives equal to zero and solve the system

$$\begin{aligned}
0 &= \Lambda_i - (\beta_{ii} I_i/N_i + \beta_{ip} P) S_i - \mu_i S_i + \nu_i R_i, \\
0 &= (\beta_{ii} I_i/N_i + \beta_{ip} P) S_i - (\mu_i + \gamma_i) I_i, \qquad i \in \{1, 2, \ldots, n\} \\
0 &= \gamma_i I_i - (\nu_i + \mu_i) R_i, \\
0 &= \sum_{i=1}^{n} c_i I_i - \mu_p P,
\end{aligned}$$

setting $I_i = 0$ for $i = 1, 2, \ldots, n$. Clearly, at the disease-free equilibrium, the number of individuals in the recovered classes and the amount of free-living pathogen in the environment are equal to zero. Therefore, model (1.12) has a unique disease-free equilibrium

$$E_0 = (\Lambda_1/\mu_1, 0, 0, \Lambda_2/\mu_2, 0, 0, \ldots, \Lambda_n/\mu_n, 0, 0, 0).$$

Moreover, the total population size for host type i is governed by the equation

$$\dot{N}_i = \Lambda_i - \mu_i N.$$

Hence, the total population size may vary in time but converges to the equilibrium $N_i^* = \Lambda_i/\mu_i$. We thus study (1.12) in the following feasible region

$$\Omega = \{(S_1, I_1, R_1, \ldots, S_n, I_n, R_n, P) \in \mathbb{R}_+^{3n+1} : S_i + I_i + R_i \leq \Lambda_i/\mu_i, i = 1, \ldots, n\}$$

which is clearly positively invariant under the flow of system (1.12).

The results regarding the local asymptotic stability of E_0 are consequence of Theorem 2 in (Van den Driessche and Watmough, 2002). For model (1.12), the matrices $\mathbf{F}$ and $\mathbf{V}$ such that $\mathbf{F} - \mathbf{V}$ corresponds to the linearization of the infectious subsystem of (1.12) are:

$$\mathbf{F} = \begin{pmatrix}
\beta_{11} & 0 & 0 & \cdots & 0 & \beta_{1p} N_1^* \\
0 & \beta_{22} & 0 & \cdots & 0 & \beta_{2p} N_2^* \\
0 & 0 & \beta_{33} & \cdots & 0 & \beta_{3p} N_3^* \\
\vdots & \vdots & \vdots & \ddots & \vdots & \vdots \\
0 & 0 & 0 & \cdots & \beta_{nn} & \beta_{np} N_n^* \\
c_1 & c_2 & c_3 & \cdots & c_n & 0
\end{pmatrix}, \tag{1.13}$$

and

$$\mathbf{V} = \begin{pmatrix} \mu_1+\gamma_1 & 0 & 0 & \cdots & 0 \\ 0 & \mu_2+\gamma_2 & 0 & \cdots & 0 \\ \vdots & \vdots & \ddots & \vdots & \vdots \\ 0 & 0 & \cdots & \mu_n+\gamma_n & 0 \\ 0 & 0 & \cdots & 0 & \mu_p \end{pmatrix}. \tag{1.14}$$

The global behavior of the disease-free equilibrium is summarized in the following result.

Theorem 1.3.1. *Let* $\mathbf{K} = \mathbf{F}\mathbf{V}^{-1}$ *with* $\mathbf{F}$ *and* $\mathbf{V}$ *given by* (1.13) *and* (1.14)*, respectively. If the basic reproduction number* $\mathscr{R}_0 = \rho(\mathbf{K})$ *satisfies* $\mathscr{R}_0 \leq 1$*, then the disease-free equilibrium* E_0 *of model* (1.12) *is globally asymptotically stable in* Ω*.*

Proof. By construction, the matrix $\mathbf{F}$ has only nonnegative entries and the matrix $\mathbf{V}$ is an M-matrix (Van den Driessche and Watmough, 2002). From matrix theory, we now that the spectral radius of $\mathbf{F}\mathbf{V}^{-1}$ and $\mathbf{V}^{-1}\mathbf{F}$ are the same; therefore, $\mathscr{R}_0 = \rho(\mathbf{F}\mathbf{V}^{-1}) = \rho(\mathbf{V}^{-1}\mathbf{F})$ (Horn and Johnson, 2013). Moreover, $(\mathbf{V}^{-1}\mathbf{F})^2$ is entry-wise positive; thus, $\mathbf{V}^{-1}\mathbf{F}$ is primitive and by Perron's theorem (Berman and Shaked-Monderer, 2012), $\mathbf{V}^{-1}\mathbf{F}$ has a positive unique left eigenvector $\mathbf{w} = (w_1, w_2 \ldots, w_n, w_p)$ such that

$$(w_1, w_2 \ldots, w_n, w_p)\mathbf{V}^{-1}\mathbf{F} = \mathscr{R}_0(w_1, w_2 \ldots, w_n, w_p).$$

Let $\mathbf{P} = (I_1, I_2, \ldots, I_n, P)^T$, $k_i = w_i/(\mu_i+\gamma_i)$ for $i = 1, 2, \ldots, n$ and $k_p = w_p/\mu_p$. Define the function

$$L = \sum_{i=1}^{n} k_i I_i + k_p P.$$

Clearly, L is a radially unbounded function whose derivative along the solutions of (1.12) in Ω satisfies

$$\begin{aligned} \dot{L} &= \sum_{i=1}^{n} k_i \left[(\beta_{ii} I_i/N_i + \beta_{ip} P)S_i - (\mu_i+\gamma_i)I_i\right] + k_p \left[\sum_{i=1}^{n} c_i I_i - \mu_p P\right] \\ &\leq \sum_{i=1}^{n} k_i \left[(\beta_{ii} I_i + \beta_{ip} P N_i^*) - (\mu_i+\gamma_i)I_i\right] + k_p \left[\sum_{i=1}^{n} c_i I_i - \mu_p P\right] \\ &= (k_1, k_2, \ldots, k_n, k_p)\,(\mathbf{F}-\mathbf{V})\mathbf{P}. \end{aligned}$$

Since

$$(k_1, k_2, \ldots, k_n, k_p) = (w_1, w_2, \ldots, w_n, w_p)\,\mathbf{V}^{-1}$$

we obtain

$$\dot{L} \leq \mathbf{w}(\mathbf{V}^{-1}\mathbf{F} - \mathbf{I})\mathbf{P} = (\mathscr{R}_0 - 1)\mathbf{w}\mathbf{P}.$$

Clearly, if $\mathscr{R}_0 \leq 1$ then $\dot{L} \leq 0$. Hence, L is a Lyapunov function for model (1.12). Moreover, since for all i the constants k_i are positive, $\dot{L} = 0$ implies that $\mathbf{P}$ is equal to the zero vector. Using $I_i = 0$ and $P = 0$, it is easy to see that $R_i \to 0$ and $S_i \to \Lambda_i/\mu_i$. Therefore, if $\mathscr{R}_0 \leq 1$, it follows from LaSalle's invariance principle (La Salle et al., 1962), that every solution of the equations in the model (1.12), with initial condition in Ω, approaches E_0 as $t \to \infty$. □

Control Strategies

When the control strategy is based on reducing the pathogen shedding by infectious hosts and minimizing exposure to environmental risk factors, we have the following result that generalizes the result obtained in section 2.1 (C).

Theorem 1.3.2. *Consider the epidemiological model (1.12) and define the target set as* $W = \{(1,n+1),(2,n+1),\ldots,(n,n+1),(n+1,1),(n+1,2),\ldots,(n+1,n)\}$. *Provided that the condition*

$$\max\{\mathscr{R}_1,\mathscr{R}_2,\ldots,\mathscr{R}_n\} < 1$$

is satisfied, the target reproduction number $\mathscr{T}_W$ *is given by*

$$\mathscr{T}_W = \sqrt{\frac{\mathscr{R}_{1p}^2}{1-\mathscr{R}_1} + \frac{\mathscr{R}_{2p}^2}{1-\mathscr{R}_2} + \cdots + \frac{\mathscr{R}_{np}^2}{1-\mathscr{R}_n}}, \tag{1.15}$$

where

$$\mathscr{R}_i = \frac{\beta_{ii}}{\mu_i + \gamma_i} \quad \textit{and} \quad \mathscr{R}_{ip} = \sqrt{\frac{c_i\beta_{ip}N_i^*}{\mu_p(\mu_i+\gamma_i)}}.$$

Proof. The $(n+1)\times(n+1)$ next-generation matrix $\mathbf{K}$ for model (1.12) is given by

$$\mathbf{K}=\begin{pmatrix} \mathscr{R}_1 & 0 & 0 & \cdots & 0 & \dfrac{\beta_{1p}N_1^*}{\mu_p} \\ 0 & \mathscr{R}_2 & 0 & \cdots & 0 & \dfrac{\beta_{2p}N_2^*}{\mu_p} \\ 0 & 0 & \mathscr{R}_3 & \cdots & 0 & \dfrac{\beta_{3p}N_3^*}{\mu_p} \\ \vdots & \vdots & \vdots & \ddots & \vdots & \vdots \\ 0 & 0 & 0 & \cdots & \mathscr{R}_n & \dfrac{\beta_{np}N_n^*}{\mu_p} \\ \dfrac{c_1}{\mu_1+\gamma_1} & \dfrac{c_2}{\mu_2+\gamma_2} & \dfrac{c_3}{\mu_3+\gamma_3} & \cdots & \dfrac{c_n}{\mu_n+\gamma_n} & 0 \end{pmatrix}, \tag{1.16}$$

which is irreducible. Since the matrix $(\mathbf{K}-\mathbf{K}_W)$ is the diagonal matrix $diag(\mathscr{R}_1,\mathscr{R}_2,\cdots,\mathscr{R}_n,0)$ it is clear that

$$\rho(K-K_W)<1 \Longleftrightarrow \max\{\mathscr{R}_1,\mathscr{R}_2,\cdots,\mathscr{R}_n\}<1.$$

Furthermore, using induction it can be proved that the characteristic polynomial of the matrix $\mathbf{K}_W\cdot(\mathbf{I}-\mathbf{K}+\mathbf{K}_W)^{-1}$

$$\begin{pmatrix} 0 & 0 & \cdots & 0 & \dfrac{\beta_{1p}N_1^*}{\mu_p} \\ 0 & 0 & \cdots & 0 & \dfrac{\beta_{2p}N_2^*}{\mu_p} \\ \vdots & \vdots & \ddots & 0 & \vdots \\ 0 & 0 & \cdots & 0 & \dfrac{\beta_{np}N_n^*}{\mu_p} \\ \dfrac{c_1/(\mu_1+\gamma_1)}{(1-\mathscr{R}_1)} & \dfrac{c_2/(\mu_2+\gamma_2)}{(1-\mathscr{R}_2)} & \cdots & \dfrac{c_n/(\mu_n+\gamma_n)}{(1-\mathscr{R}_n)} & 0 \end{pmatrix}$$

is given by

$$P(\lambda)=(-1)^{n+1}\lambda^{n+1}+(-1)^n\left(\frac{\mathscr{R}_{1p}^2}{1-\mathscr{R}_1}+\cdots+\frac{\mathscr{R}_{np}^2}{1-\mathscr{R}_n}\right)\lambda^{n-1}. \tag{1.17}$$

By definition, the value of the target reproduction number $\mathscr{T}_W$ is equal to the root of largest modulus of polynomial (1.17) which it is given by the right-hand side of (1.15). □

Several properties make the target reproduction number such a useful quantity. First, it shares the threshold property of the basic reproduction number ($\mathscr{T}_W < 1$ if and only if $\mathscr{R}_0 < 1$; and $\mathscr{T}_W = 1$ if and only if $\mathscr{R}_0 = 1$). Second, if the values of the entries W in the next-generation matrix $\mathbf{K}$ are reduced by a proportion more than $1 - 1/\mathscr{T}_W$, then the disease will die out. The only requirements for this to be true are that $\rho(\mathbf{K} - \mathbf{K}_W) < 1$ and the next-generation matrix $\mathbf{K}$ to be irreducible.

As a decision maker, one might be concerned about how to lower the value of the target reproduction number below 1. In this case, it is important to know how sensitive is $\mathscr{T}_W$ to the values of the reproduction numbers associated with the environment-to-host and host-to-host transmission cycles to decide on which of the two to invest. This can be done, for instance, using the partial derivatives of $\mathscr{T}_W$. For example, from (1.15) it is easy to prove that,

$$\frac{\partial \mathscr{T}_W}{\partial \mathscr{R}_i} \leq \frac{\partial \mathscr{T}_W}{\partial \mathscr{R}_{ip}} \iff \frac{\mathscr{R}_{ip}}{2(1-\mathscr{R}_i)} \leq 1, \quad i = 1, 2, \ldots, n.$$

Therefore, $\mathscr{T}_W$ is more sensitive to the reproduction number $\mathscr{R}_{ip}$ than to $\mathscr{R}_i$ if and only if $\mathscr{R}_{ip} \leq 2(1-\mathscr{R}_i)$, see Fig. 1.3. If other things are equal, this simple analysis tells us if it is more convenient to reduce $\mathscr{R}_i$ or $\mathscr{R}_{ip}$ when controlling the i th host type. However, this sensitivity is local since it does not take into account the simultaneous variation of input parameters.

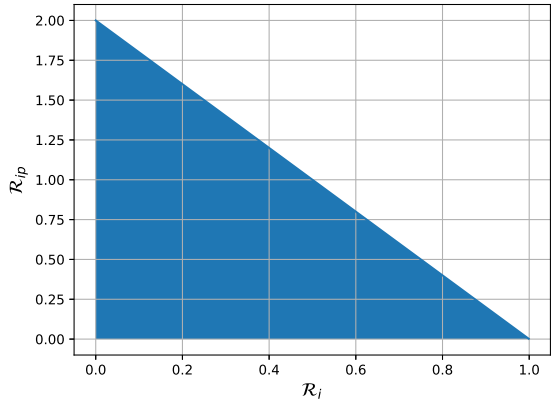

Fig. 1.3 Region (blue) in which the target reproduction number $\mathscr{T}_W$ is more sensitive to the reproduction number associated with the environment-to-host transmission $\mathscr{R}_{ip}$ than to the reproduction number of the host-to-host transmission $\mathscr{R}_i$.

The following theorem establishes the generalization of the result obtained for approach *(A)* in section 2.1.

Theorem 1.3.3. *Consider the epidemiological model (1.12) and define the target set as* $S = \{(1,n+1),(2,n+1),\ldots,(n,n+1)\}$. *Provided that the condition*

$$\max\{\mathscr{R}_1,\mathscr{R}_2,\ldots,\mathscr{R}_n\} < 1 \tag{1.18}$$

is satisfied, the target reproduction number $\mathscr{T}_S$ *is given by*

$$\mathscr{T}_S = \frac{\mathscr{R}_{1p}^2}{1-\mathscr{R}_1} + \frac{\mathscr{R}_{2p}^2}{1-\mathscr{R}_2} + \cdots + \frac{\mathscr{R}_{np}^2}{1-\mathscr{R}_n}. \tag{1.19}$$

Proof. By definition, the target matrix $\mathbf{K}_S$ is given by

$$\mathbf{K}_S = \begin{pmatrix} 0 & 0 & \cdots & 0 & \dfrac{\beta_{1p}N_1^*}{\mu_p} \\ \vdots & \vdots & \cdots & \vdots & \vdots \\ 0 & 0 & \cdots & 0 & \dfrac{\beta_{np}N_n^*}{\mu_p} \\ 0 & 0 & \cdots & 0 & 0 \end{pmatrix}. \tag{1.20}$$

Consequently, the matrix $\mathbf{K}-\mathbf{K}_S$ is a triangular matrix with $\mathscr{R}_1,\ldots,\mathscr{R}_n$ and 0 in its diagonal; hence, $\rho(\mathbf{K}-\mathbf{K}_S) < 1$ is equivalent to condition (1.18). The product $\mathbf{K}_S\cdot(\mathbf{I}-\mathbf{K}+\mathbf{K}_S)^{-1}$ is given by the following matrix

$$\begin{pmatrix} \dfrac{\mathscr{R}_{1p}^2}{1-\mathscr{R}_1} & \dfrac{c_2\beta_{1p}N_1^*}{\mu_p(\mu_2+\gamma_2)(1-\mathscr{R}_2)} & \cdots & \dfrac{c_n\beta_{1p}N_1^*}{\mu_p(\mu_n+\gamma_n)(1-\mathscr{R}_n)} & \dfrac{\beta_{1p}N_1^*}{\mu_p} \\ \dfrac{c_1\beta_{2p}N_2^*}{\mu_p(\mu_1+\gamma_1)(1-\mathscr{R}_1)} & \dfrac{\mathscr{R}_{2p}^2}{1-\mathscr{R}_2} & \cdots & \dfrac{c_n\beta_{2p}N_2^*}{\mu_p(\mu_n+\gamma_n)(1-\mathscr{R}_n)} & \dfrac{\beta_{2p}N_2^*}{\mu_p} \\ \vdots & \vdots & \cdots & \vdots & \vdots \\ \dfrac{c_1\beta_{np}N_n^*}{\mu_p(\mu_1+\gamma_1)(1-\mathscr{R}_1)} & \dfrac{c_2\beta_{np}N_n^*}{\mu_p(\mu_2+\gamma_2)(1-\mathscr{R}_2)} & \cdots & \dfrac{\mathscr{R}_{np}^2}{1-\mathscr{R}_n} & \dfrac{\beta_{np}N_n^*}{\mu_p} \\ 0 & 0 & \cdots & 0 & 0 \end{pmatrix}.$$

It is easy to see that $\mathit{rank}\left(\mathbf{K}_S\cdot(\mathbf{I}-\mathbf{K}+\mathbf{K}_S)^{-1}\right) = 1$ since all the columns of $\mathbf{K}_S\cdot(\mathbf{I}-\mathbf{K}+\mathbf{K}_S)^{-1}$ are scalar multiples of its first column. Hence, $\mathbf{K}_S\cdot(\mathbf{I}-\mathbf{K}+\mathbf{K}_S)^{-1}$ only has a nonzero

eigenvalue, which implies

$$\rho(\mathbf{K}_S \cdot (\mathbf{I}-\mathbf{K}+\mathbf{K}_S)^{-1}) = \frac{\mathscr{R}_{1p}^2}{1-\mathscr{R}_1} + \frac{\mathscr{R}_{2p}^2}{1-\mathscr{R}_2} + \cdots + \frac{\mathscr{R}_{np}^2}{1-\mathscr{R}_n}$$

because the trace of a matrix is equal to the sum of its eigenvalues. □

In cases when the control strategy focuses on reducing the shedding rate of infectious hosts, we have the following result.

Theorem 1.3.4. *Consider the epidemiological model (1.12) and define the target set as* $U = \{(n+1,1),(n+1,2),\ldots,(n+1,n)\}$. *Provided that the condition*

$$\max\{\mathscr{R}_1,\mathscr{R}_2,\ldots,\mathscr{R}_n\} < 1 \tag{1.21}$$

is satisfied, the target reproduction number $\mathscr{T}_U$ *is given by*

$$\mathscr{T}_U = \frac{\mathscr{R}_{1p}^2}{1-\mathscr{R}_1} + \frac{\mathscr{R}_{2p}^2}{1-\mathscr{R}_2} + \cdots + \frac{\mathscr{R}_{np}^2}{1-\mathscr{R}_n}. \tag{1.22}$$

Proof. It is straightforward to see that

$$\rho(\mathbf{K}-\mathbf{K}_U) < 1 \Longleftrightarrow \max\{\mathscr{R}_1,\mathscr{R}_2,\ldots,\mathscr{R}_n\} < 1.$$

Moreover, the matrix $\mathbf{K}_U \cdot (\mathbf{I}-\mathbf{K}+\mathbf{K}_U)^{-1}$ is a lower triangular matrix with 0's in the first n elements of its diagonal and

$$\frac{\mathscr{R}_{1p}^2}{1-\mathscr{R}_1} + \frac{\mathscr{R}_{2p}^2}{1-\mathscr{R}_2} + \cdots + \frac{\mathscr{R}_{np}^2}{1-\mathscr{R}_n}$$

as the last element of its diagonal. □

One of the advantages of using the target reproduction number is making a big problem smaller. Instead of struggling with the complete and probably very complex $\mathscr{R}_0$, one can handle a much smaller amount of information: some of the entries of the next-generation matrix.

Therefore, although $\mathscr{T}_S$ and $\mathscr{T}_U$ have the same value, in real life, one of the two strategies may have advantages over the other one. For instance, assuming that we want to reduce the value of the entries U of the next-generation matrix $\mathbf{K}$ (1.16) by a proportion more than $1-1/\mathscr{T}_U$, then we have to reduce the pathogen shedding rate or increase the recovery rate in each host class. But, if the objective is to reduce the entries S in $\mathbf{K}$; increasing the pathogen

clearance rate μ_p reduces all of these entries at the same time. This could be a practical advantage of the last strategy over the first one.

How multiple transmission routes affect the spread of many environmentally-driven diseases is not well-understood (Tien and Earn, 2010). Nevertheless, the host-to-host transmission pathway has been traditionally considered as the predominant cause of disease spread (Bani-Yaghoub et al., 2012). For model (1.12), infectious individuals can transmit the infection both through direct contact with a susceptible person and also by pathogen shedding into the environment. One of the basic aims of this work is to explore the role of the host-environment-host indirect transmission pathway. Therefore, control strategies *(A)*, *(B)* and *(C)* essentially focus on controlling environmental factors.

1.3.2 A Metapopulation Model with a Central Patch

Metapopulation models (see (Hanski et al., 1999) and the references therein) were first introduced in ecology, for situations where a population can be divided into a number of geographically separated sub-populations. The term metapopulation was coined by Richard Levins in 1969 to describe a model of population dynamics. The most common form of metapopulation model consists of a number of sub-populations, where each sub-population is assumed to be large. Many metapopulation models in ecology show that increasing movement among populations reduces the chance of metapopulation extinction. However, epidemiological models indicate that increased contact among populations enhances the spread of disease and can trigger epidemics.

In this section, we consider a metapopulation model with $n+1$ patches that can be thought of as cities, countries, or other geographically autonomous regions with the particularity that one of them is the gravity center that connects the other ones.

We propose a compartmental *SIRS* model for each patch. For the central patch, we are going to denote the total population at time t by $N_c(t)$, whereas $S_c(t)$, $I_c(t)$ and $R_c(t)$ give the number of susceptible, infectious and recovered individuals at time t, respectively. For the remaining n patches, the classes are denoted by $S_i(t)$, $I_i(t)$ and $R_i(t)$ with $i \in \{1,2,\ldots,n\}$. So, the total population at time t in patch i is $N_i(t) = S_i(t)+I_i(t)+R_i(t)$ for $i \in \{1,2,\ldots,n,c\} := J$.

Concerning movement, we assume that the members of the region $i \in \{1,2,\ldots,n\}$ make short-term visits to the central region and return to the home patch, while individuals in the central patch can travel to all the remaining patches and then get back home. When infectious individuals are visiting another region, they can infect the susceptible individuals of that region. Likewise, the susceptible ones that travel can be infected by infectious ones of the visited region.

For the sake of clarity, the incidence will be governed by the mass action law and we also assume that all individuals are born susceptibles. The metapopulation *SIRS* model takes the following form

$$\begin{aligned}\dot{S}_i &= \Lambda_i - (\beta_{ii}I_i + \beta_{ic}I_c)S_i - \mu_i S_i + \nu_i R_i,\\ \dot{I}_i &= (\beta_{ii}I_i + \beta_{ic}I_c)S_i - (\mu_i + \gamma_i)I_i,\\ \dot{R}_i &= \gamma_i I_i - (\nu_i + \mu_i)R_i,\end{aligned} \tag{1.23}$$

for patches $i \in \{1,2,\ldots,n\}$, while for the central patch,

$$\begin{aligned}\dot{S}_c &= \Lambda_c - \beta_{cc}S_cI_c - \sum_{i=1}^{n}\beta_{ci}S_cI_i - \mu_c S_c + \nu_c R_c,\\ \dot{I}_c &= \beta_{cc}S_cI_c + \sum_{i=1}^{n}\beta_{ci}S_cI_i - (\mu_c + \gamma_c)I_c,\\ \dot{R}_c &= \gamma_c I_c - (\nu_c + \mu_c)R_c.\end{aligned} \tag{1.24}$$

Here, Λ_i are recruitment rates, β_{ij} are the transmission rates of infectious individuals from patch j to susceptible individuals in patch i. The mortality rates are denoted by μ_i, and γ_i represent recovery rates. The average duration of the immune period for individuals in patch $i \in J$ is $1/\nu_i$. The graph associated with the dynamics of the infection process is shown in Fig. 1.4.

To see that solutions of model (1.23)-(1.24) with nonnegative initial conditions remain nonnegative consider when at least one of the phase space variables x_i is equal to zero. Direct computation gives that if $x_i = 0$, then $\dot{x}_i \geq 0$ where $x \in \{S,I,R\}$ and $i \in J$. Thus, solutions cannot become negative for future times. The total population size of the complete system $N = \sum_{i\in J} N_i$ satisfies

$$\dot{N} \leq \Lambda - \mu N, \quad \text{with} \quad \Lambda = \sum_{i\in J}\Lambda_i, \quad \mu = \min_{i\in J}\{\mu_i\};$$

therefore,

$$\limsup_{t\to\infty} N(t) \leq \Lambda/\mu.$$

It follows that solutions of (1.23)-(1.24) are bounded. Moreover, for all the patches, the total population size of the patch converges to $N_i^* = \Lambda_i/\mu_i$ with $i \in J$. Then, the region

$$\Gamma = \{(S_1,I_1,R_1,\ldots,S_c,I_c,R_c) \in \mathbb{R}_+^{3n+3} : S_i + I_i + R_i \leq \Lambda_i/\mu_i,\ i \in J\}$$

is positively invariant under the flow of (1.23)-(1.24).

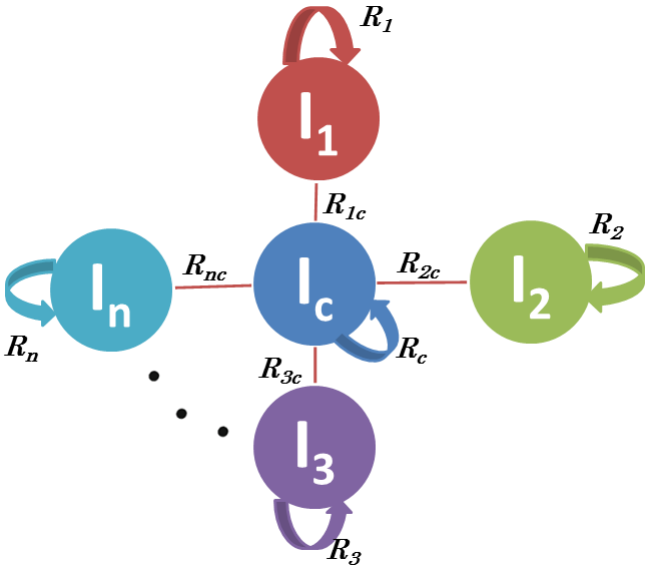

Fig. 1.4 Topological structure of the infection process for model (1.23)-(1.24). The reproduction numbers $\mathscr{R}_i$ correspond to the isolated dynamics of patch $i \in J$, while the reproduction numbers $\mathscr{R}_{ic}$ are associated with the commuting between the central patch and patch i, $1 \leq i \leq n$.

The disease-free equilibrium $\tilde{E}$ obtained by solving for S_i and R_i after setting $I_i = 0$, takes the values $S_i^* = N_i^*$ and $R_i^* = 0$ for $i \in J$. Thus,

$$\tilde{E} = (N_1^*, 0, 0, \ldots, N_n^*, 0, 0, N_c^*, 0, 0) \tag{1.25}$$

is the unique disease-free equilibrium of model (1.23)-(1.24). Assuming that the commuting between patches does not occur, that is, $\beta_{ic} = \beta_{ci} = 0$ for $i = 1, 2, \ldots, n$, we can define the basic reproduction number for each patch

$$\mathscr{R}_i = \frac{\beta_{ii} N_i^*}{\mu_i + \gamma_i}, \quad i \in J.$$

The familiar threshold property of the basic reproduction number is valid for each patch. Thus, if $\mathscr{R}_i < 1$ in patch i, the disease will be eradicated in patch i if it is not connected with other patches of the metapopulation. If $\mathscr{R}_0 > 1$, the disease will persist in patch i if it is isolated from the metapopulation.

The reproduction numbers associated with the infections caused by the commuting between the $i \in \{1,2,\ldots,n\}$ patches and the central patch, are

$$\mathscr{R}_{ic} = \sqrt{\frac{\beta_{ic}\beta_{ci}N_i^*N_c^*}{(\mu_i+\gamma_i)(\mu_c+\gamma_c)}}, \quad i \in \{1,2,\ldots,n\}$$

As in the proof of Theorem 1.3.1, constructing a suitable Lyapunov function we can prove the following result.

Theorem 1.3.5. *Let* $\mathbf{K}$ *be the next-generation matrix for model* (1.23)-(1.24) *and* $\mathscr{R}_0 = \rho(\mathbf{K})$. *If the basic reproduction number satisfies* $\mathscr{R}_0 \leq 1$, *then the disease-free equilibrium* $\tilde{E}$ *of the metapopulation model* (1.23)-(1.24) *is globally asymptotically stable in* Γ.

Since the importance of the mobility component in the persistence of diseases in metapopulation models has been proved (Arino and Van den Driessche, 2003), our control strategy shall focus on the interactions between patches rather than the local dynamics of each patch.

Theorem 1.3.6. *Provided that the condition*

$$\max\{\mathscr{R}_1,\ldots,\mathscr{R}_n,\mathscr{R}_c\} < 1 \tag{1.26}$$

is fulfilled, the target reproduction number $\mathscr{T}_Z$ *for system (1.23)-(1.24) where the target set is defined as* $Z = \{(1,n+1),(2,n+1),\ldots,(n,n+1),(n+1,1),(n+1,2),\ldots,(n+1,n)\}$ *is given by*

$$\mathscr{T}_Z = \sqrt{\frac{1}{(1-\mathscr{R}_c)}\left(\frac{\mathscr{R}_{1c}^2}{1-\mathscr{R}_1}+\frac{\mathscr{R}_{2c}^2}{1-\mathscr{R}_2}+\cdots+\frac{\mathscr{R}_{nc}^2}{1-\mathscr{R}_n}\right)}, \tag{1.27}$$

where $\mathscr{R}_i$ *and* $\mathscr{R}_{ic}$ *are the basic reproduction numbers of the within-patch transmission and the infectious caused by the commuting between the* $i \in \{1,2,\ldots,n\}$ *patches and the central patch, respectively (see Fig. 1.4).*

The proof follows the same idea that the proof of Theorem 3.1, and it is therefore omitted. Observe that in the calculated target reproduction number (1.27), in the denominator arise expressions of the form $1-\mathscr{R}_i$, $i \in J$. Thus, in a limit sense, the value of $\mathscr{T}_Z$ goes to infinity as $\mathscr{R}_i$ tend to 1. This seems to contradict the fact that

$$\mathscr{T}_Z < 1 \Leftrightarrow \mathscr{R}_0 < 1, \quad \text{and} \quad \mathscr{T}_Z = 1 \Leftrightarrow \mathscr{R}_0 = 1 \tag{1.28}$$

when the target reproduction number is well defined. However, this is not a discrepancy since $\mathscr{R}_i$, $i \in J$, are local reproduction numbers associated with submodels and relation (1.28) only applies for the basic reproduction number of the complete model.

We also want to emphasize that the conceptual idea of the design of control strategies from the topological structure of the infection process is applicable to a broad range of models beyond those where the heterogeneity is spatial. For example, infectious processes related to vector-borne diseases that affect multiple host species have an analogous structure that the one presented in Fig. 1.4, with the difference that the reproduction numbers associated with the within-species transmission are zero. In the above case, the vector has the function of transmitting the infection to the different species so it works as the common source of infection.

1.4 Discussion

In recent years, the fast development of the field of mathematical epidemiology has included a wide range of multigroup mathematical models that consider host heterogeneities. However, much remains to be understood about how such heterogeneities and the topological structure of the infection process affect the spread of infectious diseases and our capacity to control them.

Even though $\mathscr{R}_0$ is a linear measure of the strength of the infection, under the homogeneous mixing assumption, it aptly determines the control effort needed to eradicate an infection (Roberts and Heesterbeek, 2003) which is one of the fundamental tasks in the mathematical modeling of infectious diseases. However, for a large number of diseases, there are multiple factors such as physiological, geographical or even economic conditions that affect the trend of the infection and therefore the homogeneous mixing assumption is no longer valid. This might make it necessary to consider different host types where each group guarantees homogeneous mixing. Once having several host types, the basic reproduction number often appears as complex combinations of parameters that make any analysis difficult. In these cases, $\mathscr{R}_0$ does not improve our understanding of how efforts should be focused to eliminate the epidemic (Olmos et al., 2015).

In this work, we bring forward some techniques to reduce the value of $\mathscr{R}_0$ for multigroup models even without explicitly knowing its expression. Given the original model, we studied some subsystems and computed their basic reproduction numbers. These basic reproduction numbers allowed us to express the target reproduction number in a more treatable way for concrete public health interventions. In other words, our methodology focuses on preventing outbreaks at the global level by means of controlling the local dynamics of the infection process.

We started by applying these methods to a two-species model for leptospirosis. Three control policies were studied, all of them focusing on the indirect transmission caused by

the interaction between hosts and the free-living leptospira in the environment. In particular, by comparing the strategy that minimizes exposures to environmental risk factors with the one that reduces the pathogen shedding rate, we found that both target reproduction numbers are equal. Biologically, this means that both processes lead to the same outcome. Therefore, one can select the strategy that is most feasible according to the local conditions. The combination of the above strategies brings a stronger strategy because for endemic cases $1 < \mathscr{T}_W < \mathscr{T}_S = \mathscr{T}_U$ and therefore $1 - 1/\mathscr{T}_W < 1 - 1/\mathscr{T}_S$. Yet, none of these strategies is good enough to control the infection when the direct transmission cycle is endemic.

In order to study infections caused by pathogens with the ability to survive in the environment, we proposed a generalization of the previous model, namely the n-groups compartmental model (1.12). The model includes two potential routes of transmission: host-to-host and environment-to-host transmission. Traditionally, control strategies have been focused on the host-to-host transmission pathway. Nevertheless, the relative importance of the indirect infections caused via contact with a contaminated environment is uncertain (Bani-Yaghoub et al., 2012; Holt et al., 2006; Tien and Earn, 2010). Therefore, we analyzed control strategies that center on the environment-to-host and computed the target reproduction number in each case to quantify the control effort needed to eradicate the infection.

We also studied the spread of an infection among discrete geographical regions with a core region. Even though the connection of the regions is by way of short-term movement, it still allows infectious individuals to transmit the pathogen to susceptible individuals of a different region. Theorem 1.3.6 implies that if the disease can persist even in one patch we cannot eradicate the epidemic by just controlling the movement between patches in the metapopulation model (1.23)-(1.24). In fact, we also notice that the infection can persist in the population even if all the basic reproduction numbers for the transmission within patches are less than one.

Another important observation is that the topological structure of the infection process of model (1.12) is a particular case of the infection cycle that follows the metapopulation model (1.23)-(1.24). The difference is that the common source of infection in model (1.12) (namely the free-living pathogen) does not have the ability to produce within-group infections. On the other hand, the central group of the metapopulation model can produce within-group infections with a reproduction number $\mathscr{R}_c$. Also note that in qualitative terms, the strategy that aims to reduce the pathogen shedding by infectious hosts and minimize exposure to environmental risk factors in model (1.12), is equivalent to the strategy that focuses on reducing the infections caused by travel between patches in the metapopulation model. This explains the similarity in the target reproduction numbers (1.15) and (1.27) and leads us to remark that there is a connection among the cycles of infection, the basic reproduction

number and the target reproduction number. These results illustrate that understanding the topological structure of the infection process and partitioning it into simple cycles is useful to design and evaluate control strategies.

Chapter 2

Evaluating the Potential of Vaccine-Induced Type Replacement for High-Risk Human Papillomavirus

2.1 Introduction

Cervical cancer is the fourth most frequent cancer in women with an estimated $570,000$ new cases in 2018 representing 6.6% of all female cancers. Approximately 90% of deaths from cervical cancer occurred in low- and middle-income countries. In Mexico, $13,900$ cases of cervical cancer are estimated annually, with an incidence of 23.3 cases per $100,000$ women. In 2013, in the specific group of women aged 25 and over, there were $3,771$ deaths with a rate of 11.3 deaths per $100,000$ women, making cervical cancer one of the leading causes of death in Mexican women (de Salud Mexico, 2016).

It is known that a persistent infection with human papillomavirus (HPV) is the primary cause of cervical cancer and several other malignancies (Arbyn et al., 2011; Ault, 2008; Dasbach et al., 2006; Juckett et al., 2010). HPVs are small non-enveloped double-stranded DNA viruses that belong to the Papillomaviridae family. Over 150 HPV types or strains have been identified to date (Burd, 2003). HPVs infect squamous epithelia, that is, mucosal and cutaneous membranes (Kajitani et al., 2012). Based on their association with cervical cancer and other malignant carcinomas, mucosal HPVs can be classified into two groups: high-risk (HR) and low-risk (LR) types (Kajitani et al., 2012). HR HPV types include types 16, 18, 31, 33, 34, 35, 39, 45, 51, 52, 56, 58, 59, 66, 68, and 70 (Burd, 2003). HPV-16 and HPV-18 are the most prevalent HR strains, being associated with 70% of cases of cervical cancer globally (Grabowska and Riemer, 2012; Li et al., 2011).

Since 2007, in many developed countries, there have been recommendations to implement vaccination programs against HPV. At present, the degree of implementation of these programs depend on several country-specific factors including the health care system organization and the ways of funding. Currently, in Mexico there are two vaccines that protect against HPV infection: the quadrivalent vaccine Gardasil® and the bivalent vaccine Cervarix®. Both vaccines target the HR strains 16 and 18, but the quadrivalent vaccine also protect against the LR strains 6 and 11 that are responsible for approximately 90% of genital warts. The efficacy of these vaccines has been shown to be very high, being more than 90% effective at preventing diseases associated with the vaccine-targeted types ('vaccine types') (Stanley, 2010). Several studies that analyzed HPV transmission at the population level have found that vaccination of pre-adolescent girls is both highly effective and highly cost-effective to reduce diseases caused by HPV (Brisson et al., 2011; Chesson et al., 2011; Damm et al., 2017; Muller and Bauch, 2010; Prinja et al., 2017).

Nevertheless, given the vast diversity of HPV types, there have been speculations over whether vaccine types will be replaced by other HR non-vaccine-targeted types ('non-vaccine types') (Murall et al., 2014). Vaccine-induced strain replacement is a phenomenon in which vaccination leads to emergence and dominance of non-vaccine pathogen strains. This replacement is due to a decreased fitness of the vaccine types after a vaccination scheme and the fact that non-vaccine types can still infect vaccinated individuals (Martcheva et al., 2008). For the specific case of HPV, selective pressures from vaccination might cause a reduction in the size of the ecological niches dominated by HPV-16 and HPV-18, and at the same time an increase in the prevalence of other HR non-vaccine types (Peralta et al., 2014). Yet, in order to predict the outcome of a vaccination program, it is necessary to understand how HPV strains interact and what factors control strain dominance.

Coinfection with multiple HPV strains has been found in several epidemiological studies (Trottier and Franco, 2006). However, the role of coinfections with additional HPV strains on the duration of an episode with a given HPV strain is not clear. To date, the biological mechanisms that define the interactions among the broad variety of HPV strains inside a host are not well understood. For example, in (McLaughlin-Drubin and Meyers, 2004) it was reported that there can be antagonistic interactions among different HPV strains such as competition, but only at the within-cell level, with more complex multistrain relations at the population-cell level. Other studies suggest that the relations among HPV strains are synergistic in the sense that infection with one strain facilitates concurrent or subsequent infections with other strains (Elbasha and Galvani, 2005). However, independence among HPV types is also a common finding (Garnett and Waddell, 2000; Saccucci et al., 2018; Schiller and Lowy, 2012; Tota et al., 2013). This controversy implies that more clinical

and theoretical studies are needed to infer the dynamics of HR non-vaccine types after a vaccination program.

In this work, we use a within-host metapopulation model to investigate if the selective nature of HPV vaccine can induce pathogen strain replacement. The model is formulated as a nonlinear, discrete time Markov chain; the details of the formulation are given in section 2.2. We compute the basic reproduction number $\mathscr{R}_0$ and analyze the stability of the disease-free and boundary equilibria in section 2.3. In section 2.4, we study the model outcome through numerical simulations for different scenarios related to the effectiveness of the vaccine and the degree of cross-protection. We discuss the main implications of our analysis and simulations and mention future work in section 2.5.

2.2 Model formulation

Early mathematical modeling related to within-host HPV dynamics dates back to 2013. (Orlando et al., 2013) developed ecological and evolutionary models of HPV-induced epithelial lesions using partial differential equations. Their results demonstrate the link between HPV infection and ecological parameters governing cellular population dynamics and highlight somatic evolution as an alternative hypothesis for the progression of HPV-induced lesion to malignancy. Based on Levins' metapopulation framework, (Murall et al., 2014) developed the first patch model to investigate HPV type interactions and their immune responses. The authors in (Smith et al., 2015) constructed a within-host compartmental model to examine the effect of vaccination on viral eradication. The role of HPV vaccines on the evolution of virulence is discussed in (Murall et al., 2015). Using an evolutionary ecology modeling approach, they found that higher oncogene expression is favored in vaccinated hosts, leading to a higher probability of transmission before clearance by the vaccine. (Asih et al., 2016) presented a model of HPV infection allowing the progression of infected cells to cancerous forms to explore the interactions of long-term HPV infections and the risk for the development of cervical cancer.(Verma et al., 2017) constructed a mathematical model of HIV/HPV coinfection to determine the role of HIV-associated immune suppression on HPV persistence and pathogenesis. Recently, (Alizon et al., 2017) discussed the metapopulation approach as an explanatory framework to the study of the course of HPV infections.

Here, we propose a simple metapopulation model to examine the interplay of HR vaccine and non-vaccine types after vaccination. Our model is formulated as a nonlinear, discrete time Markov chain. This approach has not been used to study within-host HPV dynamics, but it has been used successfully to study the biological heterogeneity of communities on patchy landscapes (Barradas et al., 1996; Barradas and Cohen, 1994; Barradas and Tassier,

1999; CASWELL and COHEN, 1991). As remarked by Murall et al. (Murall et al., 2014), HPVs need microabrasions on the skin to infect new basal epithelial cells. Therefore, HPV infections are localized and can be conceptualized as occurring in specific areas or patches of the squamous epithelium.

The host tissue for the infection cycle of HPV is the squamous epithelium (Chow et al., 2010). HPVs are intracellular parasites that must deliver their genome into host cells. The target for HPV infection are basal epithelial cells in the cervix. In the initial phase of the infection, HPV DNA is transported into the nucleus and maintained at very low levels in the basal cells (Bedell et al., 1991; Moody and Laimins, 2010). The productive lifecycle of HPV requires differentiation of the host cell. When the virus initially enters the host basal cell, it cannot replicate until the cell matures into a keratinocyte. Once the infected keratinocytes enter the differentiating compartment in the suprabasal layers of the epithelium, the productive lifecycle occurs, and progenitor virions are released at the surface of the epithelium once the cell dies, thus the virus is nonlytic(Grabowska and Riemer, 2012; Kajitani et al., 2012).

For our model formulation, we consider the epithelium as a patchy environment that can be inhabited by HPVs. Patches, that is, localized areas of the epithelium, can be infected by multiple HPV strains and eventually produce free virions. However, since we want to study the possibility of strain replacement, we only distinguish infection with HR vaccine types (strains 16 and 18) or with HR non-vaccine types (strains 31, 33, 34, 35, 39, 45, 51, 52, 56, 58, 59, 66, 68, and 70). From now on, we are also going to refer to HR vaccine types as *species* S_1 and to HR non-vaccine types as *species* S_2.

Each patch can be in one of four possible states depending on the presence or absence of the species. The states are numbered $0, 1, 2$ or 3 and defined as follows: 0 if the patch is not infected, 1 if it is infected by species S_1, 2 if it is infected by species S_2, and 3 if both species are present in it. This is summarized in Table 2.1.

HR Vaccine-Types	HR Non-vaccine Types	State
absent	absent	0
present	absent	1
absent	present	2
present	present	3

Table 2.1 Patch states defined by the presence or absence of species.

The state of the metapopulation model as a whole is described by a vector $\mathbf{y} = (y_0.y_1, y_2, y_3) \in \mathbb{R}^4$, where the entry y_i is the proportion of patches in state i, for $i = 0, 1, 2, 3$. Note that we are assuming that all patches are identical; therefore, we are only considering the environmental

heterogeneity produced by the independence of the patches. This simplifying assumption allows us to focus our analysis on the impact of vaccination and the level of cross-protection on the prevalence of the species.

The dynamics of our model for an HPV infected epithelium is given by a nonlinear Markov chain

$$\mathbf{y}(t+1) = \mathbf{A}_{\mathbf{y}(t)}\mathbf{y}(t), \tag{2.1}$$

where the transition matrix $\mathbf{A}_{\mathbf{y}(t)}$ is a 4×4 column stochastic matrix which depends on the state $\mathbf{y}(t)$ at time t. The elements $a_{ij}(\mathbf{y}(t)) \in \mathbf{A}_{\mathbf{y}(t)}$ give the transition probability of moving from state j to state i.

We derive the transition matrix under the hypothesis of independence among HPV types. In other words, we assume that the ability to infect patches and produce virions of species S_1 is not affected by the presence of species S_2 and vice-versa.

Since infected patches can produce new virions, we assumed that the mean number of virions of species S_i infecting a patch is directly proportional to the fraction of patches containing S_i. Further, under the assumption that the infections of patches are independent events that occurs at random, that is, without neighborhood effects, we can assume that infection follows a Poisson process. Therefore, the probability C_i that a healthy patch is infected by at least one virion of species S_i is given by

$$C_1(\mathbf{y}) = 1 - \exp(-(1-\varepsilon)d_1 f_1), \tag{2.2}$$

$$C_2(\mathbf{y}) = 1 - \exp(-(1-\sigma)d_2 f_2). \tag{2.3}$$

Where no confusion seems likely to result, we will omit the dependence on $\mathbf{y}$ of the functions C_1 and C_2.

The dispersal coefficient d_i of species S_i is a constant of proportionality that combines the effect of the production of new virions in the infected patches and the success of dispersal of those virions (CASWELL and COHEN, 1991). The variables $f_1(t) = y_1(t) + y_3(t)$, and $f_2(t) = y_2(t) + y_3(t)$ represent the frequency of species S_1 and S_2 at time t, respectively.

HPV vaccines are composed of type-specific HPV L1 protein which is the major capsid protein of HPV (Stanley, 2010). These vaccines stimulate the production of antibodies that bind to the virus and prevent the infection of cells. We consider this in our model assuming that the vaccine prevents the infection of patches by species S_1 with an effectiveness ε, we take $0 \leq \varepsilon \leq 1$. The vaccine is completely effective when $\varepsilon = 1$ and useless when $\varepsilon = 0$. Moreover, it has been reported that the vaccine may provide cross-protection to non-vaccine types (Durham et al., 2012; Jenkins, 2008). The level of cross-protection is reflected in the

parameter σ, where $0 \leq \sigma < \varepsilon$. If σ is close to 0, the degree of cross-protection is low. On the contrary, if σ is close to ε, the degree of cross-protection is high.

In most cases, HPV infections are cleared by a cell-mediated immune response induced by CD8+ T-cells (Stanley, 2010). In fact, there are estimations that on average 70% of persons with a new HPV infection will clear the infection within 1 year, and approximately 90% within 2 years (Markowitz et al., 2014). However, if the viral infection is not effectively cleared, individuals can undergo neoplastic progression to high-grade precancer in the cervix and eventually to cervical cancer. In this work, we model the cell-mediated immune response as a disturbance that affects the persistence of the virus in the patches. In particular, we assume that the immune system clears species S_i, with a constant probability p_i per unit of time, $i = 1,2$.

Finally, assuming that an empty patch can be infected by either or both species at the same time, we obtain the following transition matrix

$$A_{\mathbf{y}(t)} = \begin{bmatrix} (1-C_1)(1-C_2) & p_1 & p_2 & p_1p_2 \\ C_1(1-C_2) & \bar{p}_1(1-C_2) & 0 & \bar{p}_1p_2 \\ (1-C_1)C_2 & 0 & \bar{p}_2(1-C_1) & p_1\bar{p}_2 \\ C_1C_2 & \bar{p}_1C_2 & \bar{p}_2C_1 & \bar{p}_1\bar{p}_2 \end{bmatrix} \tag{2.4}$$

where $0 < p_i < 1$, and we used the convention that $\bar{p}_i = 1 - p_i$ for p_i with $i = 1,2$.

2.3 Model analysis

The fundamental question about the model (2.1) is to determine the asymptotic behavior of the system for any well-defined initial condition. From a mathematical point of view, model (2.1) is a nonlinear, discrete time, nonautonomous dynamical system with a considerable spectrum of possible asymptotic behaviors.

The simplest outcome of the model (2.1) is the vector of state frequencies $\mathbf{y}^* \in \mathbb{R}^4$ that quantifies the densities of the species at equilibrium. This vector gives the overall picture of the host tissue after HPV infection. In addition, the prevalence of vaccine and non-vaccine types at equilibrium is easily obtained adding the corresponding elements of the state frequency vector $\mathbf{y}^*$. Besides these spatial averages, patch properties and temporal averages of patch transitions can also be computed (CASWELL and COHEN, 1991). For example, the local diversity also known as alpha diversity, measured by the expected number of species per patch is

$$\alpha = y_1 + y_2 + 2y_3,$$

and the variance in alpha diversity

$$V(\alpha) = y_1 + y_2 + 4y_3 - \alpha^2$$

can be used to measure the spatial heterogeneity in the landscape.

Between patch or beta diversity quantifies the spatial heterogeneity in species composition. One of the simplest methods to compute beta diversity is with the entropy of the state frequency vector,

$$\beta = -\sum_{i=1}^{4} y_i \log(y_i).$$

Beta diversity is at the minimum when all patches contain the same density of species and grows when all different patches types are equally abundant (CASWELL and COHEN, 1991). In this work, our main interest is to quantify quantitative differences between the prevalence of HPV non-vaccine types in the presence and absence of vaccination. Therefore, our analysis focuses on the equilibrium state frequencies.

Since the transition matrix (2.4) is column-stochastic, the phase space for model (2.1), that is, the standard 3-simplex

$$\Delta^3 = \left\{ \mathbf{y} \in \mathbb{R}^4 \mid y_0 + y_1 + y_2 + y_3 = 1,\ y_i \geq 0,\ i = 0,1,2,3 \right\} \tag{2.5}$$

is invariant under system (2.1).

To investigate the existence and stability of the equilibrium points of the model (2.1), define the functions $g_i : \Delta^3 \to \mathbb{R}$ for $i = 1,2,3,4$ as

$$\begin{aligned}
g_0(\mathbf{y}) &= (1-C_1)(1-C_2)y_0 + p_1 y_1 + p_2 y_2 + p_1 p_2 y_3 - y_0, \\
g_1(\mathbf{y}) &= C_1(1-C_2)y_0 + \bar{p}_1(1-C_2)y_1 + \bar{p}_1 p_2 y_3 - y_1, \\
g_2(\mathbf{y}) &= (1-C_1)C_2 y_0 + \bar{p}_2(1-C_1)y_2 + p_1 \bar{p}_2 y_3 - y_2, \\
g_3(\mathbf{y}) &= C_1 C_2 y_0 + \bar{p}_1 C_2 y_1 + \bar{p}_2 C_1 y_2 + \bar{p}_1 \bar{p}_2 y_3 - y_3.
\end{aligned} \tag{2.6}$$

Clearly, a vector $\mathbf{y}^* \in \Delta^3$ is an equilibrium point of the model (2.1) if and only if

$$g_i(\mathbf{y}^*) = 0, \quad i = 0,1,2,3. \tag{2.7}$$

Moreover, the variable y_i increases over time if $g_i > 0$, decreases if $g_i < 0$, and does not change if $g_i = 0$. Thus, the behavior of the solution of the model (2.1) in the simplex (2.5) is determined by the sign of the functions g_i.

If we set (2.6) equal to zero, it is easy to see that (2.1) always has a disease-free equilibrium

$$E_0 = (1,0,0,0), \tag{2.8}$$

that is, an equilibrium point in which none of the species is present.

In order to compute the within-host basic reproduction number $\mathscr{R}_0$ for the model (2.1), we adapted the method of Van den Driessche and Watmough (2002) to compute $\mathscr{R}_0$ in compartmental epidemic models using the next-generation matrix.

First, we need to write the variation in the proportions of infected patches per unit of time in the following way:

$$y_i(t+1) - y_i(t) = \mathscr{F}_i(\mathbf{y}) - \mathscr{V}_i(\mathbf{y}), \quad i = 1,2,3, \tag{2.9}$$

where $\mathscr{F}_i$ is the rate of appearance of new patches in state i, and $\mathscr{V}_i$ incorporates the remaining transitional terms, namely disease progression and recovery. For our model, these functions have the following form:

$$\begin{aligned}
\mathscr{F}_1 &= C_1(1-C_2)y_0, & \mathscr{V}_1 &= y_1 - \bar{p}_1(1-C_2)y_1 - \bar{p}_1 p_2 y_3,\\
\mathscr{F}_2 &= (1-C_1)C_2 y_0, & \mathscr{V}_2 &= y_2 - \bar{p}_2(1-C_1)y_2 - p_1\bar{p}_2 y_3,\\
\mathscr{F}_3 &= C_1C_2y_0 + \bar{p}_1C_2y_1 + \bar{p}_2C_1y_2, & \mathscr{V}_3 &= y_3 - \bar{p}_1\bar{p}_2y_3.
\end{aligned}$$

Next, we define the matrix of new infections

$$\mathbf{F} = \left[\frac{\partial \mathscr{F}_i(E_0)}{\partial y_j}\right] = \begin{bmatrix} (1-\varepsilon)d_1 & 0 & (1-\varepsilon)d_1 \\ 0 & (1-\sigma)d_2 & (1-\sigma)d_2 \\ 0 & 0 & 0 \end{bmatrix}, \tag{2.10}$$

and the matrix for transitions among states

$$\mathbf{V} = \left[\frac{\partial \mathscr{V}_i(E_0)}{\partial y_j}\right] = \begin{bmatrix} p_1 & 0 & -\bar{p}_1p_2 \\ 0 & p_2 & -p_1\bar{p}_2 \\ 0 & 0 & 1-\bar{p}_1\bar{p}_2 \end{bmatrix}. \tag{2.11}$$

Note that **F** is a non-negative matrix and **V** is a non-singular M-matrix. Finally, we define $\mathscr{R}_0$ as the spectral radius of the next-generation matrix $\mathbf{K} = \mathbf{F}\mathbf{V}^{-1}$ which is given by

$$\mathbf{K} = \begin{bmatrix} \dfrac{(1-\varepsilon)d_1}{p_1} & 0 & \dfrac{(1-\varepsilon)d_1}{p_1} \\ 0 & \dfrac{(1-\sigma)d_2}{p_2} & \dfrac{(1-\sigma)d_2}{p_2} \\ 0 & 0 & 0 \end{bmatrix} \tag{2.12}$$

thus

$$\mathscr{R}_0 = \max\{\mathscr{R}_1, \mathscr{R}_2\} \tag{2.13}$$

where

$$\mathscr{R}_1 = \frac{(1-\varepsilon)d_1}{p_1} \quad \text{and} \quad \mathscr{R}_2 = \frac{(1-\sigma)d_2}{p_2} \tag{2.14}$$

are the reproduction numbers of vaccine and non-vaccine types, respectively. The reproduction number $\mathscr{R}_i$ gives the average number of secondary virus particles that one virus of species S_i will produce in a completely susceptible target cell population Martcheva (2015).

The following result establishes the relationship between the within-host basic reproduction number and the stability of the disease-free equilibrium E_0.

Theorem 2.3.1. *The disease-free equilibrium $E_0 = (1,0,0,0)$ of the system* (2.1) *is locally asymptotically stable if the within-host basic reproduction number $\mathscr{R}_0$ is less than* 1*, that is, if*

$$\mathscr{R}_1 < 1, \quad \textit{and} \quad \mathscr{R}_2 < 1. \tag{2.15}$$

The disease-free equilibrium is unstable if at least one of the above inequalities is reversed.

Proof. Model (2.1) is a four-dimensional discrete time dynamical system of the form

$$\mathbf{y}(t+1) = f(\mathbf{y}(t)), \tag{2.16}$$

where the function $f : \Delta^3 \to \Delta^3$ has components

$$f_i(\mathbf{y}) = \sum_{j=1}^{4} a_{ij}(\mathbf{y}) y_{j-1}, \qquad i = 1,2,3,4. \tag{2.17}$$

However, since $\mathbf{y} \in \Delta^3$ i.e. $y_0 + y_1 + y_2 + y_3 = 1$, defining the function $\bar{f} = (\bar{f}_1, \bar{f}_2, \bar{f}_3)$ with

$$\bar{f}_{i-1}(y_1, y_2, y_3) = f_i(1 - (y_1 + y_2 + y_3), y_1, y_2, y_3), \quad i = 2,3,4, \tag{2.18}$$

we can reduce (2.16) to the three-dimensional system

$$\bar{\mathbf{y}}(t+1) = \bar{f}(\bar{\mathbf{y}}(t)), \quad \bar{\mathbf{y}}(t) = (y_1(t), y_2(t), y_3(t)). \tag{2.19}$$

The disease-free equilibrium $E_0 = (1,0,0,0)$ of the system (2.16) is equivalent to the equilibrium $\bar{E}_0 = (0,0,0)$ of the system (2.19). Therefore, we can determine the stability of E_0 analyzing the stability of $\bar{E}_0$.

For system (2.19), the derivative of $\bar{f}$ evaluated at the equilibrium $\bar{E}_0$ is given by the following matrix

$$D\bar{f}(\bar{E}_0) = \begin{pmatrix} (1-\varepsilon)d_1 + \bar{p}_1 & 0 & \bar{p}_1 p_2 + (1-\varepsilon)d_1 \\ 0 & (1-\sigma)d_2 + \bar{p}_2 & p_1\bar{p}_2 + (1-\sigma)d_2 \\ 0 & 0 & \bar{p}_1\bar{p}_2 \end{pmatrix}. \tag{2.20}$$

The equilibrium $\bar{E}_0$ is locally asymptotically stable if the spectral radius of the above matrix is less than 1, that is, $\rho(D\bar{f}(\bar{E}_0)) < 1$. Since $D\bar{f}(\bar{E}_0)$ is a triangular matrix and $|\bar{p}_1\bar{p}_2| < 1$, it is clear that $\rho(Df(E_0)) < 1$ if and only if $\mathscr{R}_0 < 1$. □

Besides E_0, the model (2.1) also has another boundary equilibrium points in which one of the species is present while the other is absent. The following results state this more precisely.

Theorem 2.3.2. *In the absence of the species S_2, if $\mathscr{R}_1 > 1$, the model* (2.1) *has an asymptotically stable boundary equilibrium of the form*

$$E_1 = (1 - y_1^*, y_1^*, 0, 0) \tag{2.21}$$

where y_1^* is the only positive solution of

$$(1 - e^{-(1-\varepsilon)d_1 y_1})(1 - y_1) - p_1 y_1 = 0 \tag{2.22}$$

such that $y_1^* \in (0,1)$. In other words, the solution $\mathbf{y}(t) = (y_0(t), y_1(t), y_2(t), y_3(t))$ of system (2.1) *with initial condition $\mathbf{y}_0 = (y_0(0), y_1(0), 0, 0) \in \Delta^3$, $\mathbf{y}_0 \neq E_0$, satisfies $\mathbf{y}(t) \to E_1$ as $t \to \infty$ if and only if $\mathscr{R}_1 > 1$.*

Proof. In the absence of the species S_2, that is, when $y_2(t) = 0$, coinfections are not possible, thus $y_3(t) = 0$ for all t. Under these conditions, if we set (2.6) equal to zero, we get that the

equilibrium point satisfy the following system of equations

$$(e^{-(1-\varepsilon)d_1 y_1})y_0 + p_1 y_1 = y_0 \tag{2.23}$$
$$(1-e^{-(1-\varepsilon)d_1 y_1})y_0 + \bar{p}_1 y_1 = y_1. \tag{2.24}$$

Because $y_0 = 1 - y_1$, equations (2.23) and (2.24) are equivalent. Hence, we only analyze (2.24) in the form

$$g_1(1-y_1, y_1, 0, 0) = (1-e^{-(1-\varepsilon)d_1 y_1})(1-y_1) - p_1 y_1 = 0. \tag{2.25}$$

Define $h(y_1) \equiv g_1(1-y_1, y_1, 0, 0)$. It is not difficult to see that h is a concave function such that $h(0) = 0$ and $h(1) < 0$. Therefore, the equation (2.25) has a unique positive solution $y_1^* \in (0,1)$, if and only if

$$h'(0) = (1-\varepsilon)d_1 - p_1 > 0. \tag{2.26}$$

Clearly, the condition (2.26) is fulfilled if and only if $\mathscr{R}_1 > 1$. In addition, h is positive in $(0, y_1^*)$ and negative in $(y_1^*, 1)$. □

The analogous result that establishes the existence and stability of the boundary equilibrium in which S_2 is present and S_1 is absent is stated in the next theorem. We omit the proof since it follows the same argument of the previous proof.

Theorem 2.3.3. *In the absence of the species S_1, if $\mathscr{R}_2 > 1$, the model* (2.1) *has an asymptotically stable boundary equilibrium of the form*

$$E_2 = (1-y_2^*, 0, y_2^*, 0) \tag{2.27}$$

where y_2^* is the only positive solution of

$$(1-e^{-(1-\sigma)d_2 y_2})(1-y_2) - p_2 y_2 = 0 \tag{2.28}$$

such that $y_2^* \in (0,1)$. In other words, the solution $\mathbf{y}(t) = (y_0(t), y_1(t), y_2(t), y_3(t))$ of the system (2.1) *with initial condition $\mathbf{y}_0 = (y_0(0), 0, y_2(0), 0) \in \Delta^3$, $\mathbf{y}_0 \neq E_0$, satisfies $\mathbf{y}(t) \to E_2$ as $t \to \infty$ if and only if $\mathscr{R}_2 > 1$.*

Conditions guaranteeing the existence of an interior equilibrium point are difficult to obtain by reason of the nonlinear dependence of C_i ($i = 1,2$) with respect to the frequency of the species. Nevertheless, numerical simulations indicate that if the reproduction numbers of both species are greater than 1, namely, $\mathscr{R}_1 > 1$ and $\mathscr{R}_2 > 1$, there is a unique endemic equilibrium in the interior of Δ^3 which is locally asymptotically stable.

2.4 Numerical results

In order to explore the dynamical behavior of the model, we performed multiple numerical simulations. Due to the uncertainty and the considerable variability of estimates of the parameters in the literature, for the numerical experiments, we vary our model parameters in ranges compatible with the natural history of HPV infection of the mucosal epithelia.

Some studies have estimated the persistence of HPV infection as a function of time and the clearance rate for some HPV types. For example, in Molano et al. (Molano et al., 2003), it was estimated that the median duration of a new HPV infection was 14.8 months for HR types and 11.1 months for LR types. In that study, HPV-16 had a significantly lower clearance rate than infections with LR types. HPV types phylogenetically related to HPV 16 (types 31, 33, 35, 52, 58) showed clearance rates intermediate between those of HPV-16 and LR HPV types. Other HR types, including HPV-18, did not show evidence of slower clearance rates compared with LR types. Since species S_1 includes types 16 and 18, we assume that the clearance rates for S_1 and S_2 are roughly the same. Thus, we posit that parameters p_1 and p_2, that represent the probability (per unit of time, that we choose to be one week) with which the immune system clears patches in states 1 and 2, respectively, satisfy $p_1, p_2 \in (0, 0.1]$.

Moreover, since types 16 and 18 are the most prevalent types among women (Bruni et al., 2010), it is rational to expect that $d_1 > d_2$ (to complement the analysis, we study the case $d_1 \leq d_2$ in the Appendix A). That is, HR vaccine types are better on average than HR non-vaccine types at the production and dispersal of new virions in infected patches. From an ecological point of view, if we consider that S_1 and S_2 are two species that live in the same ecological community (squamous epithelium) and compete for resources (basal cells), we could expect that S_1 is the dominant species in the absence of vaccination. Thus, we posit $d_1 \in (0, 1.5]$ and $d_2 \in (0, 0.5]$. Finally, since HPV vaccines have been shown to be highly effective (Stanley, 2010), under vaccine conditions, we set $\varepsilon = 0.9$.

To determine if HR non-vaccine HPV types can increase their niche after a vaccination scheme, we compare the prevalence of both vaccine and non-vaccine types for different scenarios related to vaccine conditions and the level of cross-protection σ. For each of the scenarios, we carried out $100,000$ simulations of the system (2.1) until in each of the simulations the vector of frequencies $\mathbf{y}(t)$ converged to a steady state $\mathbf{y}^*$. Then we quantified the results via histograms of the resulting density of the species at the steady state. The parameters p_i and d_i $(i = 1, 2)$ were sampled using uniform probability distribution in their respective range. The results of the experiments are shown in Figure 2.1. For the histograms, we split the interval $[0, 1]$ into 30 bins of the same length. Moreover, the vertical axis (observe that the scale is different for all the subfigures) indicates the relative frequency of occurrences in which the value of y_i^*, falls into a specific bin or interval.

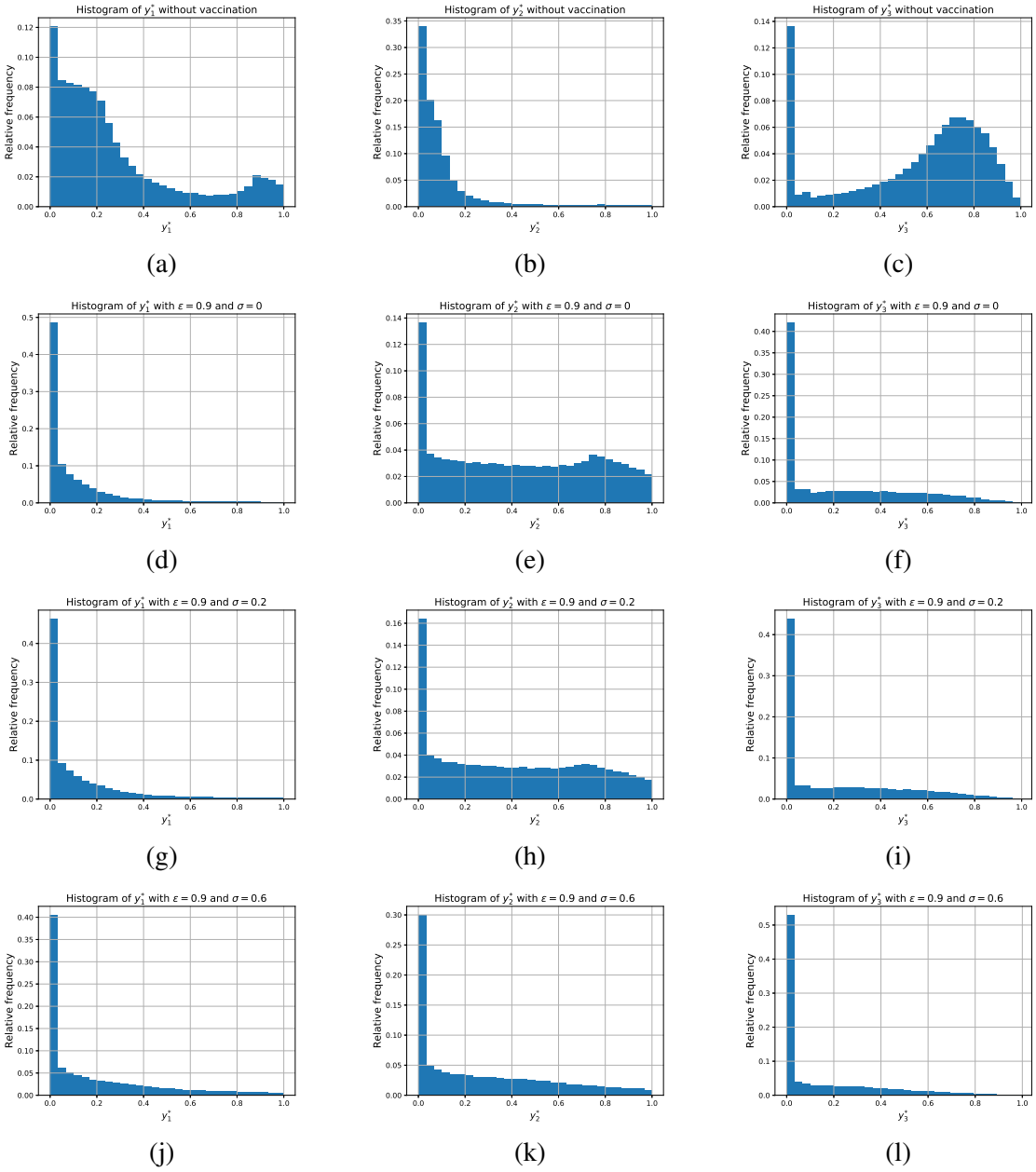

Fig. 2.1 Histograms for the state frequencies at the equilibrium of system (2.1). Columns (from left to right): (1) density of patches infected by S_1, (2) density of patches infected by S_2, (3) density of patches coinfected with S_1 and S_2. Rows (from top to bottom): (1) absence of vaccination i.e $\varepsilon = \sigma = 0$, (2) vaccination with no cross-protection i.e $\varepsilon = 0.9$, $\sigma = 0$, (3) vaccination with low cross-protection i.e $\varepsilon = 0.9$, $\sigma = 0.2$, (4) vaccination with high cross-protection i.e $\varepsilon = 0.9$, $\sigma = 0.6$. For (a)-(l), the rest of the parameters were sampled randomly in their respective intervals, $p_i \in (0, 0.1]$ $(i = 1, 2)$, and $d_1 \in (0, 1.5]$, $d_2 \in (0, 0.5]$.

In the first place, we study a scenario in which there is no vaccination, that is, the parameters ε and σ are both equal to zero. The model outcome in these conditions is plotted in Figure 2.1 (a), (b), (c). In these subfigures, the density of patches infected with vaccine-types is greater than the density of patches infected with non-vaccine types. This is an expected result since we are assuming that in the absence of vaccination S_1 is a better competitor than S_2. Moreover, the fraction of patches infected by S_1 is highly concentrated in the interval $[0, 0.2]$ and the fraction infected by S_2 in the interval $[0, 0.1]$. In addition, the first bin, that is, the interval $[0, 1/30]$ is the bin with the highest relative frequency; hence, there is also a high probability of extinction. This seems to indicate that even in the absence of vaccination the prevalence of the species is low, however, in the histogram for coinfections (Figure 2.1 (c)), one can see that the fraction of patches in the state 3 could be bigger than 0.6. Therefore, the total percentage of infected patches in the absence of vaccination might be around 90%.

In the second scenario, we analyze the effects of vaccination when there is no cross-protection, i.e, $\varepsilon = 0.9$ and $\sigma = 0$ (Figure 2.1 (d), (e), (f)). Comparing Figure 2.1 (a) and (d), it is clear that the application of the vaccine reduces significantly the infection by vaccine-types. Indeed, the relative frequency of the first bin of the histogram in Figure 2.1 (d) is nearby 0.5, which implies that there is a high probability of extinction for vaccine-types. For non-vaccine types, if we compare Figure 2.1 (e) and (b), we observe that there is a big increase in the infection with non-vaccine types. In fact, if we omit the first bin in the histogram in Figure 2.1 (e), the rest of the bins have nearly the same relative frequency. Thus, non-vaccine types have a strong possibility of infecting more than 50% of the healthy patches. Furthermore, the fraction of coinfected patches y_3^* in this case (Figure 2.1 (f)) is considerably lower than in the absence of vaccination, (Figure 2.1 (c)). In summary, for this scenario, the application of the vaccine would increase the prevalence of non-vaccine types.

In the third place, we consider vaccination with low cross-protection, that is, $\varepsilon = 0.9$ and $\sigma = 0.2$ (Figure 2.1 (g), (h), (i)). The results indicate that the outcome for this scenario is almost the same as the case without cross-protection. Lastly, we analyze vaccination with high cross-protection i.e $\varepsilon = 0.9$ and $\sigma = 0.6$ (Figure 2.1 (j), (k), (l)). Again, the application of the vaccine cause a reduction of vaccine-types, this is observed comparing y_1^* in Figure 2.1 (j) against y_1^* in Figure 2.1 (a). Nevertheless, infection by non-vaccine types (Figure 2.1 (k)) is less in relation with the cases of low (Figure 2.1 (h)) and no cross-protection (Figure 2.1 (e)). Finally, the fraction of coinfected patches is the lowest for this case. This is deduced by seeing that the relative frequency for the bin $[0, 1/30]$ is greater than 0.5 in the histogram in Figure 2.1 (l).

The above results suggest that cross-protection plays an important role to determine the possibility of vaccine-induced strain replacement. Therefore, we analyze how the structure of the solution depends on the parameter σ using bifurcation analysis. Consistent with the literature, we fixed $\varepsilon = 0.9$, so the vaccine is 90% effective at preventing infection by vaccine types. We fix the other parameters with the following values: $p_1 = 0.1$, $p_2 = 0.1$, $d_1 = 1.5$, $d_2 = 0.3$; and vary σ in the interval $0 \leq \sigma < \varepsilon$. Then, we check numerically the fraction of patches infected by vaccine $y_1^*(\sigma)$ and non-vaccine $y_2^*(\sigma)$ types at the equilibrium level as functions of σ. The results are shown in Figure 2.2.

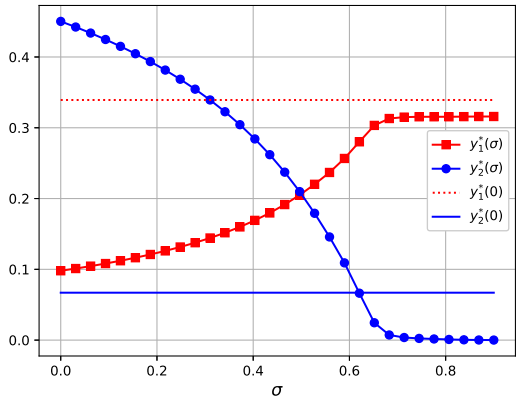

Fig. 2.2 Fraction of patches infected by vaccine $y_1^*(\sigma)$ and non-vaccine $y_2^*(\sigma)$ types as functions of σ at the equilibrium level under vaccine conditions i.e $\varepsilon = 0.9$. The straight lines $y_1^*(0)$ and $y_2^*(0)$ represent the fraction of patches infected by vaccine types and non-vaccine types, respectively, at the steady state when there is no vaccination i.e $\varepsilon = 0$ and $\sigma = 0$. The rest of parameters are fixed with the following values: $p_1 = 0.1$, $p_2 = 0.1$, $d_1 = 1.5$, $d_2 = 0.3$.

In order to have a clear way to compare the prevalence under vaccine conditions for different levels of cross-protection against the case without vaccination, we add two straight lines $y_1^*(0)$ and $y_2^*(0)$ to Figure 2.2. These lines represent the fraction of patches infected by vaccine types and non-vaccine types, respectively, at the steady state when there is no vaccination, that is, with $\varepsilon = 0$ and $\sigma = 0$. Parameters p_i and d_i for these straight lines are the same that for $y_1^*(\sigma)$ and $y_2^*(\sigma)$. From Figure 2.2, we observe that $y_1^*(\sigma)$ is a non-decreasing function of σ. Hence, from an ecological point of view, cross-protection affects positively vaccine-types. On the other hand, $y_2^*(\sigma)$ is a non-increasing function of σ. In consequence, the infection by non-vaccine types is low for high levels of cross-protection. Moreover, $y_1^*(\sigma) < y_1(0)$ for all the values of σ in its range. This implies that regardless of the level of cross-protection, the fraction of patches infected by S_1 under vaccine conditions is always less than in the absence of vaccination. Whereas, $y_2^*(\sigma) > y_2(0)$ if and only if $0 \leq \sigma < 0.62$. Thus, if $\sigma < 0.62$ there is an increase in the prevalence of infection by S_2 in comparison to

the case without vaccination. Yet, if $\sigma > 0.62$, the fraction of patches infected by S_2 is less in comparison to the case without vaccination.

2.5 Discussion

Pathogen evolution is subject to natural selection at numerous levels. For instance, pathogens compete for target cells within infected hosts but also attempt to infect more individuals at the population level. Inside a host, the immune system imposes natural selection on pathogen populations. However, the application of vaccines can modify this selection by attacking specific pathogen strains. Thus, under certain conditions, strains not targeted by the vaccine may increase in prevalence. This phenomenon has been called vaccine-induced pathogen strain replacement (Martcheva et al., 2008). Generally speaking, strain replacement is the phenomenon of substitution through time of one or more initially dominant strains of a pathogen by another strain or strains.

Many countries have implemented vaccination against infection by specific HPV strains. In Mexico, there are currently two vaccines available to prevent HPV infection: a bivalent vaccine against HPV strains 16 and 18, and a quadrivalent that protects against strains 16, 18, 6, and 11. In other countries, there is also a nonavalent vaccine directed against the four strains of the quadrivalent vaccine and five additional high-risk strains: 31, 33, 45, 52, and 58 (Damm et al., 2017). However, there are still some high-risk HPV strains not targeted by the vaccines, and there is controversy over the possibility of the emergence of non-targeted types after a vaccination program. In other words, the removal of HPVs 16 and 18 and other vaccine-targeted types as the result of vaccination may result in a positive selection pressure for other high-risk non-vaccine HPV types, leading to an increase in transmission of the latter.

In this work, we propose a metapopulation model at the within-host level to evaluate the potential of HPV strain-replacement for different levels of cross-protection. Our model considers high-risk types and classify them into two groups: vaccine-targeted types ('vaccine types'), and vaccine-non-targeted types ('non-vaccine types'). According to basic ecological principles, if HPV types compete for resources such as target cells, the application of a vaccine that prevents infections by one type may promote the emergence of the other types. On the contrary, if the interactions among types are synergistic, a vaccination scheme may reduce not only the prevalence of vaccine-types but also the prevalence of the non-vaccine types. At present, it is still unclear how the broad diversity of HPV types interact inside a host. Here, we analyzed independence among types as the main ecological interaction since it is one of the most accepted hypotheses regarding HPVs interactions (Murall et al., 2014).

The general argument in the literature is that the existence of natural type competition is a necessary condition for type replacement (Tota et al., 2013). Therefore, several studies evaluating the possibility of HPV type replacement have focussed on finding competitive interactions among HPV types (Chaturvedi et al., 2011; Mollers et al., 2014; Tota et al., 2016). Nevertheless, even in the absence of competition mechanisms, the results of this study show that type replacement is viable at the within-host level if the degree of cross-protection induced by the vaccine is not high enough. Type replacement has been observed following vaccination in Durham et al. (Durham et al., 2012). In this study, the authors reported that the prevalence of HPV types phylogenetically related to HPV-16 (types 39, 45, 59, and 68) and HPV-18 (types 39, 45, 59, and 68) increased by 50% and 29% following vaccination, respectively. However, a number of epidemiological studies have shown only occasional increases in the prevalence of HPV types not targeted by the vaccine, suggesting a low probability of type replacement (Kahn et al., 2012; Mesher et al., 2016; Saccucci et al., 2018). Hence, monitoring for possible type replacement remains a very important task.

For the particular case of our model, the degree of cross-protection must be greater than 62% to avoid an increase in the prevalence of non-vaccine types in comparison to the case in which there is no vaccination. However, although the currently available HPV vaccines provide more than 90% of protection against infection with its targeted types, these vaccines based on virus-like particles of the major capsid protein L1 do not generate a significant degree of cross-protection (Tumban et al., 2011). Nevertheless, the negative impact of type replacement in the health system is somehow mitigated due to the fact that infection with non-vaccine types implies lower cervical cancer risk than infection with vaccine-types.

The patch dynamics model presented here is simple and only considers two spatial scales: local within-patch interactions and the dynamics of the metapopulation as a whole. Many natural extensions are possible to improve the realism of the model. For instance, instead of grouping HPVs as vaccine and non-vaccine types, the phylogenetic clades based on the L1 sequences of HPV can be used to have a finer classification. In this regard, since high-risk strains targeted only by the nonavalent vaccine were considered non-vaccine types, examining scenarios for the nonavalent vaccine is still needed. Moreover, we postulated that the immune system clears infected patches with a constant probability, yet, the clearance rates for HPV strains are not constant in time. In addition, it is also possible to link this model with an epidemic model in order to study pathogen evolution and the reciprocal feedback between within- and between-host dynamics. Currently, we are working on these extensions and the study of other ecological scenarios besides the case of independence among HPV strains.

Appendix A

HPV types 16 and 18 are the most prevalent types in cervical cancer globally but not necessarily the most common in early, usually asymptomatic, infections. Moreover, the distribution of HPV types is known to vary across different geographical regions. Therefore, it is instructive to analyze the model outcome if the $d_1 > d_2$ assumption is relaxed.

In order to determine if vaccine-induced type replacement is possible when $d_1 \leq d_2$, we compare the prevalence of both vaccine and non-vaccine types for two scenarios: (i) no vaccination ($\varepsilon = 0$, $\sigma = 0$), and (ii) vaccination with low cross-protection ($\varepsilon = 0.9$, $\sigma = 0.2$). As in the main text, for each of the scenarios, we carried out $100,000$ simulations of the system (2.1) until in each of the simulations the vector of frequencies $\mathbf{y}(t)$ converged to a steady state $\mathbf{y}^*$. Then, we quantify the results via histograms of the resulting density of the species at the steady state (see Figure 2.3). Here, the parameters d_i ($i = 1,2$) were sampled using uniform probability distribution in the interval $d_i \in [0,1]$.

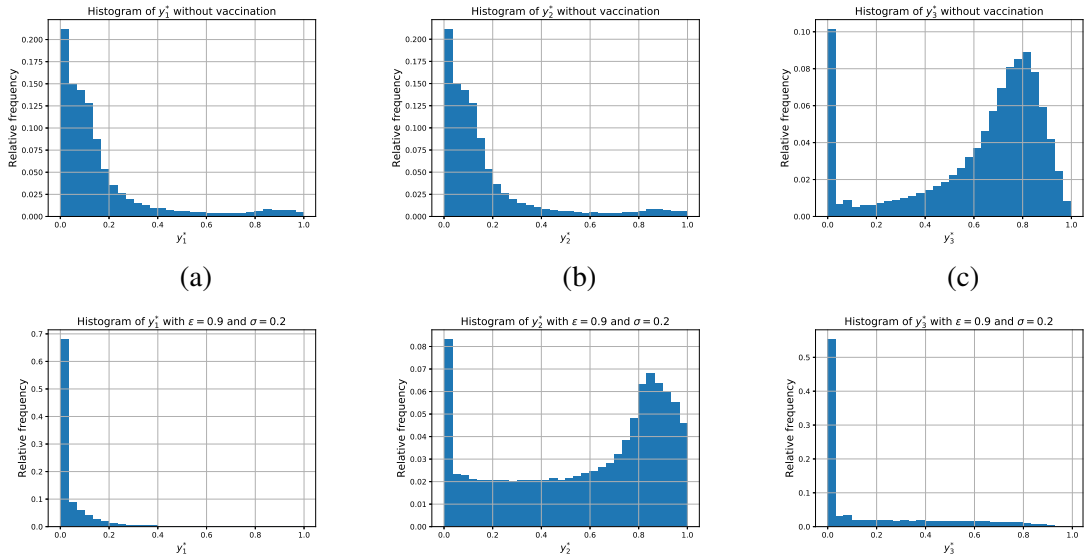

Fig. 2.3 Histograms for the state frequencies at the equilibrium of system (2.1). Columns (from left to right): (1) density of patches infected by S_1, (2) density of patches infected by S_2, (3) density of patches coinfected with S_1 and S_2. Rows (from top to bottom): (1) absence of vaccination i.e $\varepsilon = \sigma = 0$, (2) vaccination with low cross-protection i.e $\varepsilon = 0.9$, $\sigma = 0.2$. For (a)-(f), the parameters were sampled randomly in the following intervals, $p_i \in (0, 0.1]$, and $d_i \in (0,1]$ ($i = 1,2$).

If there is no vaccination, the density of patches infected by S_1 (Figure 2.3 (a)) and S_2 (Figure 2.3) is identical. This result is logical since the parameters d_1 and d_2 have the same

range. The fraction of coinfected patches, in this case, can be very high (Figure 2.3 (c)). Following vaccination, infection by vaccine-types decreases significantly (Figure 2.3 (d)) and there is a clear increase in the density of patches infected by non-vaccine types (Figure 2.3). Moreover, the fraction of coinfected patches are considerably lower than in the absence of vaccination (Figure 2.3 (f)). Therefore, the result that type replacement is possible when cross-protection is low (which is the more realistic case) does not depend on the dispersal coefficients d_1 and d_2.

Chapter 3

Optimal Control Against the Human Papillomavirus

3.1 Introduction

Human papillomavirus (HPV) is the leading etiological factor for the development of cervical cancer. According to the World Health Organization (WHO) report, cervical cancer is the fourth most frequent cancer in women with approximately 570,000 new cases reported in 2018. This fact makes the design, implementation, and maintenance of effective preventing policies against cervical cancer a highly relevant public health problem. Moreover, HPV is the most common sexually transmitted infection globally and most people are infected at some point in their lives. This consideration motivates research on the design and development of cost-effective vaccination and screening programs against HPV infection.

An HPV infection is caused by human papillomavirus, a DNA virus from the papillomavirus family, of which over 170 types are known. More than 40 types are transmitted through sexual contact and infect the anus and genitals. These types are typically spread by sustained direct skin-to-skin contact, with vaginal and anal sex being the most common methods. Other HPV types can cause common warts like hand warts and plantar warts on the feet but these are not sexually transmitted. Most people with HPV have no symptoms and feel totally fine, so they usually do not even know they are infected. However, although most genital HPV infections are not harmful at all and go away on their own, some infections persist and can cause cervical cancer. Risk factors for persistent genital HPV infections, which increases the risk for developing cancer, include early age of first sexual intercourse, multiple partners, smoking, and immunosuppression.

On October 5th of 2018, the US Food and Drug Administration (FDA) approved the nonavalent vaccine Gardasil-9 against HPV infection for use in women and men aged 27 to 45 (FDA, 2018). Earlier, the FDA approved the vaccine for persons between the ages of 9 to 26. Gardasil-9 protects against HPV types 6, 11, 16, and 18 (that are already targeted by the quadrivalent HPV vaccine Gardasil) and against the next five most common oncogenic viral types, namely, HPV 31, 33, 45, 52 and 58. These nine HPV types are responsible for the majority of HPV-associated diseases (Brisson et al., 2016). In addition to the nonavalent and quadrivalent vaccines, there is also an FDA-approved bivalent vaccine (Cervarix) that targets HPV types 16 and 18.

The introduction of HPV vaccines is changing the epidemiology of cervical cancer and other HPV-associated diseases each year. Since HPV-associated morbidity and mortality are usually considerably higher in females than in males, in the majority of countries the primary target group of HPV vaccination programs is adolescent school girls aged 9–14 (Seto et al., 2012). However, considering that Gardasil-9 has been licensed for a broader age range in both males and females, it is essential to analyze the potential health benefits of extending vaccination to males, as well as older individuals, versus a higher economic cost of such programs.

To examine the dynamics of HPV spread and control, numerous mathematical models have been proposed (Alsaleh and Gumel, 2014; Bogaards et al., 2011; Elbasha and Dasbach, 2010; Elbasha et al., 2007; Garnett et al., 2006; Guerrero et al., 2015; Kim and Goldie, 2009; Malik et al., 2013; Newall et al., 2007; Saldaña and Barradas, 2019; Smith et al., 2011). While these and other recent studies analyzed different strategies for HPV control and brought important insight into the problem, the majority of them did not take into account the optimality of these interventions. The study of optimality, however, is of particular relevance in the allocation of limited public health resources. In this context, the application of optimal control theory has proven to be an important tool for evaluating and optimizing various detection, prevention, therapy, vaccination, and other intervention programs (Sharomi and Malik, 2017).

So far, to the best of the authors' knowledge, for the case of HPV infection only a few studies have been done using the optimal control framework to assess the impact of vaccination programs (Brown and White, 2011; Malik et al., 2016). Brown and White (Brown and White, 2011) explored how to target vaccination in the UK. This study highlights the importance of including a catch-up vaccination policy in order to control the spread of the infection. In a recently published paper, Malik et al (Malik et al., 2016) analyzed the optimal control strategies for a vaccination program administering the bivalent, quadrivalent and nonavalent HPV vaccines to the female population. In particular, they explored scenarios

where the three vaccines are used simultaneously compared with the case where the bivalent and quadrivalent vaccines were initially used and then, during the program, one or both of them are replaced by the nonavalent vaccine.

The purpose of this work is to assess the cost-effectiveness of the most practical interventions policies used against HPV. We consider a two-sex epidemic model consisting of ordinary differential equations based on the susceptible-infected-vaccinated-susceptible (SIVS) compartmental structure. The model includes vaccination in both females and males where we distinguish between vaccines given before and after sexual initiation. Moreover, we also consider females' screening. We prove that our model is mathematically and biologically well-posed. Important threshold quantities, namely, the basic and the effective reproduction numbers are used to determine the stability of the disease-free equilibrium. Then, we define a suitable cost function and a cost-effectiveness ratio to evaluate the performance of health care interventions against HPV. Furthermore, we apply the theory of optimal control to obtain time-dependent health care interventions and investigate the potential public health impact of HPV vaccination programs.

3.2 Model formulation

In this study, we propose and study a compartmental model for the transmission dynamics of the HPV types targeted by the nonavalent vaccine Gardasil-9. The model classifies the hosts' population at time t denoted by $N(t)$ according to gender and infection status. We subdivide the total female population $N_f(t)$ into four mutually exclusive compartments: unvaccinated susceptibles $S_f(t)$, vaccinated susceptibles $V_f(t)$, and infectious females unaware $U_f(t)$ and aware $I_f(t)$ of their infection, thus

$$N_f(t) = S_f(t) + V_f(t) + U_f(t) + I_f(t). \tag{3.1}$$

The total male population $N_m(t)$ consist of three compartments: unvaccinated susceptibles $S_m(t)$, vaccinated susceptibles $V_m(t)$ and infectious males $I_m(t)$, so that

$$N_m = S_m(t) + V_m(t) + I_m(t). \tag{3.2}$$

We assume that individuals enter the sexually active population as singles at a constant rate Λ_k ($k = f, m$). Females and males leave the population by death or ceasing sexual activity at per capita rates μ_f and μ_m, respectively. In this study, we distinguish between vaccination prior and after sexual initiation. In particular, a fraction w_1 of females and a fraction w_2 of males are vaccinated before they enter the sexually active class and thus are recruited into

their vaccinated compartment. Moreover, the susceptible sexually active females and males are vaccinated at rates u_1 and u_2 per unit of time, respectively. The vaccine reduces the force of infection by a factor $0 \leq \varepsilon \leq 1$; thus, the vaccine is completely effective when $\varepsilon = 0$ and ineffective when $\varepsilon = 1$. Therefore $1-\varepsilon$ is the vaccine effectiveness. The vaccine-induced immunity wanes at a rate θ. Both males and females can clear the infection naturally with per capita rates γ_m and γ_f, respectively. No permanent immunity is assumed after that.

Susceptible females become infected at a rate β_m following effective contact with an infectious male. After the acquisition of HPV infection, a fraction p of the infected females may develop symptoms and become aware of their infection entering the $I_f(t)$ class. The remaining infected females do not realize their infection and move to the unaware class $U_f(t)$. However, the screening program may allow the unaware infected females to detect their infection at a rate α.

Susceptible males can be infected by unaware infected females $U_f(t)$ at a rate β_f and by aware infected females $I_f(t)$ at a rate $\tilde{\beta}_f$. We assume that $0 < \tilde{\beta}_f < \beta_f$ since a female conscious of her infection can take precautions like condom use to reduce the possibility of transmission. Since HPV infection is transmitted (in most cases) sexually, we model the transmission via the standard incidence (Martcheva, 2015).

The model resulting from these assumptions is governed by the following system of differential equations:

$$
\begin{aligned}
\dot{S}_f &= (1-w_1)\Lambda_f - \beta_m S_f \frac{I_m}{N_m} - (u_1+\mu_f)S_f + \gamma_f(U_f+I_f) + \theta V_f,\\
\dot{U}_f &= \left(S_f + \varepsilon V_f\right)(1-p)\beta_m \frac{I_m}{N_m} - (\gamma_f+\alpha+\mu_f)U_f,\\
\dot{I}_f &= \left(S_f + \varepsilon V_f\right) p\beta_m \frac{I_m}{N_m} + \alpha U_f - (\gamma_f+\mu_f)I_f,\\
\dot{V}_f &= w_1\Lambda_f + u_1 S_f - \varepsilon\beta_m V_f \frac{I_m}{N_m} - (\mu_f+\theta)V_f,\\
\dot{S}_m &= (1-w_2)\Lambda_m - \left(\beta_f \frac{U_f}{N_f} + \tilde{\beta}_f \frac{I_f}{N_f}\right) S_m - (u_2+\mu_m)S_m + \gamma_m I_m + \theta V_m,\\
\dot{I}_m &= \left(\beta_f \frac{U_f}{N_f} + \tilde{\beta}_f \frac{I_f}{N_f}\right)(S_m + \varepsilon V_m) - (\gamma_m+\mu_m)I_m,\\
\dot{V}_m &= w_2\Lambda_m - \left(\beta_f \frac{U_f}{N_f} + \tilde{\beta}_f \frac{I_f}{N_f}\right)\varepsilon V_m + u_2 S_m - (\mu_m+\theta)V_m,
\end{aligned}
\tag{3.3}
$$

Here all the parameters are assumed to be non-negative. The intervention measures, namely, the screening and vaccination rates will be called controls and denoted by vector $c = (w_1, w_2, u_1, u_2, \alpha)$.

Before going any further, we need to mention that our model, as any other, is limited and simplifies reality in many respects. This simplification is achieved by making some assumptions that can make the model feasible for mathematical analysis. First, we are assuming that the screening tests are 100% effective. Besides, both, the HPV test and the Pap test are valid screening methods. The HPV test looks for cervical infection by high-risk types and the Pap test is used to find cell changes or abnormal cells which may be pre-cancer. Yet, since both tests can be done at the same time (with the same swab), in our modeling approach we do not make a distinction between both screening methods. Finally, the Center for Disease Control recommends a co-test every 5 years or a Pap test every 3 years. However, in this work, we first consider a constant screening rate α.

3.3 Mathematical analysis of the HPV model

3.3.1 Boundedness and positivity of the solutions

The following result shows that the usual boundedness, positiveness, and continuity of the solutions of system (3.3) hold in a biologically feasible region.

Proposition 3.3.1. *The feasible region* $\tilde{\Omega} = \left\{x \in \mathbb{R}^7_+ : N_k \leq \Lambda_k/\mu_k,\ k = f,m\right\}$ *where* $x = (S_f, U_f, I_f, V_f, S_m, I_m, V_m)^T$ *is the vector for the states variables, is positively-invariant and attracting with respect to the flow of system* (3.3).

Proof. From system (3.3), it is easy to note that the total population size for gender $k = f,m$ is governed by the equation

$$\dot{N}_k = \Lambda_k - \mu_k N_k.$$

Direct computation gives

$$N_k(t) = \left(N_k(0) - \frac{\Lambda_k}{\mu_k}\right) e^{-\mu_k t} + \frac{\Lambda_k}{\mu_k}. \tag{3.4}$$

Therefore, the total population may vary in time, but converges asymptotically to the value $N_k^* = \Lambda_k/\mu_k$.

On account of (3.4), if $N_k(0) \in \tilde{\Omega}$, then $N_k(t) \in \tilde{\Omega}$ for all $t > 0$. Hence, $\tilde{\Omega}$ is positively-invariant. Furthermore, $N_k(t) > \Lambda_k/\mu_k$ implies $\dot{N}_k(t) < 0$; hence the solution either enter $\tilde{\Omega}$ in finite time, or approach its equilibrium value N_k^* as $t \to \infty$. In consequence, the region $\tilde{\Omega}$ is attracting. Thus, system (3.3) is mathematically and epidemiologically well-posed in $\tilde{\Omega}$. □

3.3.2 Constant population and disease-free equilibria

A standard assumption in mathematical epidemiology is that the host population remains approximately constant over the time of an epidemic outbreak. For the majority of infectious diseases, the transmission happens on a time scale, which is fast compared to the time scale of demographic changes. Thus, the population could be considered as constant (Brauer and Castillo-Chavez, 2012).

In the following, we consider a constant population. In mathematical terms, we assume $\Lambda_k = r_k N_k$ ($k = f, m$), where the per capita recruitment rate, r_k, is equal to the per capita rate of ceasing sexual activity, μ_k. Please observe that $r_k N_k$ is the total number of individuals recruited into the sexually active population per unit of time. Moreover, without loss of generality, we consider a rescaling of our model assuming that $N_f = 1$ and $N_m = 1$. Then, the state variables are expressed as fractions of the populations of each gender and we can rewrite system (3.3) as follows:

$$\begin{aligned}
\dot{S}_f &= (1-w_1)\mu_f - \beta_m S_f I_m - (u_1+\mu_f)S_f + \gamma_f(U_f+I_f) + \theta V_f,\\
\dot{U}_f &= (S_f+\varepsilon V_f)(1-p)\beta_m I_m - (\gamma_f+\alpha+\mu_f)U_f,\\
\dot{I}_f &= (S_f+\varepsilon V_f)p\beta_m I_m + \alpha U_f - (\gamma_f+\mu_f)I_f,\\
\dot{V}_f &= w_1\mu_f + u_1 S_f - \varepsilon\beta_m V_f I_m - (\mu_f+\theta)V_f,\\
\dot{S}_m &= (1-w_2)\mu_m - (\beta_f U_f + \tilde{\beta}_f I_f)S_m - (u_2+\mu_m)S_m + \gamma_m I_m + \theta V_m,\\
\dot{I}_m &= (\beta_f U_f + \tilde{\beta}_f I_f)(S_m+\varepsilon V_m) - (\gamma_m+\mu_m)I_m,\\
\dot{V}_m &= w_2\mu_m - (\beta_f U_f + \tilde{\beta}_f I_f)\varepsilon V_m + u_2 S_m - (\mu_m+\theta)V_m.
\end{aligned} \tag{3.5}$$

The biologically feasible region for system (3.5) is

$$\Omega = \left\{x \in \mathbb{R}^7_+ : S_f + U_f + I_f + V_f = 1,\ S_m + I_m + V_m = 1\right\}. \tag{3.6}$$

We focus primarily on system (3.5) hereafter. Nevertheless, we have to stress that the equality of the per capita recruitment and ceasing sexual activity rates is just a matter of convenience and is not an assumption of importance for further analysis.

Model (3.5) always has a disease-free equilibrium state $E_\circ(c)$. To compute the coordinates of the disease-free equilibrium, we set the rates of change of all state variables equal to zero.

Solving the system of algebraic equations, we obtain $U_f^\circ(c) = I_f^\circ(c) = I_m^\circ(c) = 0$, and

$$S_f^\circ(c) = \frac{(1-w_1)\mu_f + \theta}{u_1 + \mu_f + \theta}, \quad V_f^\circ(c) = \frac{w_1\mu_f + u_1}{u_1 + \mu_f + \theta},$$
$$S_m^\circ(c) = \frac{(1-w_2)\mu_m + \theta}{u_2 + \mu_m + \theta}, \quad V_m^\circ(c) = \frac{w_2\mu_m + u_2}{u_2 + \mu_m + \theta}.$$

The coordinates of the equilibrium $E_\circ(c)$ depend on the magnitude of the control measures, namely, the screening and vaccination rates. Indeed, from the definition of $E_\circ(c)$ it is clear that $S_f^\circ(0) = 1$ and $S_m^\circ(0) = 1$. Therefore, in the absence of controls, at the disease-free equilibrium the total population remains fully susceptible as can be expected.

3.3.3 The reproduction numbers

Several risk factors and characteristics of communicable diseases may be of interest to public health officials in formulating responses to a possible disease outbreak. The basic reproduction number $\mathscr{R}_0$ is considered as one of the central and most often used metrics in the area of mathematical epidemiology (Heffernan et al., 2005). Historically, $\mathscr{R}_0$ was described as the average number of secondary infections that an infectious individual can generate in a totally susceptible population during his entire period of infectiousness (Diekmann et al., 1990). The definition of $\mathscr{R}_0$ assumes a fully susceptible population and, hence, control measures such as mass vaccination that reduce the number of susceptible individuals in the population should, technically not reduce the value of $\mathscr{R}_0$ (Delamater et al., 2019). Therefore, alongside to $\mathscr{R}_0$ we introduce the effective reproduction number, denoted here as $\mathscr{R}_e$, which is defined as the actual average number of secondary cases per a primary case (Nishiura and Chowell, 2009). $\mathscr{R}_e$ does not assume the complete susceptibility of the population; and, therefore, vaccination and other control measures could potentially reduce the value of $\mathscr{R}_e$. Consequently, in the presence of vaccination, the effective reproduction number can be a better metric for understanding the transmissibility of infectious diseases (Delamater et al., 2019).

Mathematically, both reproduction numbers can be computed via the next-generation operator introduced by Diekmann and his collaborators. Under this approach, it is necessary to study the subsystem that describes the production of new infections and changes in the state among the infected individuals (Saldaña and Barradas, 2018). The Jacobian matrix $\mathbf{J}$ of this subsystem at the disease-free equilibrium is decomposed as $\mathbf{J} = \mathbf{F} - \mathbf{V}$, where $\mathbf{F}$ is the transmission part and $\mathbf{V}$ describes changes in the infection status. The next-generation matrix is defined as $\mathbf{K} = \mathbf{F}\mathbf{V}^{-1}$, and $\mathscr{R}_0 = \rho(\mathbf{K})$, where $\rho(\cdot)$ denotes the spectral radius.

In the absence of controls, the infectious subsystem of (3.5) is

$$\begin{aligned}\dot{U}_f &= (1-p)\beta_m S_f I_m - (\gamma_f+\mu_f)U_f,\\ \dot{I}_f &= p\beta_m S_f I_m - (\gamma_f+\mu_f)I_f,\\ \dot{I}_m &= (\beta_f U_f + \tilde{\beta}_f I_f)S_m - (\gamma_m+\mu_m)I_m.\end{aligned}$$

Consequently,

$$\mathbf{F} = \begin{bmatrix} 0 & 0 & (1-p)\beta_m S_f^\circ(0) \\ 0 & 0 & p\beta_m S_f^\circ(0) \\ \beta_f S_m^\circ(0) & \tilde{\beta}_f S_m^\circ(0) & 0 \end{bmatrix}, \quad \mathbf{V} = \begin{bmatrix} \gamma_f+\mu_f & 0 & 0 \\ 0 & \gamma_f+\mu_f & 0 \\ 0 & 0 & \gamma_m+\mu_m \end{bmatrix}.$$

The product $\mathbf{FV}^{-1}$ gives us the following next-generation matrix:

$$\mathbf{K} = \begin{bmatrix} 0 & 0 & \dfrac{(1-p)\beta_m}{\gamma_m+\mu_m} \\ 0 & 0 & \dfrac{p\beta_m}{\gamma_m+\mu_m} \\ \dfrac{\beta_f}{\gamma_f+\mu_f} & \dfrac{\tilde{\beta}_f}{\gamma_f+\mu_f} & 0 \end{bmatrix}. \tag{3.7}$$

Hence, the basic reproduction number can be calculated as

$$\mathscr{R}_0 = \sqrt{\frac{\beta_m}{\gamma_m+\mu_m}\left(p\frac{\tilde{\beta}_f}{\gamma_f+\mu_f} + (1-p)\frac{\beta_f}{\gamma_f+\mu_f}\right)}. \tag{3.8}$$

For non-zero controls, the same method allows us to compute the effective reproduction number. Let $H_f(c) = S_f^\circ(c) + \varepsilon V_f^\circ(c)$ and $H_m(c) = S_m^\circ(c) + \varepsilon V_m^\circ(c)$. Then, we get the following next-generation matrix:

$$\tilde{\mathbf{K}}(c) = \begin{bmatrix} 0 & 0 & K_{13}(c) \\ 0 & 0 & K_{23}(c) \\ K_{31}(c) & K_{32}(c) & 0 \end{bmatrix}, \tag{3.9}$$

where

$$K_{13}(c) = \frac{(1-p)\beta_m H_f(c)}{\gamma_m + \mu_m}, \quad K_{23}(c) = \frac{p\beta_m H_f(c)}{\gamma_m + \mu_m},$$
$$K_{31}(c) = \left(\beta_f + \frac{\tilde{\beta}_f \alpha}{\gamma_f + \mu_f}\right) \frac{H_m(c)}{\gamma_f + \alpha + \mu_f}, \quad K_{32}(c) = \frac{\tilde{\beta}_f H_m(c)}{\gamma_f + \mu_f}.$$

The effective reproduction number is the spectral radius of $\tilde{\mathbf{K}}$, and is given by

$$\mathscr{R}_e(c) = \sqrt{\frac{\beta_m H_f(c)}{\gamma_m + \mu_m}\left[p\frac{\tilde{\beta}_f H_m(c)}{\gamma_f + \mu_f} + \frac{(1-p)}{\gamma_f + \alpha + \mu_f}\left(\beta_f H_m(c) + \alpha\frac{\tilde{\beta}_f H_m(c)}{\gamma_f + \mu_f}\right)\right]}. \tag{3.10}$$

The effective reproduction number, $\mathscr{R}_e(c)$, depends directly on the interventions intended to control the disease's spread. Further, note that $\mathscr{R}_e(\mathbf{0}) = \mathscr{R}_0$ and that $\mathscr{R}_0 < 1$ implies $\mathscr{R}_e(c) < 1$; but the opposite implication is not true.

To interpret the biological meaning of the effective reproduction number, we need the following components. During his infection period, $(\gamma_m + \mu_m)^{-1}$, an infectious male produces on average $\beta_m H_f(c)$ infections in females. Therefore,

$$T_m^f(c) = \frac{\beta_m H_f(c)}{\gamma_m + \mu_m}$$

is the infection transfer from the infectious males to females. An infectious female aware of her infection produces on average $\tilde{\beta}_f H_m(c)$ infections during her infectious period, $(\gamma_f + \mu_f)^{-1}$. As a result,

$$T_{I_f}^m(c) = \frac{\tilde{\beta}_f H_m(c)}{\gamma_f + \mu_f}$$

is the infection transfer from the aware infectious females to males. Analogously,

$$T_{U_f}^m(c) = \frac{\beta_f H_m(c)}{\gamma_f + \alpha + \mu_f}$$

is the infection transfer from the unaware infectious females to males. Moreover, a fraction $\alpha/(\gamma_f + \alpha + \mu_f)$ of unaware infected females becomes aware of the infection via screening. Hence

$$T_f^m(c) = pT_{I_f}^m(c) + (1-p)\left(T_{U_f}^m(c) + \frac{\alpha}{\gamma_f + \alpha + \mu_f} T_{I_f}^m(c)\right)$$

is the infection transfer from females to males. Hence, the effective reproduction number (3.10) is the geometric mean of the terms $T_m^f(c)$ and $T_f^m(c)$, that is,

$$\mathscr{R}_e(c) = \sqrt{T_m^f(c) \cdot T_f^m(c)}. \tag{3.11}$$

As a consequence of the van den Driessche theorem (Van den Driessche and Watmough, 2002), $\mathscr{R}_e(c)$ is a threshold value and we establish the following result regarding the local stability of the disease-free equilibrium.

Corollary 3.3.2. *The disease-free equilibrium $E_\circ(c)$ of system* (3.5) *is locally asymptotically stable for $\mathscr{R}_e(c) < 1$ and unstable for $\mathscr{R}_e(c) > 1$.*

Corollary 3.3.2 implies that, if initial infection levels are sufficiently low, reducing and maintaining $\mathscr{R}_e(c) < 1$ ensures disease's elimination. On the contrary, if the value of $\mathscr{R}_e(c)$ is higher than unity, the disease can persist in the population.

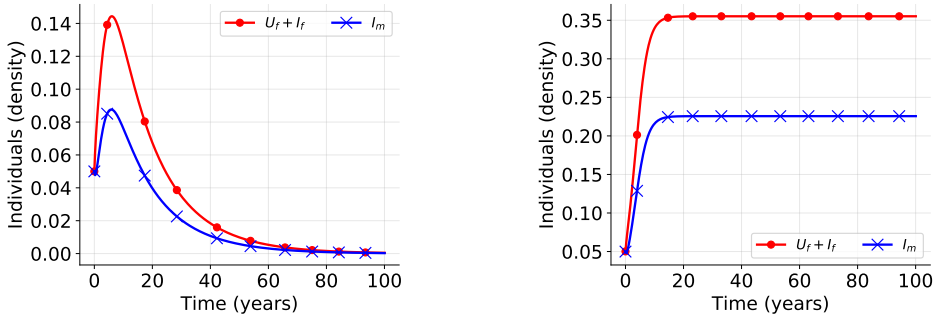

(a) (b)

Fig. 3.1 Prevalence levels for model (3.5) with $\mathscr{R}_e(c) = 0.9479 < 1$ (a) and $\mathscr{R}_e(c) = 1.4151 > 1$ (b). In case (a) the values of the screening and vaccination rates are $w_1 = 0.1$, $w_2 = 0.07$, $u_1 = 0.05$, $u_2 = 0.03$, and $\alpha = 0.1$. In case (b), the screening and vaccination rates are taken equal to zero. The rest of the parameters are as described in Table 3.1. The initial conditions are: $S_f = 0.94$, $U_f(0) = 0.04$, $I_f(0) = 0.02$, $V_f(0) = 0$, $S_m = 0.94$, $I_m(0) = 0.06$, $V_m(0) = 0$.

In order to demonstrate the importance of the control interventions to reduce the value of the effective reproduction number below 1, we firstly show the behavior of the model in the absence of control and under health care interventions with constant control parameters. Fig. 3.1 illustrates these two possibilities. In Fig. 3.1(a), we choose screening and vaccination rates that guarantee $\mathscr{R}_e(c) < 1$, so that the infection eventually decreases to zero. On the contrary, in Fig. 3.1 (b), the screening and vaccination rates are taken equal to zero, thus giving $\mathscr{R}_e(0) > 1$, so the system converges to an endemic equilibrium. Other parameters are fixed with their baseline values in Table 3.1.

3.3.4 Model parameters

Parameters values, units, and source of estimation are summarized in Table 3.1. In the next sections, we use these values unless otherwise is stated. Next, we outline their selection:

Parameter	Range	Mean Value	Units	Source
$1-\varepsilon$	$[0.8,1]$	0.9	*adimensional*	(Brisson et al., 2016)
$1/\theta$	$[5,15]$	10	*year*	(Huh et al., 2017)
β_m	$[0.05,5]$	4.0	$year^{-1}$	(Brisson et al., 2016)
β_f	$[0.05,5]$	4.0	$year^{-1}$	(Brisson et al., 2016)
$\tilde{\beta}_f$	$[0.025,2.5]$	2.0	$year^{-1}$	Estimated
$1/\gamma_f$	$[0.83,2]$	1.3	*year*	(Muñoz et al., 2004)
$1/\gamma_m$	$[0.33,1.2]$	0.6	*year*	(Anic and Giuliano, 2011)
p	$[0,1]$	0.2	*adimensional*	Estimated
$1/\mu_f$	$[15,50]$	30	*year*	Estimated
$1/\mu_m$	$[15,50]$	30	*year*	Estimated

Table 3.1 Estimated values, units and source of estimation for the parameters of the HPV model (3.5).

(i) *Vaccine efficacy*, $1-\varepsilon$. Although clinical trials are still underway, there is evidence indicating efficacy of around 90% for the nonavalent HPV vaccine Gardasil-9 (Brisson et al., 2016). We set $1-\varepsilon \in [0.8,1]$.

(ii) *Vaccine protection*, $1/\theta$. The exact duration of vaccine protection is unknown, but clinical trials (Huh et al., 2017) have shown sustained efficacy for more than 5 years. We assume that the protection is from 5 to 15 years, thus $1/\theta \in [5,15]$ *years*.

(iii) *Transmission rates*, β_m, β_f, and $\tilde{\beta}_f$. Transmission rates are the product of the average number of sexual contacts per unit of time and the probability of infection transfer per contact. We assume that both genders have between 1 and 5 sexual partners per year and per-act transmission probability range $5-100\%$ (Brisson et al., 2016). We set $\beta_i \in [0.05,5]$ $year^{-1}$ with $i \in \{f,m\}$. We also assume that the aware infected females take measures, such as condom use, that decrease the probability of infection transfer. Thus $\tilde{\beta}_f \in [0.025,2.5]$ $year^{-1}$.

(iv) *Females's infectious period*, $1/\gamma_f$. The mean duration of a new genital HPV infection in women is 14.8 months for oncogenic types and 11.1 months for non-oncogenic types (Muñoz et al., 2004). Since the majority of the types targeted by Gardasil-9 are

oncogenic, we assume that the female infectious period is between 9 months and 2 years, thus $1/\gamma_f \in [0.83, 2]$ *year*.

(v) *Male's infectious period*, $1/\gamma_m$. For men, most of the HPV infections clear in less than 12 months. Studies (see (Anic and Giuliano, 2011) and the references therein) report average clearance time of 5.9 to 7.5 months. We set $1/\gamma_m \in [0.33, 1.2]$ *year*.

(vi) *Fraction of females that become aware of their infection*, p. Since p is a fraction, $p \in [0,1]$.

(vii) *Periods of sexual activity*, $1/\mu_f$, and $1/\mu_m$. We assume that the average duration of the sexual activity period for both, males and females, is between 15 and 50 years, therefore $\mu_f^{-1}, \mu_m^{-1} \in [15, 50]$ *years*.

It is important to mention that we are assuming homogeneous mixing among individuals. Therefore, sexual contacts are instantaneous and every contact is with another individual of the population. One major implication of this assumption is that for the transmission rates, β_m, β_f, and $\tilde{\beta}_f$, the per-act transmission probability is equal to the transmission probability per partner. Although this assumption is very common for compartmental epidemic models in the literature, we remark it represents a limitation in our model (see Chapter 4).

3.4 Cost-effectiveness analysis for constant controls

Human health improved dramatically during the last century, yet grave inequities in health persist. To make further progress in health, meet new challenges, and redress inequities, resources must be deployed effectively. This requires knowledge about which interventions actually work, information about how much they cost, and experience with their implementation and delivery.

Cost-effectiveness analysis helps identify ways to redirect resources to achieve more. It demonstrates not only the utility of allocating resources from ineffective to effective interventions, but also the utility of allocating resources from less to more cost-effective interventions. Cost-effectiveness analysis is a method for assessing the gains in health relative to the costs of different health interventions. It is not the only criterion for deciding how to allocate resources, but it is an important one, because it directly relates the financial and scientific implications of different interventions.

Results of a cost-effectiveness analysis are summarized using a cost-effectiveness ratio. In this ratio, the basic calculation involves dividing the cost of an intervention in monetary units by the expected health gain measured in natural units such as number of lives saved.

ID	Strategy description	w_1	w_2	u_1	u_2	α
S_1	All Controls	✓	✓	✓	✓	✓
S_2	Vaccination prior to sexual initiation	✓	✓			
S_3	Vaccination of sexually active individuals			✓	✓	
S_4	Females' vaccination	✓		✓		
S_5	Males' vaccination		✓		✓	
S_6	Vaccination prior to sexual initiation and screening	✓	✓			✓
S_7	Vaccination of sexually active individuals and screening			✓	✓	✓
S_8	Females' vaccination and screening	✓		✓		✓

Table 3.2 Control interventions analyzed in this work.

Cost-effectiveness analysis are always comparative, as the ratios evaluate the costs and benefits of each strategy relative to the next-most effective strategy (Goldie et al., 2006). This means that the costs and clinical benefits associated with the intervention of interest should be compared to all other reasonable options.

In the following, we carry out a cost-effectiveness analysis to investigate the most cost-effective control strategy against HPV transmission. To conduct a cost-effectiveness analysis, researchers also need to specify the health intervention in some detail. A health intervention is a deliberate activity that aims to improve someone's health by reducing the risk, the duration, or the severity of a health problem. We propose realistic strategies based on the combination of the five controls incorporated into our model. These strategies are shown in Table 3.2. For each strategy, the controls not marked with a checkmark are regarded as inactive.

The main objective is to compare the health outcomes of the proposed interventions with respect to their application costs. To this end, we introduce an incremental cost-effectiveness ratio (ICER), which is a summary measure representing the economic value of an intervention, compared with an alternative (comparator). It is usually the main output or result of an economic evaluation. An ICER is usually calculated by dividing the difference in total costs (incremental cost) by the difference in the chosen measure of health outcome or effect (incremental effect) to provide a ratio of *extra cost per extra unit of health effect* – for the more expensive intervention vs the alternative.

Mathematically speaking, for two strategies S_1 and S_2, we define the ICER as

$$ICER(S_1,S_2) = \frac{C(S_2)-C(S_1)}{E(S_2)-E(S_1)}, \tag{3.12}$$

provided that $E(S_1) \neq E(S_2)$.

We also define the average cost-effectiveness ratio (ACER) for a strategy S alone as

$$ICER(S) = \frac{C(S)}{E(S)}. \tag{3.13}$$

Function $C(\cdot)$ measures the costs. For analyses conducted from a societal perspective, costs must reflect resource use, not only the intervention itself, but also for the downstream events that follow. Key cost categories include: (i) direct health-care costs (e.g. screening test, clinic visit, laboratory test, specimen transport, subsequent health-care visits for treatment, further tests, etc. (ii) Direct non-health-care costs (e.g. patient transportation costs, child or dependent care, time spend with family for caregiving, etc. (iii) Patient time costs (e.g. the time spend by the patient receiving care). (iv) Programmatic costs (e.g. costs incurred at the administrative levels rather than the point and care delivery). However, the identification, measurement, and valuation of these resources is in practice very difficult.

The function $E(\cdot)$ measures the effectiveness of the intervention using some appropriate health outcome. Health units for measuring the population impact can be disease-specific clinical outcomes, such as the number of cases prevented. Although such clinical outcomes are easily understood, a disadvantage is that results can only be compared to studies using the same outcome. In order to compare ratios across different interventions and diseases, the denominator must be expressed in a common metric, such as life expectancy, years of life lost (calculated by subtracting the age at which death occurs from life expectancy at that age), quality adjusted life years (a unit for measuring the health gain associated with a clinical or public health intervention) (Okosun et al., 2011).

In this study, we measure the effectiveness of the intervention S computing its cumulative level of infection averted using the following functional:

$$E(S) = \int_0^T \left(U_f(t) - \tilde{U}_f(t)\right) + \left(I_f(t) - \tilde{I}_f(t)\right) dt, \tag{3.14}$$

where $U_f(t)$ are the infected unaware females for no control scenario at time t and $\tilde{U}_f(t)$ are the infected unaware females under intervention S (analogously for the infected aware females I_f). The functional (3.14) focuses on the females because they are at a considerable higher risk of developing severe disease (e.g. cervical cancer) after an HPV infection. Nevertheless, we need to mention that in the context of HPV, cost-effectiveness analysis usually quantify the efficacy of the control strategies in terms of the reduction in cervical cancer associated deaths. Yet, since in our model we do not consider an explicit compartment for women with cervical cancer, we cannot use this metric to measure the effectiveness of the strategies. This is a major limitation of our model which will be improved in a future work.

To compute the costs, we propose the following functional:

$$C(S) = \int_0^T M(S) + B_1\tilde{U}_f(t) + B_2\tilde{I}_f(t)dt, \tag{3.15}$$

where

$$M(S) = A_1(w_1\mu_f + w_2\mu_m) + A_2(u_1\tilde{S}_f(t) + u_2\tilde{S}_m(t)) + A_3\alpha(\tilde{U}_f(t) + \tilde{S}_f(t)). \tag{3.16}$$

The parameters A_i $(i = 1,2,3)$ are positive constants associated with the relative costs of vaccination and screening, and parameters B_j $(j = 1,2)$ represent the medical and social costs associated with the illness. The terms $(w_1\mu_f + w_2\mu_m)$ and $(u_1\tilde{S}_f(t) + u_2\tilde{S}_m(t))$ count the number of vaccinations given prior and after sexual initiation, respectively, and $\alpha(\tilde{U}_f(t) + \tilde{S}_f(t))$ counts the number of individuals that are screened.

The costs attributable to the vaccination includes the price of the vaccine, the cost of delivery, as well as other administration associated costs. It is logical to expect that delivering the vaccine to school boys and girls is cheaper than vaccination of the sexually active individuals; hence, $A_1 < A_2$. Since the costs of screening and follow up are uncertain, for simplicity, we assume that $A_3 \approx A_1$; that is, the costs associated with screening and juveniles vaccination are of the same magnitude. Moreover, it is also considered that unaware infected females are at greater risk of developing HPV-induced cervical cancer than aware infected females; therefore, it can be expected that $B_1 \geq B_2$. Under these considerations, as a base case, we assume $A_1 = 1$, $A_2 = 5$, $A_3 = 1$, $B_1 = 15$, $B_2 = 10$. Moreover, a time horizon of $T = 100$ years is chosen because in this time frame the majority of the benefits and cost of vaccination can be recognized (Elbasha and Dasbach, 2010).

3.5 Interpreting the results of the CEA

In the simple case of comparing two interventions, the current standard and an alternative, the analysis applies the principle of strong dominance. Strong dominance favors a strategy that is both more effective and less costly. In other words, we say a strategy is strongly dominated by an alternative, if the alternative is more effective and less costly. However, it is very common that the alternative intervention is more effective but also more costly. In this case, strong dominance provides no guidance and the decision maker must decide if the greater effectiveness justifies the cost of achieving it. This is usually done with a cost-effectiveness threshold. There are several types of threshold. In health-related analyses, a very common

threshold is the so-called willingness-to-pay threshold which represents an estimate of what a consumer of health care might be prepared to pay for the health benefit.

In some studies that compare multiple interventions, an additional dominance principle is applied. As in the case when comparing two interventions, the analyst first applies the principle of strong dominance. Any of the competing interventions is ruled out if these is another intervention that is both more effective and less costly. The analyst may then apply the principle of extended dominance (sometimes called "weak dominance"). The list of interventions, trimmed of strongly dominated alternatives, is ordered by effectiveness. Each intervention is compared to the next most effective alternative by calculating the incremental cost-effectiveness ratio. Extended dominance rules out any intervention that has an incremental cost-effectiveness ratio that is greater than that of a more effective intervention. The decision maker prefers the more effective intervention with a lower incremental cost-effectiveness ratio. By approving the more effective interventions.

In this work, we attempt to systematize the analysis using a CEA algorithm. Our proposed algorithm uses the extended dominance principle to compare the strategies. However, we do not ruled out from the beginning strongly dominated strategies because we want to rank all the strategies. Moreover, our algorithm uses the ACER as a cost-effectiveness threshold. Our algorithm is structured as follows:

Cost-Effectiveness Algorithm

1. The list of strategies with their corresponding costs and effectiveness is sorted from lowest to highest costs. Let S_A and S_B be the first and the second elements of the sorted list, respectively.
2. The $ACER(S_A)$ of the first element of the list S_A is computed.
3. The $ICER(S_A, S_B)$ between the first two elements of the list S_A, S_B is computed.
4. The following conditions are assessed:
   - If $ICER(S_A, S_B) \leq 0$, then S_A has higher effectiveness than S_B; hence, we keep S_A and remove S_B.
   - If $ICER(S_A, S_B) \geq ACER(S_A)$, then S_B has higher effectiveness than S_A, but in proportion is less cost-effective than S_A; hence, we keep S_A and remove S_B.
   - If $0 < ICER(S_A, S_B) < ACER(S_A)$, then S_B has higher effectiveness than S_A and is in proportion more cost-effective than S_A; hence, we keep S_B and remove S_A.
5. We return to STEP 2 until we find the most cost-effective strategy.

To fairly compare the proposed strategies (see Table 3.2), we set the values for the screening and vaccination rates in such a way that the value of the effective reproduction number $\mathscr{R}_e(c)$ is the same for all the strategies. Then, we compute the corresponding costs and the total infection averted over the time horizon for each intervention. These data allow us to use the CE algorithm and rank the interventions in order of increasing cost-effectiveness ratios. The results are summarized in Table 3.3.

The results of the cost-effectiveness analysis suggest that the strategy S_4 (female's vaccination) is the most cost-effective intervention and S_2 (vaccination before sexual initiation) is the strategy with the second-best performance. These results coincide with several studies that have analyzed HPV transmission at the population level finding that vaccination of pre-adolescent girls is both highly effective and highly cost-effective to reduce the disease burden caused by HPV, see Seto et al. (2012) and the references therein. However, regardless of the independence of the cost function (3.15) from infected males, the third most cost-effective strategy is S_5 (male's vaccination). This result is somehow unexpected; however, it could be explained by the fact that for a heterosexual population, the eradication of the infection can

Strategy	$C(S_i)$	$E(S_i)$	Rank
S_1 ($w_1 = 0.03$, $w_2 = 0.03$, $u_1 = 0.05$, $u_2 = 0.05$, $\alpha = 0.1$)	\$ 70.33	31.77	# 7
S_2 ($w_1 = 0.81$ $w_2 = 0.81$)	\$ 47.86	31.04	# 2
S_3 ($u_1 = 0.068$, $u_2 = 0.05$)	\$ 69.07	31.71	# 6
S_4 ($w_1 = 0.3$, $u_1 = 0.127$)	\$ 49.24	32.43	# 1
S_5 ($w_2 = 0.3$, $u_2 = 0.119$)	\$ 55.07	31.86	# 3
S_6 ($w_1 = 0.66$ $w_2 = 0.6$, $\alpha = 0.4$)	\$ 59.50	31.99	# 5
S_7 ($u_1 = 0.046$, $u_2 = 0.05$, $\alpha = 0.2$)	\$ 73.30	32.01	# 8
S_8 ($w_1 = 0.15$, $u_1 = 0.1$, $\alpha = 0.3$)	\$ 58.03	32.65	# 4

Table 3.3 Control strategies with fixed constant controls together with their costs and cumulative level of infection averted. The ranking of the strategies is according to the ICER algorithm. For all the strategies, the value of the effective reproduction number is $\mathscr{R}_e(c) = 0.9$.

be achieved by vaccinating a considerable proportion of a single-sex. On the other hand, the strategy with the worst performance is S_7 (vaccination of sexually active individuals with female's screening), thus, even assuming a medium duration of protection for the vaccine (20 years), it is plausible to vaccinate individuals before sexual debut avoiding the potential of an HPV infection.

The simulations of the HPV model showing the effects of strategy S_4, which is the most cost-effective control strategy according to the ICER results in Table 3.3, are illustrated in Fig. 3.2. The simulations show that the number of infected individuals decreases to zero after an approximate time of 40 years. Furthermore, the fraction of vaccinated females increases until it reaches a value of 0.62, whereas the fraction of vaccinated males is maintained at zero.

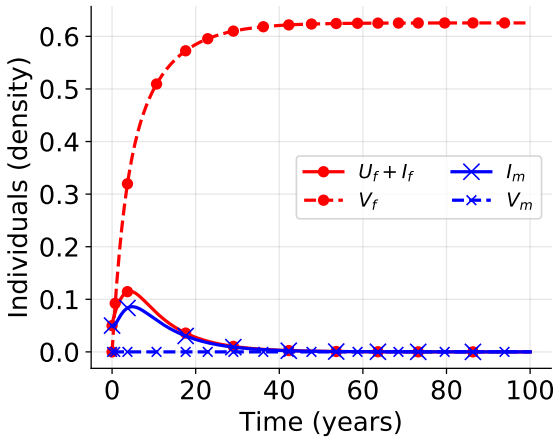

Fig. 3.2 Dynamics of model (3.5) state variables under intervention S_4 fixed constant controls $w_1 = 0.3$ and $u_1 = 0.127$

3.6 The optimal control problem

In the previous sections, we analyzed the qualitative properties of the HPV model (3.5) and performed a cost-effectiveness analysis for constant control policies. Constant control analysis is helpful to understand the mean behavior of the model. However, such a constant control scheme disregards the changing dynamics of the infection and thereby can be a fragile strategy.

For monetary and time resources, as well as disease elimination, it is essential to find the right time and the right amount of control administration. Therefore, it is valuable to incorporate time-dependent screening and vaccination into our model and explore the most cost-effective strategy via the optimal control theory.

We formulate an optimal control problem incorporating the following five time-dependent controls:

- $w_1(\cdot)$ and $w_2(\cdot)$ are the controls representing the fraction of females and males, respectively, that are vaccinated prior to sexual initiation.
- $u_1(\cdot)$ and $u_2(\cdot)$ are the controls representing the per capita vaccination rates of susceptible sexually active females and males, respectively.
- $\alpha(\cdot)$ is the control representing the per capita screening rate for females.

By definition, the controls are subject to the next constraints

$$0 \leq w_1(t), w_2(t), u_1(t), u_2(t), \alpha(t) \leq 1. \tag{3.17}$$

With these controls and taking into consideration the constant population size assumption, we can write model (3.5) as the following system of five equations:

$$\begin{aligned}
\dot{U}_f &= \big((1-U_f-I_f-V_f)+\varepsilon V_f\big)(1-p)\beta_m I_m - (\gamma_f+\alpha(t)+\mu_f)U_f,\\
\dot{I}_f &= \big((1-U_f-I_f-V_f)+\varepsilon V_f\big)\, p\beta_m I_m + \alpha(t)U_f - (\gamma_f+\mu_f)I_f,\\
\dot{V}_f &= w_1(t)\mu_f + u_1(t)(1-U_f-I_f-V_f) - \varepsilon\beta_m V_f I_m - (\mu_f+\theta)V_f,\\
\dot{I}_m &= (\beta_f U_f + \tilde{\beta}_f I_f)((1-I_m-V_m)+\varepsilon V_m) - (\gamma_m+\mu_m)I_m,\\
\dot{V}_m &= w_2(t)\mu_m - (\beta_f U_f + \tilde{\beta}_f I_f)\varepsilon V_m + u_2(t)(1-I_m-V_m) - (\mu_m+\theta)V_m,
\end{aligned} \tag{3.18}$$

complemented by initial conditions

$$0 \leq U_f(0), I_f(0), V_f(0), I_m(0), V_m(0) \leq 1. \tag{3.19}$$

The control model (3.18) is defined on a finite time interval $[0,T]$ and the set of admissible controls, denoted $D(T)$, is defined as the set of all possible Lebesgue measurable functions which for almost all $t \in [0,T]$ satisfy constraints (3.17).

For an optimal control problem, it is necessary to define a quantitative criterion to evaluate the performance of the admissible controls. In mathematical terms, this quantitative criterion leads to the definition of an objective functional, and an optimal control is one that minimizes (or maximizes) this functional. For the control model (3.18) and the set of admissible controls $D(T)$, we want to minimize the overall impact of the infection and the level of efforts that would be needed to control the infection over T years. Thus, we consider system (3.18) together with the following objective functional

$$J(c) = \int_0^T B_1 U_f + B_2 I_f + \frac{1}{2}\left(A_1(w_1^2 + w_2^2) + A_2(u_1^2 + u_2^2) + A_3\alpha^2\right) dt. \tag{3.20}$$

It is generally assumed that the quadratic terms penalize high levels of control administration (to avoid costly interventions) because "increasing the availability of vaccines and other resources often leads to a waste" Sharomi and Malik (2017). The origin of the sum of weighted squares in the controls is in engineering applications, where it is clearly interpreted as the energy spent on the control action. In the context of disease control, it is also commonly assumed that this type of functional implies minimization of certain economic costs (Brown and White, 2011; Buonomo et al., 2014; Camacho and Jerez, 2018; Malik et al., 2016; Okosun et al., 2011, 2013). Nevertheless, it is important to mention that the sum of weighted squares of the controls is probably the most common form of the objective functional in the literature due to its mathematical convenience. In particular, for functionals of these type, it is possible, by virtue of the Pontryagin maximum principle, to obtain the optimal controls as explicit functions of the state and adjoint variables Grigorieva et al. (2018).

For the sake of simplicity and comparison, in this paper the objective functional (3.20) considers the sum of weighted squares of the controls and also uses the same weight parameters of the cost function (3.15). The general optimal control problem is to find optimal vaccination and screening rates $c^* = (w_1(t)^*(t), w_2^*(t), u_1^*(t), u_2^*(t), \alpha^*(t))$ such that

$$J(c^*) = \min_{c \in D(T)} J(c)$$

subject to the dynamics of the HPV control model (3.18).

Here, we must clarify the following: (i) Although optimal controls c^* are expected to be more cost-effective than constant controls, this is not known *a priori* because c^* minimize the objective functional (3.20) and the ICER measures the cost using (3.15); (ii) The cost

function (3.15) can also be used as an objective functional for the optimal control; however, generally speaking, an optimal control problem could have multiple goals and therefore, the objective functional may include other factors besides costs.

3.7 The Pontryagin maximum principle

Pontryagin's maximum principle is used in optimal control theory to find the best possible control for taking a dynamical system from one state to another, especially in the presence of constraints for the state or input controls. It states that it is necessary for any optimal control along with the optimal state trajectory to solve the so-called Hamiltonian system, which is a two-point boundary value problem, plus a maximum condition of the Hamiltonian. These necessary conditions become sufficient under certain convexity conditions on the objective and constraint functions.

Widely regarded as a milestone in optimal control theory, the significance of the maximum principle lies in the fact that maximizing the Hamiltonian is much easier than the original infinite-dimensional control problem; rather than maximizing over a function space, the problem is converted to a pointwise optimization. The maximum principle was formulated in 1956 by the Russian mathematician Lev Pontryagin and his students, and its initial application was to the maximization of the terminal speed of a rocket. The result was derived using ideas from the classical calculus of variations. After a slight perturbation of the optimal control, one considers the first-order term of a Taylor expansion with respect to the perturbation; sending the perturbation to zero leads to a variational inequality from which the maximum principle follows.

In this section, we prove the existence of solutions for the optimal control problem (3.6). We also obtain the optimality system associated with the control model (3.18) and the set of admissible controls $D(T)$. The optimality system correspond to complement the control model (3.18) with a dual system for adjoint variables. This system will allow us to characterize the optimal controls in terms of the state and adjoint variables. Let us introduce the states $x = (U_f, I_f, V_f, I_m, V_m)^T$, the controls $c = (w_1, w_2, u_1, u_2, \alpha)^T$ and denote the right-hand side of the control model (3.18) as the vector function $F(t,x,c)$. For the objective functional (3.20), the optimal control problem of the HPV epidemic model is

$$\min_{c\in D(T)} J(c) = \min_{c\in D(T)} \int_0^T L(t,x(t),c(t))$$

where

$$L(t,x,c) = B_1U_f + B_2I_f + \frac{1}{2}(A_1(w_1^2+w_2^2) + A_2(u_1^2+u_2^2) + A_3\alpha^2) \tag{3.21}$$

subject to the dynamics of the control model (3.18) with given initial conditions (3.19).

We call a pair of states and controls (x,c) satisfying both (3.18) and $c \in D(T)$ a feasible pair. Theorem 4.1 in (Fleming and Rishel, 1975, Chapter III) ensures the existence of an optimal control and the corresponding solution for this problem. In particular, this existence theorem states that the following conditions are sufficient to guarantee the existence of an optimal control for (3.18):

(H1) F is continuous, and there exist positive constants K_1 and K_2 such that

(a) $|F(t,x,c)| \leq K_1(1+|x|+|c|)$

(b) $|F(t,\tilde{x},c)-F(t,x,c)| \leq K_2|\tilde{x}-x|(1+|c|)$

hold for all $t \in [0,T]$. Moreover, F can be written as $F(t,x,c) = \phi(t,x)+\psi(t,x)c$.

(H2) The set of admissible controls $D(T)$ is closed and convex. Moreover, there is at least one feasible pair $(x(t),c(t))$ satisfying both (3.18) and (3.17).

(H3) $L(t,x,\cdot)$ is convex on $D(T)$, and $L(t,x,c) \geq K_3|c|^{\beta}-K_4$, $K_3>0$, $K_4 \in \mathbb{R}$, $\beta > 1$.

Theorem 3.7.1. *Consider the optimal control problem with control model* (3.18) *and cost functional* (3.20). *Then there exist* $c^* = (w_1^*, w_2^*, u_1^*, u_2^*, \alpha^*) \in D(T)$ *such that* $\min J(c)_{c\in D(T)} = J(c^*)$.

Proof. Due to the a priori boundedness of the solutions of the control model (3.18), and the differentiability of the function F, it follows that (a) and (b) in (H1) are ensured by suitable bounds on the partial derivatives of F and on $F(t,0,0)$. Moreover, the state equations are linear with respect to the controls c, and thus $F(t,x,c) = \phi(t,x)+\psi(t,x)c$. The existence of a feasible pair is guaranteed by the Caratheodory theorem (Lukes, 1982, pp. 182) for initial value problems. Moreover, for bounded controls on a finite time interval, $D(T)$ is clearly closed and convex, and, hence, (H2) is satisfied as well. The integrand (3.21) of the cost functional is positive and quadratic with respect to the controls; therefore, $L(t,x,\cdot)$ is convex on $D(T)$. Furthermore, defining $K_3 = \min\{A_1,A_2,A_3\}$, we have $L(t,x,c) \geq (1/2)K_3|c|^2$, thus verifying (H3) and completing the proof. □

3.7.1 Characterization of the optimal controls

Here, we obtain the optimality system that corresponds to complement the control model (3.18) with a dual system for adjoint variables. Then, we can achieve the characterization of the optimal controls in terms of the state and adjoint variables.

The Pontryagin maximum principle converts the optimal control problem (3.6) into a problem of minimizing pointwise the Hamiltonian

$$\begin{aligned} H =& B_1 U_f + B_2 I_f + \frac{1}{2}\left[A_1(w_1^2 + w_2^2) + A_2(u_1^2 + u_2^2) + A_3\alpha_2\right] \\ &+ \psi_1 \dot{U}_f + \psi_2 \dot{I}_f + \psi_3 \dot{V}_f + \psi_4 \dot{I}_m + \psi_5 \dot{V}_m \end{aligned} \tag{3.22}$$

with respect to the controls. Here, ψ_i for $i = 1, \ldots, 5$ are adjoint variables which satisfy the following system of differential equations:

$$\begin{aligned} \dot{\psi}_1 =& -B_1 + [(1-p)\beta_m I_m + \gamma_f + \alpha^* + \mu_f]\psi_1 + (p\beta_m I_m - \alpha^*)\psi_2 \\ &+ u_1^*\psi_3 - \beta_f[(1 - I_m - V_m) + \varepsilon V_m]\psi_4 + \beta_f \varepsilon V_m \psi_5, \\ \dot{\psi}_2 =& -B_2 + (1-p)\beta_m I_m \psi_1 + (p\beta_m I_m + \gamma_f + \mu_f)\psi_2 + u_1^*\psi_3 \\ &- \tilde{\beta}_f[(1 - I_m - V_m) + \varepsilon V_m]\psi_4 + \tilde{\beta}_f \varepsilon V_m \psi_5, \\ \dot{\psi}_3 =& [(1-p)\psi_1 + p\psi_2](1-\varepsilon)\beta_m I_m + (\varepsilon\beta_m I_m + u_1^* + \mu_f + \theta)\psi_3, \\ \dot{\psi}_4 =& -\beta_m((1 - U_f - I_f - V_f) + \varepsilon V_f)[(1-p)\psi_1 + p\psi_2] + \varepsilon\beta_m V_f \psi_3 \\ &+ (\beta_f U_f + \tilde{\beta}_f I_f + \gamma_m + \mu_m)\psi_4 + u_2^*\psi_5, \\ \dot{\psi}_5 =& (\beta_f U_f + \tilde{\beta}_f I_f)((1-\varepsilon)\psi_4 + \varepsilon\psi_5) + (u_2^* + \theta + \mu_m)\psi_5, \end{aligned} \tag{3.23}$$

with transversality conditions $\psi_k(T) = 0$ for $k = 1, \ldots, 5$. For this control problem, applying the maximum principle from (Pontryagin, 2018), we obtain the following characterization for the optimal controls:

$$\begin{aligned} w_1^*(t) &= \min\left\{1, \max\left\{0, -\frac{\mu_f}{A_1}\psi_3(t)\right\}\right\}, \\ w_2^*(t) &= \min\left\{1, \max\left\{0, -\frac{\mu_m}{A_1}\psi_5(t)\right\}\right\}, \\ u_1^*(t) &= \min\left\{u_{max}, \max\left\{0, -\frac{1}{A_2}(1 - U_f(t) - I_f(t) - V_f(t))\psi_3(t)\right\}\right\}, \\ u_2^*(t) &= \min\left\{u_{max}, \max\left\{0, -\frac{1}{A_2}(1 - I_m(t) - V_m(t))\psi_5(t)\right\}\right\}, \\ \alpha^*(t) &= \min\left\{\alpha_{max}, \max\left\{0, \frac{1}{A_3}(\psi_1(t) - \psi_2(t))U_f(t)\right\}\right\}. \end{aligned} \tag{3.24}$$

The control model (3.18), the system of differential equations for the adjoints (3.23) and the control characterization above form the optimality system. The optimal control solutions can be obtained solving the optimality system. In particular, we can obtain time-dependent

versions of the control strategies in Table 3.2 choosing the corresponding control parameters as active and turning off the rest of control parameters.

In order to obtain approximations of our optimality systems, we use the forward-backward sweep method (FBSM) from (Lenhart and Workman, 2007). This iterative scheme begins with an initial guess on the controls; then, the state equations are solved forward in time. After that, since the transversality conditions for our problems are posed at the final time T, the system for the adjoint variables is solved backward in time. The controls are updated using a convex combination of the previous controls and the new control obtained substituting the states and adjoints into its characterization. This process is repeated until a convergence criteria is satisfied. For solving the state and adjoint systems, we use a fourth order Runge-Kutta scheme. The time-dependent profiles for the control strategies (denoted $S_i^*(t)$, $i = 1,2,\ldots,8$) are shown in Fig. 3.3.

3.7.2 Cost-effectiveness analysis for time-dependent control strategies

Next, we want to determine the most cost-effective of the time-dependent control strategies $S_i^*(t)$ ($i = 1,2,\ldots,8$) illustrated in Fig. 3.3. As in the case of constant controls, we need to compare the costs and the effectiveness of the interventions. This is done using the cost-effectiveness ICER algorithm presented in Section 3.4. The results of this analysis can be found in Table 3.4.

Strategy	$C(S_i^*)$	$E(S_i^*)$	Rank
$S_1^*(t)$	\$ 64.48	31.76	#8
$S_2^*(t)$	\$ 48.65	30.86	#3
$S_3^*(t)$	\$ 64.04	31.69	#7
$S_4^*(t)$	\$ 47.92	32.39	#1
$S_5^*(t)$	\$ 53.69	31.82	#4
$S_6^*(t)$	\$ 59.23	31.85	#5
$S_7^*(t)$	\$ 64.36	31.99	#6
$S_8^*(t)$	\$ 50.80	32.61	#2

Table 3.4 Costs, cumulative level of infection averted, and rank according to the ICER algorithm for the control strategies with time-dependent control strategies.

The results presented in Table 3.4 indicate that $S_4^*(t)$ is the most cost-effective strategy. This result coincides with the CEA results for the constant control case (see Table 3.3). Hence, female's vaccination is the intervention with the best performance for control of HPV infection. Nevertheless, for time-dependent control strategies, the second most cost-effective intervention is female's vaccination and screening, $S_8^*(t)$; whereas for constant

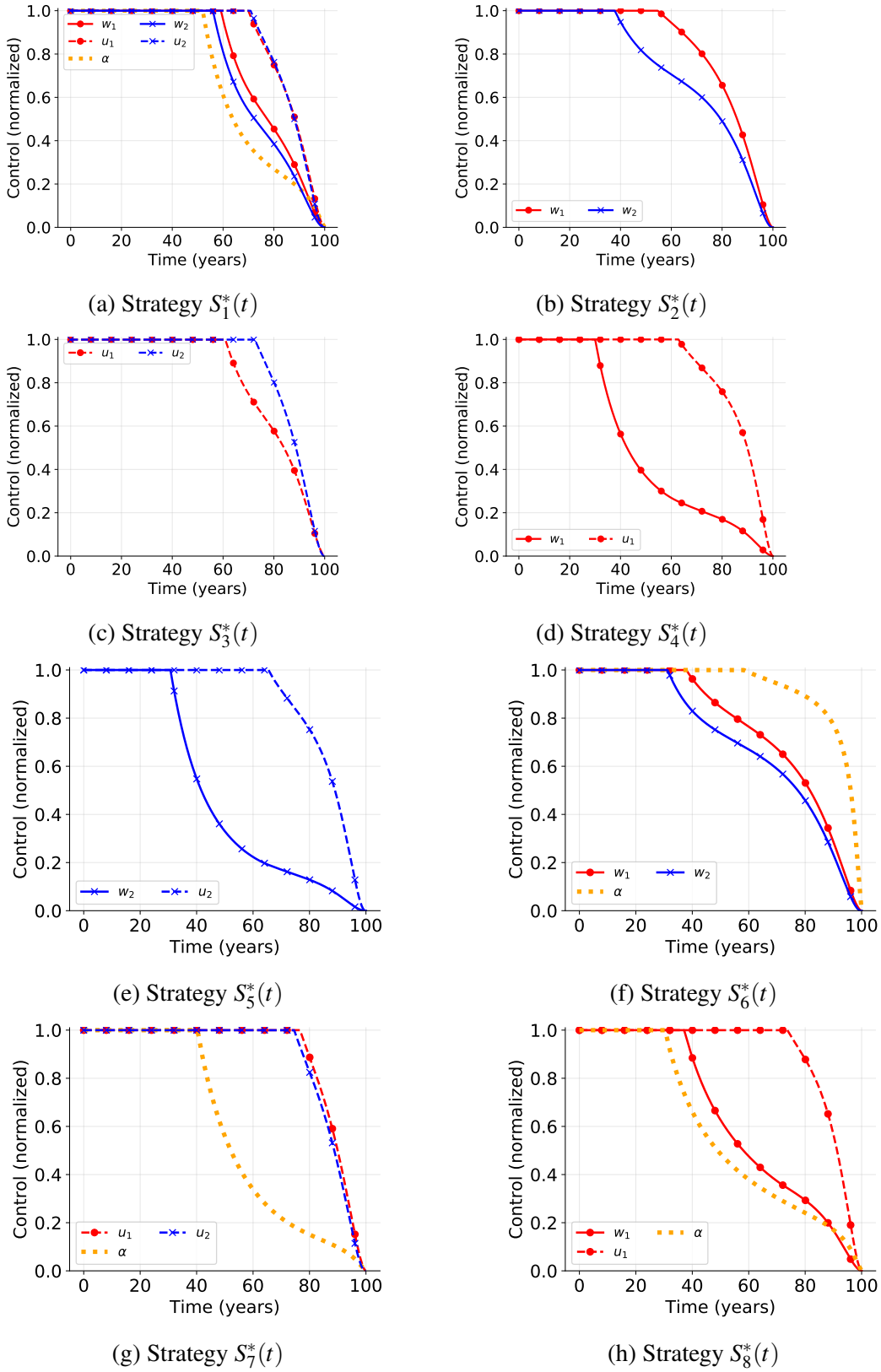

(a) Strategy $S_1^*(t)$

(b) Strategy $S_2^*(t)$

(c) Strategy $S_3^*(t)$

(d) Strategy $S_4^*(t)$

(e) Strategy $S_5^*(t)$

(f) Strategy $S_6^*(t)$

(g) Strategy $S_7^*(t)$

(h) Strategy $S_8^*(t)$

Fig. 3.3 Time-dependent profiles of the control strategies derived by the numerical solution of the optimality system.

control strategies, vaccination prior to sexual initiation, S_2, is the second most cost-effective intervention. Therefore, the CEA rankings for the constant and the time-dependent control case differ. Moreover, it is uncertain if the time-dependent control strategies outperforms the constant control strategies as expected. Thus, we shall use the ICER and the ACER to compare constant control strategies S_i (see Table 3.3) against the time-dependent control strategies $S_i^*(t)$ (see Fig. 3.3).

First, we compare the most cost-effective control strategies with constant and time-dependent controls, that is, S_4 versus $S_4^*(t)$. For this, we need the following computations:

$$ACER(S_4^*(t)) = \frac{47.92}{32.39} = 1.479,$$

$$ICER(S_4^*(t), S_4) = \frac{49.24 - 47.92}{32.43 - 32.39} = 33.00.$$

These computations imply that $ICER(S_4^*(t), S_4) > ACER(S_4^*(t))$. Hence, although strategy S_4 has higher effectiveness than strategy $S_4^*(t)$, in proportion, S_4 is less cost-effective than $S_4^*(t)$. In particular, the value of $ICER(S_4^*(t), S_4)$ shows a cost saving of \$ 33 for strategy $S_4^*(t)$ over strategy S_4. Consequently, in this case, the time-dependent control outperform the constant control.

Next, we compare the second most cost-effective constant control strategy S_2 against the second most cost-effective time-dependent control strategy $S_8^*(t)$. The cost-effective ratios are:

$$ACER(S_2) = \frac{47.86}{31.04} = 1.54,$$

$$ICER(S_2, S_8^*(t)) = \frac{50.80 - 47.86}{32.61 - 31.04} = 1.87.$$

Clearly, $ICER(S_2, S_8^*(t)) > ACER(S_2)$. Thus, the comparison shows a cost saving of \$ 1.87 for strategy S_2 over strategy $S_8^*(t)$. Therefore, in this case, the constant control outperform the time-dependent control.

Finally, we compare the third most cost-effective control strategies, that is, S_5 against $S_2^*(t)$. The ICER is calculated as follows:

$$ACER(S_2^*(t)) = \frac{48.65}{30.86} = 1.57,$$

$$ICER(S_2^*(t), S_5) = \frac{55.07 - 48.65}{31.86 - 30.86} = 6.42.$$

The comparison between strategies S_5 and $S_2^*(t)$ shows a cost saving of \$ 6.42 for strategy $S_2^*(t)$ over strategy S_5. Hence, in this case, the time-dependent control outperform the constant control.

On the whole, the intervention with the best performance is the time-dependent strategy $S_4^*(t)$ (see Fig. 3.4 for the simulations of the HPV model showing the effects of strategy S_4^*). Nevertheless, generally speaking, time-dependent control strategies obtained by the solution of the optimal control problem are not always more cost-effective than constant control strategies.

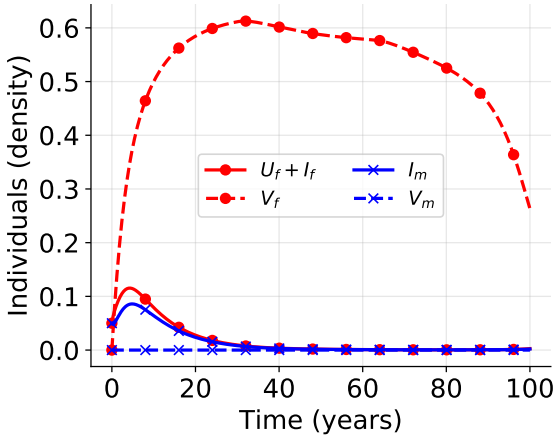

Fig. 3.4 Simulations of the HPV model showing the effects of the time-dependent control strategy $S_4^*(t)$ with optimal controls w_1^* and u_1^* illustrated in Fig. 3.3 (d).

3.8 Discussion and concluding remarks

Since the introduction of HPV vaccines over a decade ago, HPV vaccination programs have been implemented in several countries. However, there are large discrepancies in coverage and targeted groups of vaccination strategies among countries (Soe et al., 2018). The vaccination program depends on country-specific factors, such as the economic and geographical constraints as well as the health care system organization. In several countries, prophylactic vaccination of pre-adolescent females has been introduced supported by modeled evaluations that have found this intervention to be cost-effective. Vaccination of pre-adolescent males may also be cost-effective if females' coverage is below 50% (Canfell et al., 2012). Therefore, it is important to investigate under which conditions the inclusion of males and adult females into existing vaccination programs is cost-effective.

This work aimed to assess the cost-effectiveness of HPV health care interventions. We considered a two-sex compartmental epidemic model of HPV infection in which we

incorporated the control parameters representing screening, vaccination of pre-adolescent boys and girls, and vaccination of sexually active adults. We analyzed the model with constant control parameters and computed both, the basic and the effective reproduction numbers to determine the stability properties of the model. Then, we proposed constant control strategies based on combinations of the five controls incorporated in our model and used the ICER methodology to identify which strategy delivers the best effectiveness for the money invested.

Comparisons of the cost-effectiveness of the proposed constant control strategies consistently show that females' vaccination, including pre-adolescent girls and adult women, is the most cost-effective strategy. Then, the next strategy with the best performance is the vaccination of school-boys and -girls before sexual initiation. Furthermore, the third most cost-effective strategy is males' vaccination. This result is unexpected because the cost function (3.15) does not depend on the presence of HPV infected males. Therefore, a very adequate choice to balance cost and protection is increasing vaccine uptake among all eligible females and extending coverage to high-risk males sub-groups.

Secondly, we considered the control parameters to be time-dependent and formulated an optimal control problem. We used the Pontryagin maximum principle to derive the necessary conditions for the optimal control and obtained numerical approximations via the forward-backward sweep method. This allowed us to obtain time-dependent versions of the control strategies. As in the case for constant controls, we used the ICER methodology to identify the strategy with the best performance to control HPV infection. The results confirm that the females' vaccination is the most cost-effective strategy. For this intervention, the numerical computations (see Fig. 3.3 (b)) indicate that initially, the vaccination rates should be applied at the maximum level and after approximately half of the time interval, these rates should gradually be reduced reaching zero at the final time.

The objective functional (3.20) of the optimal control problem considers the sum of weighted squares in the controls. This penalizes high levels of control administration but differs from the costs derived from function $C(S)$. Therefore, when comparing constant against time-dependent control policies, it is not known *a priori* which of the strategies is the most cost-effective. Therefore, we used the ICER methodology to compare constant against time-dependent control strategies that are optimal in the sense that they minimize functional (3.20). The results indicate that time-dependent controls are not always more cost-effective than constant controls. Therefore, one must be very careful with the election of the objective functional for optimal control problems in epidemiology. Finally, we remark that our model-based cost-effectiveness analyses are sensitive to the weight parameters in the cost function and thus, the conclusions must be taken with caution. Nevertheless, model

parameters can be calibrated to match data of HPV vaccine price and delivery cost for specific geographical regions.

Chapter 4

The Role of Behavioral Changes and Prompt Treatment in the Control of Sexually Transmitted Infections

4.1 Introduction

[1] Mathematical models are an important tool for understanding the spread of diseases in populations. A better sense of the transmission characteristics of infectious diseases can lead to an improvement of our capacity to prevent and control them. Therefore, in recent years, there has been a growing interest in the field of mathematical epidemiology. In particular, many models have been proposed to examine the transmission of sexually transmitted infections (STIs), and the impact of various control policies (Chen and Ghani, 2010; Dasbach et al., 2006; Elbasha and Galvani, 2005; Heijne et al., 2011, 2013; Muller and Bauch, 2010).

Classical epidemic models for sexually transmitted infections usually overlooked the existence of sexual partnerships. This is partly because they assume homogeneous mixing among individuals. In other words, these models suppose that sexual contacts are instantaneous and every contact is with another individual of the population; therefore, the entire population is all the time at risk of contracting the infection. These assumptions may be comprehensible when modeling a group of highly promiscuous individuals but it may not always be valid for the average population. In fact, in real life scenarios, sexual partnerships usually have nonzero length; and there is also a positive time gap between partnerships (Foxman et al., 2006; Muller and Bauch, 2010).

[1] This Chapter is based on (Saldaña and Barradas, 2019)

To deal with such dynamic properties of sexually transmitted infections, pair formation models were first introduced into the field of mathematical epidemiology by Dietz and Hadeler (Dietz and Hadeler, 1988). They modified models from mathematical demography to include transmission of infection in an age-structured two-sex population. Simplified versions of this pair formation epidemic model were later formulated by Kretzschmar and Dietz and compared with models, which do not take partnership duration into account. Since then, pair formation models have been used in many variants, have been implemented into simulation models for STIs, and have been applied to analyze the impact of public health interventions.

The explicit inclusion of sexual partnerships is important to address the fact that transmission only takes place when a susceptible individual and an infected one form a sexual partnership. Therefore, as remarked in (Muller and Bauch, 2010), two susceptible individuals that form a pair can be considered temporarily immune as long as they do not separate. For a pair of two infected individuals, if the partnership lasts enough they can clear the infection before the partnership ends and avoid transmission to future partners. These examples show that transmission in a model that includes sexual partnerships (pair model) could be slower than in a classical homogeneous mixing model.

Another interesting subject of research that has been shown to bring rich dynamics in epidemiological models (Villavicencio Pulido et al., 2017; Wang et al., 2012; Wang, 2006; Zhang and Liu, 2008) is the role played by the recovery function on the spread of infections. Assuming a recovery rate proportional to the size of the infectious class is not satisfactory due to the fact that the health-care system is limited when the number of infected individuals is large. Incorporating a general recovery function is necessary to evaluate situations like these. Moreover, a general recovery function can also describe different control policies and behavioral changes in the population related to the number of infectious individuals.

The present work includes pair formation considering nonzero length partnerships as an explicit variable of the model and capturing the dynamics of partnership formation and dissolution. The pair model proposed below generalizes the work presented in (Kretzschmar and Dietz, 1998) to an SIS (susceptible-infectious-susceptible) structure. The new model incorporates a general recovery function that allows studying situations in which, for instance, behavioral changes occur or medical resources are limited. We shall analyze how the recovery function affects the equilibrium level of prevalence and other possible effects in the context of the persistence of the disease in the population.

The structure of this chapter is as follows. In the next section, we describe the underlying assumptions that govern our model equations. In section 4.3, we calculate the expression for the basic reproduction number and investigate the stability of the equilibrium points. In sec-

tion 4.4, we perform a global sensibility analysis to identify the parameters or combinations of parameters that contribute the most to the variance of $\mathscr{R}_0$. In section 4.5, we propose and study two different recovery functions. Bifurcation analysis is used as a tool to explore the structure of the model's solution for a plausible range of parameter values. The role of the pair formation process is analyzed in section 4.6. Finally, the conclusions and a discussion are presented in section 4.7.

4.2 Model Formulation

The compartmental *SIS* model proposed below describes the pair formation process and the spread of an infection within partnerships. Single individuals form monogamous sexual partnerships at a constant rate ρ per unit of time and the partnerships break up at a rate σ per unit of time. Transmission of the infection can only occur within partnerships, with ϕ being the number of sex acts per unit of time and h the transmission probability per contact.

As pointed out in Dietz and Hadeler (1988), if the pair formation process is considered only as a social act and sexual contacts occur within a pair with a certain rate, for a high separation rate there could be partnerships without a sexual contact during their existence. These pairs would be irrelevant for the infection process. Hence, we shall assume that every partnership starts with a sexual contact.

Individuals enter the sexually active phase of their lives at a constant rate ν as singles and leave the sexually active population at a rate μ. Moreover, for simplicity, we are going to omit the relation between the infectious disease and the pair formation process. Therefore, being infected does not bias individual's tendency neither to form or break partnerships, nor to have sexual contacts Kretzschmar and Dietz (1998).

The model equations resulting from these assumptions are

$$\begin{aligned}
\frac{dX_0}{dt} &= \nu + (\sigma+\mu)(2P_{00}+P_{01}) - (\mu+\rho)X_0 + \Phi(I)X_1,\\
\frac{dX_1}{dt} &= (\sigma+\mu)(2P_{11}+P_{01}) - (\mu+\rho)X_1 - \Phi(I)X_1,\\
\frac{dP_{00}}{dt} &= \frac{1}{2}\rho\frac{X_0^2}{X} - (\sigma+2\mu)P_{00} + \Phi(I)P_{01},\\
\frac{dP_{01}}{dt} &= \rho(1-h)\frac{X_0X_1}{X} - (\sigma+\phi h+2\mu)P_{01} - \Phi(I)P_{01} + 2\Phi(I)P_{11},\\
\frac{dP_{11}}{dt} &= \frac{1}{2}\rho\frac{X_1^2}{X} + \rho h\frac{X_0X_1}{X} + \phi hP_{01} - (\sigma+2\mu)P_{11} - 2\Phi(I)P_{11},
\end{aligned} \tag{4.1}$$

Variable	Description
X_0	Single susceptible individuals
X_1	Single infected individuals
P_{00}	Pairs with two susceptible individuals
P_{01}	Pairs with a susceptible and an infected individuals
P_{11}	Pairs with two infected individuals
X	Total number of singles
P	Total number of pairs
u_T	Public health control: treatment of infected individuals
u_C	Public health control: condom promotion

Table 4.1 State variables for model (4.1).

Parameter	Description	Units
ν	Recruitment rate	individuals year^{-1}
μ	Rate of leaving the sexually active population	year^{-1}
ρ	Rate of pair formation	year^{-1}
σ	Separation rate	year^{-1}
ϕ	Contact frequency within partnerships	year^{-1}
$1/\gamma$	Infectious period in the absence of treatment	year
h	Transmission probability per contact	dimensionless

Table 4.2 Interpretation and units for the parameters of model (4.1).

where $I(t) = X_1(t) + P_{01}(t) + 2P_{11}(t)$ is the total prevalence at time t and all the parameters are assumed to be non-negative. Tables 4.1 and 4.2 summarize the model variables and parameters.

Before going any further it is important to emphasize the role of the function $\Phi(I)$. In our system $\Phi(I)$ represents the impact on the population due to the efforts (decisions, plans or actions) undertaken by the health care system to control the disease. In other words, the function $\Phi(I)$ model public health strategies to reduce the prevalence of the infection. In mathematical terms, the function $\Phi(I)$ is a non-negative function that increase the recovery rate of infected individuals as a consequence of the application of public health strategies.

It is worth mentioning that when the function $\Phi(I)$ is assumed constant, then the infection clearance rate, and consequently the mean recovery time, depends only on the biology of the pair pathogen-human and permanent health policies. In particular, no additional control interventions depending on the number of infected individuals are included. Allowing the recovery function $\Phi(I)$ to change with I takes into consideration modifications in control policies due to a perceived hazard: the level of prevalence of the infection. Therefore, $\Phi(0) = \gamma > 0$ represents the infection clearance rate under normal conditions. These conditions might include the natural immune response and any other permanent health policy that influences the recovery time of a single infected individual. The quotient $1/\Phi(I)$ can be interpreted as

the mean recovery time when the level of prevalence is I. In particular, $1/\gamma$ is the recovery time when no additional density-dependent treatment or actions are taken by the infectious individual or society's health sectors.

4.3 Model Analysis

Note that the total population size $N = X_0 + X_1 + 2(P_{00} + P_{01} + P_{11})$ satisfies $N' = -\mu N + \nu$. Therefore, by adding the equations of the pair model (4.1) we obtain

$$N(t) \leq N(0)e^{-\mu t} + \frac{\nu}{\mu}\left(1 - e^{-\mu t}\right). \tag{4.2}$$

If we consider the set

$$\Omega = \{(X_0, X_1, P_{00}, P_{01}, P_{11}) \in \mathbb{R}^5_+ \mid X_0 + X_1 + 2(P_{00} + P_{01} + P_{11}) \leq \nu/\mu\},$$

then, from (4.2), we get that if $N(0) \in \Omega$ then $N(t) \in \Omega$ for all $t > 0$. We say that Ω is a positively invariant set under (4.1).

Now, let $X = X_0 + X_1$ be the total number of singles and $P = P_{00} + P_{01} + P_{11}$ the total number of pairs. From (4.1), observe that the dynamics of singles and pairs are described by the the following system of differential equations:

$$X' = \nu + 2(\sigma + \mu)P - (\mu + \rho)X, \tag{4.3}$$

$$P' = \frac{1}{2}\rho X - (\sigma + 2\mu)P. \tag{4.4}$$

The partnership dynamics (4.3)–(4.4) has a unique equilibrium point (X^*, P^*):

$$X^* = \frac{\nu(\sigma + 2\mu)}{\mu(\sigma + 2\mu + \rho)}, \qquad P^* = \frac{\nu\rho}{2\mu(\sigma + 2\mu + \rho)}. \tag{4.5}$$

Let the initial conditions of (4.3)–(4.4) be the equilibrium point (X^*, P^*) (4.5). In this case we say that the pair formation process is at equilibrium. This assumption implies that $X' = 0$ and $P' = 0$, so the total population size is constant with $N = \nu/\mu$. Thus, assuming equilibrium of the pair formation process we may reduce model (4.1) to the following three dimensional

system in terms of the proportions $\bar{X}_1 = X_1/N$, $\bar{P}_{01} = P_{01}/N$, $\bar{I} = I/N$,

$$\begin{aligned}
\frac{d\bar{X}_1}{dt} &= (\sigma+\mu)\bar{I} - (2\mu+\rho+\sigma)\bar{X}_1 - \bar{\Phi}(\bar{I})\bar{X}_1, \\
\frac{d\bar{P}_{01}}{dt} &= \rho(1-h)\bar{X}_1\left(1-\frac{\bar{X}_1}{\bar{X}^*}\right) - (\sigma+\phi h+2\mu)\bar{P}_{01} + \bar{\Phi}(\bar{I})(\bar{I}-\bar{X}_1-2\bar{P}_{01}), \\
\frac{d\bar{I}}{dt} &= \rho h\bar{X}_1\left(1-\frac{\bar{X}_1}{\bar{X}^*}\right) + \phi h\bar{P}_{01} - \mu\bar{I} - \bar{\Phi}(\bar{I})\bar{I},
\end{aligned} \tag{4.6}$$

where

$$\bar{X}^* = \frac{(\sigma+2\mu)}{(\sigma+2\mu+\rho)}, \qquad \bar{P}^* = \frac{\rho}{2(\sigma+2\mu+\rho)} \tag{4.7}$$

are the proportions of singles and pairs at the equilibrium level of partnership dynamics. To avoid clumsy notation, from now on we are going to omit the bars in the variables of the model (4.6).

4.3.1 The basic reproduction number

In this section, we compute the basic reproduction number for the reduced model (4.6). We shall consider the special case in which the function $\Phi(I)$ takes its value at zero, that is, $\Phi(0) = \gamma$. Thus, we consider the following model:

$$\begin{aligned}
\frac{d\bar{X}_1}{dt} &= (\sigma+\mu)\bar{I} - (2\mu+\rho+\sigma)\bar{X}_1 - \gamma\bar{X}_1, \\
\frac{d\bar{P}_{01}}{dt} &= \rho(1-h)\bar{X}_1\left(1-\frac{\bar{X}_1}{\bar{X}^*}\right) - (\sigma+\phi h+2\mu)\bar{P}_{01} + \gamma(\bar{I}-\bar{X}_1-2\bar{P}_{01}), \\
\frac{d\bar{I}}{dt} &= \rho h\bar{X}_1\left(1-\frac{\bar{X}_1}{\bar{X}^*}\right) + \phi h\bar{P}_{01} - \mu\bar{I} - \gamma\bar{I},
\end{aligned} \tag{4.8}$$

The basic reproduction number $\mathscr{R}_0$ for pair models is defined as the expected number of secondary infections one typical infectious individual will produce during his/her infectious period starting in a P_{11} partnership in a completely susceptible population (Heijne et al., 2013). A point to consider when computing $\mathscr{R}_0$ for pair models with nonzero recovery rate is that infected individuals can clear their infection before the partnership ends, but they can get reinfected if their partner is still infectious. These reinfections should be included in the computation of $\mathscr{R}_0$.

For the computation of the basic reproduction number we need the following components:

(i) The probability that the initial infectious individual (initial case) is still infectious when separating from a partner.

(ii) The probability that the initial case is still infectious when he/she forms a new partnership.

(iii) The transmission probability per partnership.

(iv) The number of new partners during the infectious period and the number of reinfections for each partner.

First, we compute the probability that the initial case is still infected when separating from a P_{11} partnership. The initial case can reach the state X_1 by direct separation from the P_{11} with a probability

$$\mathbb{P}(P_{11} \to X_1) = \frac{\sigma+\mu}{\sigma+2\mu+2\gamma} \tag{4.9}$$

or by first passing through P_{01} with a probability

$$\mathbb{P}(P_{11} \to P_{01})\mathbb{P}(P_{01} \to X_1) = \left(\frac{\gamma}{\sigma+2\mu+2\gamma}\right)\left(\frac{\sigma+\mu}{\sigma+\phi h+2\mu+\gamma}\right) \tag{4.10}$$

The probability p_t of the initial case still being infected after separation when there are no reinfections is the sum of equations (4.9) and (4.10),

$$p_t = \frac{(\sigma+\mu)(\sigma+\phi h+2\mu+2\gamma)}{(\sigma+2\mu+2\gamma)(\sigma+\phi h+2\mu+\gamma)} \tag{4.11}$$

In addition, the initial case can reach the state X_1 after m loops of clearance-reinfection of his/her partner. For that reason, we need to examine the case that one or more reinfections take place before separation. A reinfection occurs with a probability

$$p_r = \left(\frac{\gamma}{\sigma+2\mu+2\gamma}\right)\left(\frac{\phi h}{\sigma+\phi h+2\mu+\gamma}\right). \tag{4.12}$$

Thus, the probability that clearance and reinfection happen exactly m times before separation of the partnership is p_r^m, $m \in \mathbb{N}$. Therefore, the probability that at least one reinfection occurs is

$$\sum_{m=1}^{\infty} p_r^m = \frac{p_r}{1-p_r} = \frac{\gamma\phi h}{(\sigma+2\mu+\gamma)(\sigma+\phi h+2\mu+2\gamma)} \tag{4.13}$$

As a consequence, the probability p_s that an individual who started in a P_{11} partnership is still infectious after separation is given by

$$p_s = p_t\left(1+\frac{p_r}{1-p_r}\right) = \frac{\sigma+\mu}{\sigma+2\mu+\gamma}. \tag{4.14}$$

Seeing that

$$p_d = \rho/(\rho+\gamma+\mu) \tag{4.15}$$

is the probability that the initial case is still infectious and sexually active when he/she forms a new partnership, and

$$h_p = h(\sigma+\phi+2\mu+\gamma)/(\sigma+\phi h+2\mu+\gamma) \tag{4.16}$$

is the transmission probability per partnership, we conclude that

$$\mathscr{R}_c = h_p \sum_{i=1}^{\infty} (p_d p_s)^i = \frac{h\rho(\sigma+\mu)(\sigma+\phi+\gamma+2\mu)}{(\gamma+\mu)(\sigma+\gamma+2\mu+\rho)(\sigma+\phi h+\gamma+2\mu)} \tag{4.17}$$

is the average number of individuals that the initial case will infect during his/her infectious period in a completely susceptible population. $\mathscr{R}_c$ is known as the case reproduction number (Heijne et al., 2013). If we add the expected number of reinfections in the starting and the subsequent partnerships of the initial case $(p_r/(1-p_r))(\mathscr{R}_c+1)$ to the case reproduction number $\mathscr{R}_c$, we obtain the following expression for the basic reproduction number

$$\mathscr{R}_0 = \frac{h[\rho(\sigma+\mu)(\sigma+\phi+2\gamma+2\mu)+\gamma\phi(\gamma+\mu+\rho)]}{(\gamma+\mu)(\sigma+\gamma+2\mu+\rho)(\sigma+\phi h+2\gamma+2\mu)} \tag{4.18}$$

4.3.2 Equilibrium points and stability analysis

A triplet (X_1^*, P_{01}^*, I^*) is called an endemic equilibrium point of model (4.8) if $I^* > 0$ and if the triplet satisfies the following non-linear system:

$$X_1^* = \frac{(\sigma+\mu)I^*}{2\mu+\rho+\sigma+\gamma}, \tag{4.19}$$

$$P_{01}^* = \frac{\rho(1-h)X_1^*}{\sigma+\phi h+2\mu+2\gamma}\left(1-\frac{X_1^*}{X^*}\right) + \frac{\gamma(I^*-X_1^*)}{\sigma+\phi h+2\mu+2\gamma}, \tag{4.20}$$

$$I^* = \frac{\rho h X_1^*}{\mu+\gamma}\left(1-\frac{X_1^*}{X^*}\right) + \frac{\phi h P_{01}^*}{\mu+\gamma}. \tag{4.21}$$

System (4.19)–(4.21) comes from setting the left-hand side of (4.8) equal to zero. Assume that (X_1^*, P_{01}^*, I^*) is an endemic equilibrium point. From (4.19) we can see that $I^* > X_1^* > 0$. In addition, given that $X_1^* \leq X^*$, from equation (4.20) we deduce that $I^* > P_{01}^* > 0$. In

summary, if (X_1^*, P_{01}^*, I^*) is an endemic equilibrium point then

$$I^* > 0, \quad I^* > X_1^* > 0, \quad I^* > P_{01}^* > 0.$$

Substituting the values of X_1^* and P_{01}^* in equation (4.21) and solving for I^*, we get:

$$I^* = (\mathscr{R}_0 - 1)\frac{(\mu+\gamma)(\sigma+\phi h+2\mu+2\gamma)(2\mu+\rho+\sigma+\gamma)^2 X^*}{\rho h(\sigma+2\gamma+2\mu+\phi)(\sigma+\mu)^2}. \tag{4.22}$$

This, in turn, can be used to explicitly determine the values of X_1 and P_{01} at the endemic equilibrium. Moreover, when $\mathscr{R}_0 > 1$ all the factors on the right-hand side of expression (4.22) are positive. Therefore, $I^* > 0$ exists if and only if $\mathscr{R}_0 > 1$. The following result summarizes the role of the basic reproduction number in the dynamics of the disease.

Theorem 4.3.1. *For the reduced model* (4.8)*, the disease-free equilibrium* $E_0 = (0,0,0)$ *always exists and it is locally asymptotically stable if and only if* $\mathscr{R}_0 < 1$*. For* $\mathscr{R}_0 > 1$*, the vector* $E_1 = \left(X_1^*, P_{01}^*, I^*\right)$*, where* X_1^**,* P_{01}^* *and* I^* *are given by the solution of system* (4.19)–(4.21)*, is the only endemic equilibrium point of model* (4.8) *and it is locally asymptotically stable.*

Proof. It is straightforward to see that $E_0 = (0,0,0)$ is the disease-free equilibrium for model (4.8). To investigate the local stability of the equilibrium points, we compute the Jacobian matrix of the model (4.8):

$$J(X_1, P_{01}, I) = \begin{pmatrix} J_{11} & 0 & \sigma+\mu \\ J_{21} & J_{22} & \gamma \\ J_{31} & \phi h & -(\mu+\gamma) \end{pmatrix},$$

where:

$$J_{11} = 2\mu+\rho+\sigma-\gamma, \quad J_{21} = \rho(1-h)\left(1-\frac{2X_1}{X^*}\right)-\gamma,$$
$$J_{22} = -(\sigma+\phi h+2\mu+2\gamma), \quad J_{31} = \rho h\left(1-\frac{2X_1}{X^*}\right).$$

The characteristic polynomial for the Jacobian matrix evaluated at the disease-free equilibrium $J(E_0)$ is $P_1(\lambda) = \lambda^3 + a_2\lambda^2 + a_1\lambda + a_0(1-\mathscr{R}_0)$ where:

$$\begin{aligned} a_2 &= 2\sigma + 4\gamma + 5\mu + \rho + h\phi, \\ a_1 &= (\sigma + 2\gamma + 2\mu + h\phi)(\sigma + \gamma + 2\mu + \rho) \\ &\quad + (\gamma + \mu)(2\sigma + 3\gamma + 4\mu + \rho + h\phi), \\ &\quad - h(\rho(\sigma + \mu) + \gamma\phi), \\ a_0 &= (\sigma + 2\gamma + 2\mu + h\phi)(\gamma + \mu)(\sigma + \gamma + 2\mu + \rho). \end{aligned}$$

Note that coefficients a_i are positive for $i = 0, 1, 2$. Thus, $P_1(\lambda)$ is an strictly increasing function for $\lambda \in \mathbb{R}^+$. Furthermore, $P_1(0) > 0$ if and only if $\mathscr{R}_0 < 1$. In consequence, if $\mathscr{R}_0 < 1$, then the roots of the polynomial $P_1(\lambda)$ have negative real part. However, $P_1(\lambda)$ has a unique positive real root if $\mathscr{R}_0 > 1$. Therefore, the disease-free equilibrium is locally asymptotically stable if $\mathscr{R}_0 < 1$, and it is unstable if $\mathscr{R}_0 > 1$.

We have already established that for $\mathscr{R}_0 > 1$ the point $E_1 = \left(X_1^*, P_{01}^*, I^*\right)$ is the only endemic equilibrium for model (4.8). The characteristic polynomial for the Jacobian matrix evaluated at the endemic equilibrium $J(E_1)$ is $P_2(\lambda) = \lambda^3 + b_2\lambda^2 + b_1\lambda + b_0(\mathscr{R}_0 - 1)$ where

$$b_2 = a_2 > 0, \quad b_1 = a_1 + h\rho(\sigma + \mu)\left(\frac{2X_1^*}{X^*}\right) > 0, \quad b_0 = a_0 > 0.$$

Seeing that $P_2(0) > 0$ if $\mathscr{R}_0 > 1$, and that $P_2(\lambda)$ is an increasing function of λ when $\lambda > 0$, we obtain the local asymptotic stability of E_1. □

4.4 Sobol's indices for $\mathscr{R}_0$

In this section, we will perform a Sobol sensibility analysis Saltelli et al. (2004, 1999) to evaluate the relative contribution of each individual parameter, as well as the interactions among parameters to the overall variance of the basic reproduction number (4.18). This will allow us to identify the parameters or combinations of parameters that influence the most the value of the basic reproduction number. This is important in order to plan appropriate control policies.

Due to the uncertainty in parameters' values that appear in the definition of $\mathscr{R}_0$, we are going to explore plausible ranges for them. The assumptions made for the sensitivity analysis and the corresponding ranges for the parameters are listed below:

- The number of new partners varies from 1 up to 4 per year.

- The percentage of people in a partnership at the equilibrium level ranges from 50% to a maximum of 80%.
- The pair formation rate is between $2/year$ and $20/year$. The separation rate, σ, lies between $1.027/year$ and $7.77/year$. (Equation (4.7) i.e the fraction of singles and pairs at the steady state was used to estimate the ranges for ρ and σ).
- The duration of the infectious period under normal conditions is between 0.5 and 2 years Juckett et al. (2010), therefore $\gamma \in [0.5, 2]\ year^{-1}$.
- The transmission probability per contact, h, lies in the interval $[0.01, 0.3]$.
- The contact frequency within partnerships, ϕ, varies from 26 contacts up to 156 contacts per year.

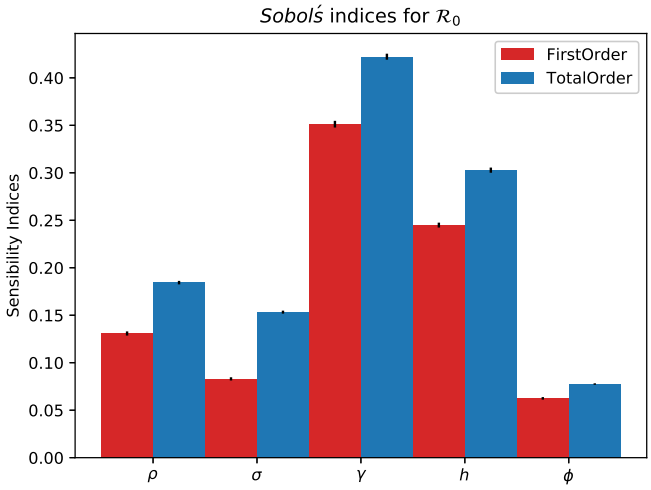

Fig. 4.1 Sobol's indices for $\mathscr{R}_0$ (first and total order). The ranges explored for the parameters are $\rho \in [1.25, 8]$, $\sigma \in [1.777, 19.77]$, $\gamma \in [0.5, 2]$, $h \in [0.01, 0.3]$ and $\phi \in [26, 156]$. The vertical black lines in the indices represent confidence and can be interpreted as error bars.

The results shown in figure 4.1 indicate that the dominant parameter contributing with about 35% of the variability of $\mathscr{R}_0$ is γ, the recovery rate under normal conditions. The transmission probability per contact, h, is also a very influential parameter with a first-order index of 0.2449. The influence of the behavioral parameters ρ and σ on $\mathscr{R}_0$ is smaller but not negligible. This is because although their first-order indices are not very high, the sum of their total-order sensibility indices is above 0.30. This suggests that both ρ, and σ have strong compound interactions with the remaining parameters. On the other hand, the contact

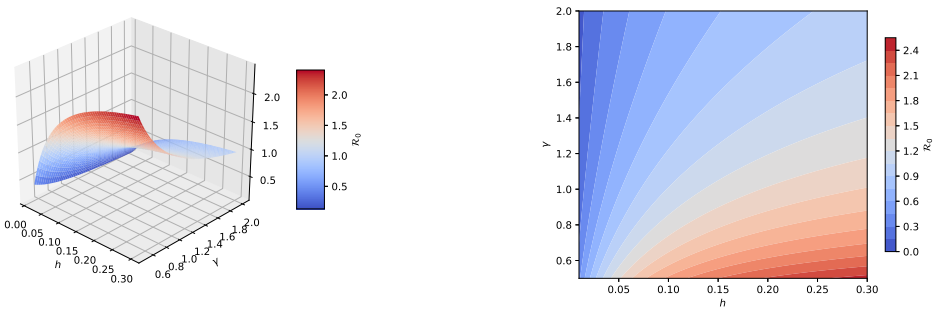

(a) $\mathscr{R}_0$ as function of γ and h.

(b) Contour plot of $\mathscr{R}_0$ as function of γ and h.

Fig. 4.2 $\mathscr{R}_0$ and its dependency on the parameters γ and h.

frequency within partnerships, ϕ, has only a weak influence on $\mathscr{R}_0$. The dark marks on top of the bars in figure 4.1 represent 95% confidence intervals for the sensibility indices. Notice that they are very small.

We also computed the second-order sensibility indices to measure the contribution to the variance of $\mathscr{R}_0$ caused by the interaction of two model inputs. Within the ranges explored, the combination of γ and σ influences the variance of $\mathscr{R}_0$ more than any other combination of two parameters. Our sensibility analysis also indicates that there is a significant interaction between the parameters γ and h, and also between ρ and σ.

Given the relevance of γ and h, we plotted the basic reproduction number (4.18) as a function of them. As expected, $\mathscr{R}_0$ is a non-increasing function of the recovery rate γ. The opposite pattern is seen for $\mathscr{R}_0$ as a function of the transmission probability per contact, i.e. $\mathscr{R}_0$ is a non-decreasing function of h (see figure 4.2).

These results suggest that public health efforts should focus primarily on increasing γ, the recovery rate under normal conditions. This can be achieved, for example, through a permanent program of screening, diagnosis, and treatment of cases. An improvement of clinical services and training of health personnel can also help to increase γ. In addition, a reduction of h, the transmission probability per contact, is likewise essential to eradicate the disease. Among the different ways of doing that, barrier methods stand out because they are relatively low-cost, accessible and effective in reducing h.

Finally, the control of the parameters ρ and σ can also be significant to reduce the transmission of the infection. For this reason, efforts to maintain public awareness of STIs and health education are an essential component to control them. These behavioral interventions are useful for reducing individuals' risk of contracting and transmitting STIs. Although in real life situations these strategies are often difficult to implement, their benefits

can be considerable. Among the expected effects are a reduced number of sexual partners, delayed sexual debut and mutual monogamy.

4.5 Equilibrium prevalence versus recovery function

In this section, we study through numerical examples the relationship between the prevalence at the equilibrium level and the form of the function $\Phi(I)$. For this, we perform numerical bifurcation analysis using the software **AUTO-07p** developed by Eusebius Doedel. Different forms for $\Phi(I)$ have been proposed in the literature to model different scenarios. For example, in (Villavicencio Pulido et al., 2017) Villavicencio-Pulido et al. studied a model where the recovery function is a Michaelis-Menten equation which corresponds to a non-convex saturation function. They also considered an exponential recovery function whose effect caused the appearance of a backward bifurcation.

Researchers have also explored treatment functions in epidemiological models (Eckalbar and Eckalbar, 2011; Wang et al., 2012; Wang, 2006; Zhang and Liu, 2008). The idea is that public health authorities will mobilize their resources to fight perceived infections depending on the level of prevalence. For instance, in (He et al., 2013) a quadratic treatment function was proposed to model the fact that society's capacity for providing treatment is limited and can decline after critical equipment and supplies are exhausted or health-care workers fall victim to the disease. In this work, we analyze two different forms for the recovery function related to particular control policies to understand how recovery influences the equilibrium level of prevalence.

4.5.1 A sigmoid recovery function

Here, the treatment function $\Phi(I)$ takes the form of a sigmoid curve,

$$\Phi(I) = \frac{M}{1+\exp\left[-k(I-I_0)\right]}, \quad 0 < I_0 < 1,\ 0 < M. \tag{4.23}$$

The quotient $1/M$ is the minimum time needed to recover from the disease when undergoing treatment. Therefore, the parameter M satisfies $M > \gamma$. The parameter I_0 represents an alert level of prevalence after which the response of the public health authorities begins to grow faster until saturation begins. The parameter k models the speed of resource allocation per new infected case. In particular, when k is big, the reaction of the system is almost negligible for $I < I_0$ and, nearest to the maximum capacity for $I > I_0$. On the other hand, when k is small, the system takes more into account the gradual increase or decrease in the prevalence.

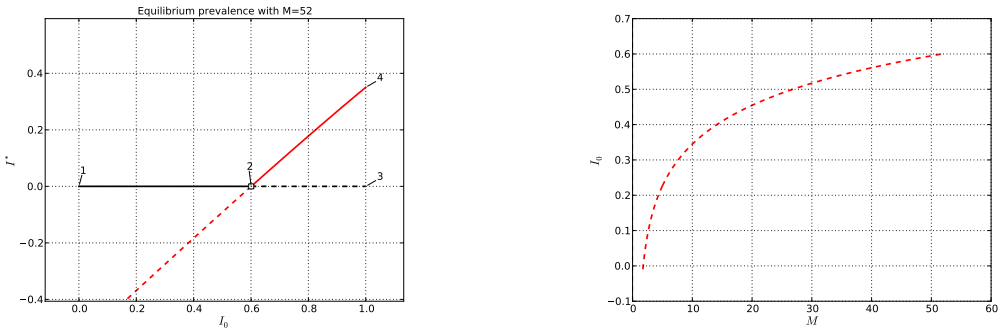

(a) Parameter I_0 versus the equilibrium prevalence I^*, with $M = 52$.

(b) Two parameter continuation of the bifurcation point 2 in (a).

Fig. 4.3 Part (a) shows how the prevalence at the steady state depends on the alert level of prevalence. Part (b) shows a relationship between I_0 and M that guarantees $\mathscr{R}_0 = 1$.

Note that despite the fact that there are no estimates of k, given that $\Phi(0) = \gamma$, the parameter k can be used to calibrate the value of $\mathscr{R}_0$.

From the definition of $\Phi(I)$, it is not difficult to understand the effects of the parameter I_0. For low values of I_0, the system tries to control the epidemic since the first cases with a strong response whose growth is weakened over time by the consumption of resources. In contrast, for high values of I_0, the initial stage of the response is slow but becomes faster when the alert level of prevalence is reached and grows to the carrying capacity of the system.

We are interested in finding conditions on the parameters I_0 and M that guarantee the eradication of the disease. This is essential because it will allow us to know how fast we should act to control an outbreak, given the recovery time from the infection. To find these conditions, we explore by means of a bifurcation diagram how the structure of the solution of model (4.6) depends on the alert level of prevalence, I_0, for a fixed value of M. The parameter I_0 will vary between 0 and 1, while the other parameters are fixed and $k = 6.74$. In particular, the value of M will be 52 so that the minimum recovery time is close to one week.

The resulting bifurcation diagram is plotted in figure 4.3 (a). The bifurcation parameter I_0 is shown on the horizontal axis of the plot and the vertical axis shows the prevalence of system (4.6) at the steady state. As usual, stable solutions are represented by a solid line and unstable ones with a dotted line. White squares symbolize static bifurcation points. The results indicate that the disease-free equilibrium point begins being stable for small values of I_0, but loses its stability when I_0 reaches the value 0.6006. At this value, the system has a transcritical bifurcation with bifurcation point 2 and consequently a stable endemic equilibrium appears. This indicates that the alert level of prevalence should be less than 60% of the population to successfully control the disease when the minimum time to recover is

roughly one week. Note that in these conditions, the maximum percentage of the population that is infected at the steady state is 35.051%.

The bifurcation point 2 is of paramount importance because it gives the exact relationship between I_0 and M for which the value of the basic reproduction number $\mathscr{R}_0$ is equal to 1. The bifurcation diagram in figure 4.3 (a) shows this relationship for $M = 52$. But, this can be obtained for any value of M. We proceed to show that, through the continuation in two parameters of the bifurcation point 2. The result is plotted in figure 4.3 (b), where the horizontal axis corresponds to M and the vertical axis to I_0. From this figure, we can deduce the alert level of prevalence needed to control the disease according to the minimum recovery time. For example, when the minimum time needed to recover is nearly one month, that is, when $M = 12$, the alert level of prevalence should be less than 38% to successfully control the disease. This can be found drawing a vertical line at $M = 12$ in figure 4.3 (b).

4.5.2 A saturated treatment function

Treatment is one of the most efficient ways to control the spread of a variety of infectious diseases, see Wang (2006) and the references therein. Nevertheless, due to logistic and economic constraints, any community or city has a maximum capacity for treatment of a disease. We are going to considered this phenomenon in our model introducing the saturated treatment function

$$T(I) = \gamma I/(1+aI) \tag{4.24}$$

proposed in (Zhang and Liu, 2008). The treatment function can be interpreted as the product of a recovery function and the prevalence, that is, $T(I) = \Phi(I)I$. Thus, to include (4.24) in our model it is enough to assume that $\Phi(I) = \gamma/(1+aI)$.

The function $T(I)$ describes the effect of delayed treatment when the population of infected individuals is large, and medical resources are limited. This is reflected through the parameter $a \geq 0$, which measure the extent of the effect of there being a delay in the treatment of infected individuals (Wang et al., 2012; Zhang and Liu, 2008). Note that $T(I) \sim \gamma I$ for small I; therefore, the treatment rate is proportional to the number of infected individuals when the prevalence is low. But, when the fraction of infected individuals is close to 1, it tends to a saturation level, since $T(I) \sim \gamma/(1+a)$. This appears to be more acceptable than the conventional constant rate.

In order to get a better understanding of how delayed treatment can affect the dynamics of our model, we will perform numerical bifurcation analysis with respect to the parameter γ and two different values of a. The first value proposed is $a = 0.1$; hence, in this case,

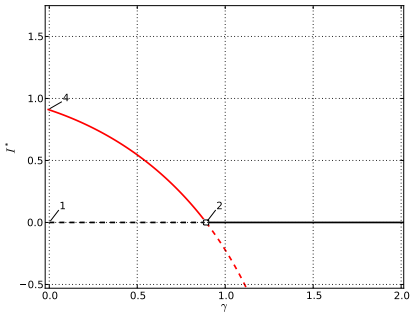

(a) Parameter γ versus I^*, with $a = 0.1$.

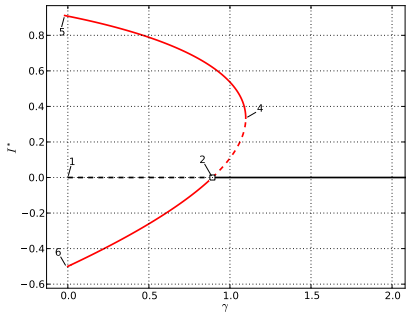

(b) Parameter γ versus I^*, with $a = 2$.

Fig. 4.4 Bifurcation diagrams corresponding to $a = 0.1$ (a) and $a = 2$ (b).

treatment delays are negligible. For the second value, $a = 2$, the effect of delays in treatment is more pronounced.

The results can be observed in figure 4.4. In figure 4.4 (a), that is, when there are no treatment delays, the system has a transcritical bifurcation at $\gamma = 0.8917$ designated by the bifurcation point 2. Hence, in this case, the model presents classical behavior in the sense that the basic reproduction number aptly determines the threshold for disease's eradication. However, the model exhibits a backward bifurcation in the presence of treatment delays, see figure 4.4 (b). Therefore, public health authorities should guarantee a minimum level of efficiency for the treatment of infected individuals to avoid the danger that a backward bifurcation represents.

4.6 The role of the pair formation process

The explicit inclusion of sexual partnerships in epidemiological models for STIs is necessary because most of these infections are transmitted within a partnership of two individuals who engage in sexual intercourse and have repeated sexual contacts with each other (Heijne et al., 2013). The pair formation process can impact the transmission dynamics in different ways. For example, if the mean time of partnership duration is short, the number of sexual acts within the partnership could not be enough to transmit the infection. On the other hand, if the partnership duration is long, infected individuals can clear the infection before the partnership ends, and the number of partners during the infectious period is low.

In this section, we shall study how partnership duration affects the spread of the disease. In order to do that, we shall analyze the dynamics of the system (4.6) for different values of the separation rate σ. Clearly, the duration of partnerships is inversely related to the value of

the separation rate. Consequently, we can explore the formulation of pairs in comparison to what would occur in a non-pair model taking a large value for σ.

It should be noted that changes in the separation rate when the rest of the parameters are fixed, not only change the duration of partnerships. It also modifies the expected number of partners per unit of time and the total number of pairs. Hence, the rate of pair formation should also be changing to ensure that the percentage of people in a partnership remains constant. If ρ is fixed, it can be difficult to know if dynamical changes when σ increases are due to the duration of partnerships or solely to the decline in the total number of pairs (Heijne et al., 2011; Muller and Bauch, 2010).

Let us now analyze how the structure of the solution depends on the separation rate. We check numerically the stability of the equilibria and the dependence of the basic reproduction number on the parameter σ, see figure 4.5. The recovery function used was $\Phi(I) = \gamma/(1+aI)$ with $\gamma = 1$, $a = 0.1$. In the bifurcation diagram shown in figure 4.5 (a), we varied the

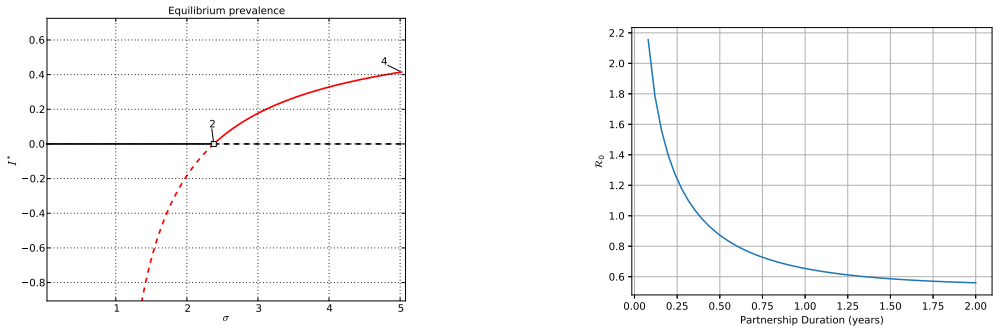

(a) Equilibrium prevalence versus σ.

(b) $\mathcal{R}_0$ as function of partnership duration.

Fig. 4.5 (a) Bifurcation diagram of model (4.6) with respect to σ. (b) Dependence of $\mathcal{R}_0$ with respect to σ through partnership duration.

parameter σ in the interval $[0,5]$. In this diagram the value of ρ changes with σ in such a way that the percentage of people in a partnership is constant consistent with published data Johnson et al. (2001). In figure 4.5 (b), the basic reproduction number is plotted as a function of the mean duration of partnerships which in turn depends on σ. In fact, partnership's duration is long for small values of σ and short when σ is big.

In figure 4.5 (b) it can be observed that $\mathcal{R}_0$ is a non-increasing function of partnership duration, this implies that non-pair models overestimate the value of the basic reproduction number which is logical since they implicitly assume a highly promiscuous behavior in the population. The bifurcation diagram in figure 4.5 (a) confirms that something similar happens for the equilibrium prevalence. Since for small values of σ (i.e. large partnership duration) the disease-free equilibrium is stable because, among other things, the number of partners in

the infectious period is not enough to maintain the infection. However, as σ increases and reaches the value of 2.3836 a forward bifurcation occurs causing the loss of stability of the disease-free equilibrium and giving rise to an endemic equilibrium whose value increases with σ.

4.7 Discussion

In this work, we have analyzed the relationship between the recovery function and the prevalence in an epidemic *SIS* model with nonzero partnership length. The main purpose of incorporating general recovery functions was to study the different scenarios that can occur when treating infected individuals. This contemplates, for instance, logistic limitations to treat infected individuals when their number is large or behavioral changes related to the prevalence of the infection.

Due to the uncertainty in parameters' values and the complexity of the expression for the basic reproduction number $\mathscr{R}_0$, we have performed a sensibility analysis in order to get a better insight of how input parameters influence the variance of $\mathscr{R}_0$. The results of this analysis suggest that control strategies should center principally on increasing the recovery rate under normal conditions, γ, which is natural. However, a non-obvious conclusion of the sensibility analysis is that the parameters ρ and σ have a significant influence on the basic reproduction number, $\mathscr{R}_0$. Therefore, behavioral interventions that aim to reduce individuals' risk to transmit and contract the infection are relevant to control STIs. Moreover, in section 4.6, we showed that $\mathscr{R}_0$ is a non-increasing function of partnership duration and that the endemic equilibrium is stable when σ is large. This coincides with previous studies that showed that non-pair models overestimate the value of $\mathscr{R}_0$ compared to models where partnerships are explicitly included (Chen et al., 2009; Heijne et al., 2011; Muller and Bauch, 2010).

The inclusion of a general recovery function provided interesting insight into how saturation and delays in treatment affect the dynamics of epidemiological models. First, from the sigmoid recovery function (4.23), we established a relationship between the inverse of the minimum recovery time, M, and the alert level of prevalence, I_0, that guarantees $\mathscr{R}_0 = 1$. In practical terms, this relationship determines when public health authorities should act to successfully control disease's transmission given the minimum recovery time $1/M$. Second, when the saturated treatment function $T(I) = \gamma I/(1+aI)$ is used to describe delays in treatment, we showed numerically that a backward bifurcation can occur when such delays are considerable. This is undesirable in terms of control strategies because driving $\mathscr{R}_0$ below

1 is no longer enough to eradicate the disease. Therefore, timely treatment is of paramount importance to avoid the risk that represents a backward bifurcation.

Our model focuses on capturing the pair formation process and the effects of the recovery function. Thus, many natural extensions are possible to improve the realism of the model. For example, we did not take into consideration that sometimes individuals have contacts outside their partnerships. The existence of sexual risk group is another important aspect that should be addressed when modeling STIs. In addition, omitting the relationship between the infectious disease and the pair formation process is not realistic and deserves further studies. Currently, we are working on these extensions and the inclusion of optimal control theory to study the balance between cost and effectiveness of public health interventions.

References

Adler, B. and de la Peña Moctezuma, A. (2010). Leptospira and leptospirosis. *Veterinary microbiology*, 140(3):287–296.

Alizon, S., Murall, C., and Bravo, I. (2017). Why human papillomavirus acute infections matter. *Viruses*, 9(10):293.

Alsaleh, A. A. and Gumel, A. B. (2014). Analysis of risk-structured vaccination model for the dynamics of oncogenic and warts-causing hpv types. *Bulletin of mathematical biology*, 76(7):1670–1726.

Anic, G. M. and Giuliano, A. R. (2011). Genital hpv infection and related lesions in men. *Preventive medicine*, 53:S36–S41.

Arbyn, M., Castellsagué, X., de Sanjosé, S., Bruni, L., Saraiya, M., Bray, F., and Ferlay, J. (2011). Worldwide burden of cervical cancer in 2008. *Annals of oncology*, 22(12):2675–2686.

Arino, J. and Portet, S. (2015). Epidemiological implications of mobility between a large urban centre and smaller satellite cities. *Journal of mathematical biology*, 71(5):1243–1265.

Arino, J. and Van den Driessche, P. (2003). A multi-city epidemic model. *Mathematical Population Studies*, 10(3):175–193.

Asih, T. S. N., Lenhart, S., Wise, S., Aryati, L., Adi-Kusumo, F., Hardianti, M. S., and Forde, J. (2016). The dynamics of hpv infection and cervical cancer cells. *Bulletin of mathematical biology*, 78(1):4–20.

Ault, K. A. (2008). Human papillomavirus vaccines: an update for gynecologists. *Clinical obstetrics and gynecology*, 51(3):527–532.

Baca-Carrasco, D., Olmos, D., and Barradas, I. (2015). A mathematical model for human and animal leptospirosis. *Journal of Biological Systems*, 23(supp01):S55–S65.

Baca-Carrasco, D. and Velasco-Hernández, J. X. (2016). Sex, mosquitoes and epidemics: An evaluation of zika disease dynamics. *Bulletin of Mathematical Biology*, 78(11):2228–2242.

Bani-Yaghoub, M., Gautam, R., Shuai, Z., van den Driessche, P., and Ivanek, R. (2012). Reproduction numbers for infections with free-living pathogens growing in the environment. *Journal of biological dynamics*, 6(2):923–940.

Barradas, I., Caswell, H., and Cohen, J. E. (1996). Competition during colonization vs competition after colonization in disturbed environments: a metapopulation approach. *Bulletin of Mathematical Biology*, 58(6):1187–1207.

Barradas, I. and Cohen, J. E. (1994). Disturbances allow coexistence of competing species. *Journal of Mathematical Biology*, 32(7):663–676.

Barradas, I. and Tassier, K. (1999). Reducing competition vs. improving resistance to disturbances in the environment. *Journal of Mathematical Biology*, 39(6):518–532.

Bedell, M. A., Hudson, J. B., Golub, T. R., Turyk, M. E., Hosken, M., Wilbanks, G. D., and Laimins, L. A. (1991). Amplification of human papillomavirus genomes in vitro is dependent on epithelial differentiation. *Journal of virology*, 65(5):2254–2260.

Berman, A. and Shaked-Monderer, N. (2012). Non-negative matrices and digraphs. In *Computational Complexity*, pages 2082–2095. Springer.

Bogaards, J. A., Kretzschmar, M., Xiridou, M., Meijer, C. J., Berkhof, J., and Wallinga, J. (2011). Sex-specific immunization for sexually transmitted infections such as human papillomavirus: insights from mathematical models. *PLoS medicine*, 8(12):e1001147.

Brauer, F. (2017). Mathematical epidemiology: Past, present, and future. *Infectious Disease Modelling*, 2(2):113–127.

Brauer, F. and Castillo-Chavez, C. (2012). *Mathematical models in population biology and epidemiology*, volume 40. Springer.

Brisson, M., Laprise, J.-F., Chesson, H. W., Drolet, M., Malagón, T., Boily, M.-C., and Markowitz, L. E. (2016). Health and economic impact of switching from a 4-valent to a 9-valent hpv vaccination program in the united states. *JNCI: Journal of the National Cancer Institute*, 108(1).

Brisson, M., van de Velde, N., Franco, E. L., Drolet, M., and Boily, M.-C. (2011). Incremental impact of adding boys to current human papillomavirus vaccination programs: role of herd immunity. *Journal of Infectious Diseases*, 204(3):372–376.

Brown, V. L. and White, K. J. (2011). The role of optimal control in assessing the most cost-effective implementation of a vaccination programme: Hpv as a case study. *Mathematical biosciences*, 231(2):126–134.

Bruni, L., Diaz, M., Castellsagué, M., Ferrer, E., Bosch, F. X., and de Sanjosé, S. (2010). Cervical human papillomavirus prevalence in 5 continents: meta-analysis of 1 million women with normal cytological findings. *Journal of Infectious Diseases*, 202(12):1789–1799.

Buonomo, B., Lacitignola, D., and Vargas-De-León, C. (2014). Qualitative analysis and optimal control of an epidemic model with vaccination and treatment. *Mathematics and Computers in Simulation*, 100:88–102.

Burd, E. M. (2003). Human papillomavirus and cervical cancer. *Clinical microbiology reviews*, 16(1):1–17.

Camacho, A. and Jerez, S. (2018). Bone metastasis treatment modeling via optimal control. *Journal of mathematical biology*, pages 1–30.

Canfell, K., Chesson, H., Kulasingam, S. L., Berkhof, J., Diaz, M., and Kim, J. J. (2012). Modeling preventative strategies against human papillomavirus-related disease in developed countries. *Vaccine*, 30:F157–F167.

CASWELL, H. and COHEN, J. E. (1991). Disturbance, interspecific interaction and diversity in metapopulations. In *Metapopulation dynamics: Empirical and theoretical investigations*, pages 193–218. Elsevier.

Chaturvedi, A. K., Katki, H. A., Hildesheim, A., Rodríguez, A. C., Quint, W., Schiffman, M., Van Doorn, L.-J., Porras, C., Wacholder, S., Gonzalez, P., et al. (2011). Human papillomavirus infection with multiple types: pattern of coinfection and risk of cervical disease. *The Journal of infectious diseases*, 203(7):910–920.

Chen, M. I. and Ghani, A. C. (2010). Republished paper: Populations and partnerships: insights from metapopulation and pair models into the epidemiology of gonorrhoea and other sexually transmitted infections. *Sexually transmitted infections*, 86(Suppl 3):iii63–iii69.

Chen, M. I., Ghani, A. C., and Edmunds, W. J. (2009). A metapopulation modelling framework for gonorrhoea and other sexually transmitted infections in heterosexual populations. *Journal of The Royal Society Interface*, 6(38):775–791.

Chesson, H. W., Ekwueme, D. U., Saraiya, M., Dunne, E. F., and Markowitz, L. E. (2011). The cost-effectiveness of male hpv vaccination in the united states. *Vaccine*, 29(46):8443–8450.

Chow, L. T., Broker, T. R., and Steinberg, B. M. (2010). The natural history of human papillomavirus infections of the mucosal epithelia. *Apmis*, 118(6-7):422–449.

Damm, O., Horn, J., Mikolajczyk, R. T., Kretzschmar, M. E., Kaufmann, A. M., Deleré, Y., Ultsch, B., Wichmann, O., Krämer, A., and Greiner, W. (2017). Cost-effectiveness of human papillomavirus vaccination in germany. *Cost Effectiveness and Resource Allocation*, 15(1):18.

Dasbach, E. J., Elbasha, E. H., and Insinga, R. P. (2006). Mathematical models for predicting the epidemiologic and economic impact of vaccination against human papillomavirus infection and disease. *Epidemiologic reviews*, 28(1):88–100.

de Salud Mexico, S. (2016). Hoja de datos sobre cancer de cuello uterino.

Delamater, P. L., Street, E. J., Leslie, T. F., Yang, Y. T., and Jacobsen, K. H. (2019). Complexity of the basic reproduction number ($\mathscr{R}_0$). *Emerging infectious diseases*, 25(1):1.

Diekmann, O., Heesterbeek, J. A. P., and Metz, J. A. (1990). On the definition and the computation of the basic reproduction ratio r 0 in models for infectious diseases in heterogeneous populations. *Journal of mathematical biology*, 28(4):365–382.

Dietz, K. and Hadeler, K. (1988). Epidemiological models for sexually transmitted diseases. *Journal of mathematical biology*, 26(1):1–25.

Durham, D. P., Poolman, E. M., Ibuka, Y., Townsend, J. P., and Galvani, A. P. (2012). Reevaluation of epidemiological data demonstrates that it is consistent with cross-immunity among human papillomavirus types. *The Journal of infectious diseases*, 206(8):1291–1298.

Eckalbar, J. C. and Eckalbar, W. L. (2011). Dynamics of an epidemic model with quadratic treatment. *Nonlinear Analysis: Real World Applications*, 12(1):320–332.

Edwards, R., Kim, S., and van den Driessche, P. (2010). A multigroup model for a heterosexually transmitted disease. *Mathematical biosciences*, 224(2):87–94.

Elbasha, E. H. and Dasbach, E. J. (2010). Impact of vaccinating boys and men against hpv in the united states. *Vaccine*, 28(42):6858–6867.

Elbasha, E. H., Dasbach, E. J., and Insinga, R. P. (2007). Model for assessing human papillomavirus vaccination strategies. *Emerging infectious diseases*, 13(1):28.

Elbasha, E. H. and Galvani, A. P. (2005). Vaccination against multiple hpv types. *Mathematical biosciences*, 197(1):88–117.

Evangelista, K. V. and Coburn, J. (2010). Leptospira as an emerging pathogen: a review of its biology, pathogenesis and host immune responses. *Future microbiology*, 5(9):1413–1425.

FDA, U. S. (2018). Fda approves expanded use of gardasil-9 to include individuals 27 through 45 years old. Available at https://bit.ly/2zVRxa9. Accessed: 2019-02-22.

Fleming, W. and Rishel, R. (1975). Deterministic and stochastic optimal control.

Foxman, B., Newman, M., Percha, B., Holmes, K. K., and Aral, S. O. (2006). Measures of sexual partnerships: lengths, gaps, overlaps, and sexually transmitted infection. *Sexually transmitted diseases*, 33(4):209–214.

Ganoza, C. A., Matthias, M. A., Collins-Richards, D., Brouwer, K. C., Cunningham, C. B., Segura, E. R., Gilman, R. H., Gotuzzo, E., and Vinetz, J. M. (2006). Determining risk for severe leptospirosis by molecular analysis of environmental surface waters for pathogenic leptospira. *PLoS medicine*, 3(8):e308.

Garira, W., Mathebula, D., and Netshikweta, R. (2014). A mathematical modelling framework for linked within-host and between-host dynamics for infections with free-living pathogens in the environment. *Mathematical biosciences*, 256:58–78.

Garnett, G. P., Kim, J. J., French, K., and Goldie, S. J. (2006). Modelling the impact of hpv vaccines on cervical cancer and screening programmes. *Vaccine*, 24:S178–S186.

Garnett, G. P. and Waddell, H. C. (2000). Public health paradoxes and the epidemiological impact of an hpv vaccine. *Journal of Clinical Virology*, 19(1):101–111.

Goldie, S. J., Goldhaber-Fiebert, J. D., and Garnett, G. P. (2006). Public health policy for cervical cancer prevention: the role of decision science, economic evaluation, and mathematical modeling. *Vaccine*, 24:S155–S163.

Grabowska, A. K. and Riemer, A. B. (2012). Suppl 2: The invisible enemy–how human papillomaviruses avoid recognition and clearance by the host immune system. *The open virology journal*, 6:249.

Grigorieva, E., Khailov, E., and Korobeinikov, A. (2018). Optimal control for an seir epidemic model with nonlinear incidence rate. *Studies in Applied Mathematics*, 141(3):353–398.

Guerrero, A. M., Genuino, A. J., Santillan, M., Praditsitthikorn, N., Chantarastapornchit, V., Teerawattananon, Y., Alejandria, M., and Toral, J. A. (2015). A cost-utility analysis of cervical cancer screening and human papillomavirus vaccination in the philippines. *BMC public health*, 15(1):730.

Hanski, I. et al. (1999). *Metapopulation ecology*. Oxford University Press.

He, Y., Gao, S., Lv, H., and Liu, Y. (2013). Asymptotic behavior of an seir epidemic model with quadratic treatment. *Journal of Applied Mathematics and Computing*, 42(1-2):245–257.

Heesterbeek, J. A. P. (2002). A brief history of r0 and a recipe for its calculation. *Acta biotheoretica*, 50(3):189–204.

Heffernan, J. M., Smith, R. J., and Wahl, L. M. (2005). Perspectives on the basic reproductive ratio. *Journal of the Royal Society Interface*, 2(4):281–293.

Heijne, J. C., Althaus, C. L., Herzog, S. A., Kretzschmar, M., and Low, N. (2011). The role of reinfection and partner notification in the efficacy of chlamydia screening programs. *Journal of infectious diseases*, 203(3):372–377.

Heijne, J. C., Herzog, S. A., Althaus, C. L., Low, N., and Kretzschmar, M. (2013). Case and partnership reproduction numbers for a curable sexually transmitted infection. *Journal of theoretical biology*, 331:38–47.

Holt, J., Davis, S., and Leirs, H. (2006). A model of leptospirosis infection in an african rodent to determine risk to humans: seasonal fluctuations and the impact of rodent control. *Acta tropica*, 99(2):218–225.

Horn, R. A. and Johnson, C. R. (2013). Matrix analysis, 2nd.

Huh, W. K., Joura, E. A., Giuliano, A. R., Iversen, O.-E., de Andrade, R. P., Ault, K. A., Bartholomew, D., Cestero, R. M., Fedrizzi, E. N., Hirschberg, A. L., et al. (2017). Final efficacy, immunogenicity, and safety analyses of a nine-valent human papillomavirus vaccine in women aged 16–26 years: a randomised, double-blind trial. *The Lancet*, 390(10108):2143–2159.

Jenkins, D. (2008). A review of cross-protection against oncogenic hpv by an hpv-16/18 as04-adjuvanted cervical cancer vaccine: importance of virological and clinical endpoints and implications for mass vaccination in cervical cancer prevention. *Gynecologic oncology*, 110(3):S18–S25.

Johnson, A. M., Mercer, C. H., Erens, B., Copas, A. J., McManus, S., Wellings, K., Fenton, K. A., Korovessis, C., Macdowall, W., Nanchahal, K., et al. (2001). Sexual behaviour in britain: partnerships, practices, and hiv risk behaviours. *The Lancet*, 358(9296):1835–1842.

Juckett, G., Hartman-Adams, H., et al. (2010). Human papillomavirus: clinical manifestations and prevention. *American family physician*, 82(10):1209.

Kahn, J. A., Brown, D. R., Ding, L., Widdice, L. E., Shew, M. L., Glynn, S., and Bernstein, D. I. (2012). Vaccine-type human papillomavirus and evidence of herd protection after vaccine introduction. *Pediatrics*, 130(2):e249–e256.

Kajitani, N., Satsuka, A., Kawate, A., and Sakai, H. (2012). Productive lifecycle of human papillomaviruses that depends upon squamous epithelial differentiation. *Frontiers in microbiology*, 3:152.

Keeling, M., Tildesley, M., House, T., and Danon, L. (2013). The mathematics of vaccination. *Math. Today*, 49:40–43.

Kermack, W. O. and McKendrick, A. G. (1927). A contribution to the mathematical theory of epidemics. *Proceedings of the royal society of london. Series A, Containing papers of a mathematical and physical character*, 115(772):700–721.

Kermack, W. O. and McKendrick, A. G. (1932). Contributions to the mathematical theory of epidemics. ii.—the problem of endemicity. *Proceedings of the Royal Society of London. Series A, containing papers of a mathematical and physical character*, 138(834):55–83.

Kermack, W. O. and McKendrick, A. G. (1933). Contributions to the mathematical theory of epidemics. iii.—further studies of the problem of endemicity. *Proceedings of the Royal Society of London. Series A, Containing Papers of a Mathematical and Physical Character*, 141(843):94–122.

Kim, J. J. and Goldie, S. J. (2009). Cost effectiveness analysis of including boys in a human papillomavirus vaccination programme in the united states. *Bmj*, 339:b3884.

Knipl, D. (2016). A new approach for designing disease intervention strategies in metapopulation models. *Journal of biological dynamics*, 10(1):71–94.

Ko, A. I., Reis, M. G., Dourado, C. M. R., Johnson, W. D., Riley, L. W., Group, S. L. S., et al. (1999). Urban epidemic of severe leptospirosis in brazil. *The Lancet*, 354(9181):820–825.

Kretzschmar, M. and Dietz, K. (1998). The effect of pair formation and variable infectivity on the spread of an infection without recovery. *Mathematical biosciences*, 148(1):83–113.

La Salle, J., Lefschetz, S., and Alverson, R. (1962). Stability by liapunov's direct method with applications. *Physics Today*, 15:59.

Lajmanovich, A. and Yorke, J. A. (1976). A deterministic model for gonorrhea in a nonhomogeneous population. *Mathematical Biosciences*, 28(3-4):221–236.

Leirs, H., Stenseth, N. C., Nichols, J. D., Hines, J. E., Verhagen, R., and Verheyen, W. (1997). Stochastic seasonality and nonlinear density-dependent factors regulate population size in an african rodent. *Nature*, 389(6647):176.

Lenhart, S. and Workman, J. T. (2007). *Optimal control applied to biological models*. Crc Press.

Li, N., Franceschi, S., Howell-Jones, R., Snijders, P. J., and Clifford, G. M. (2011). Human papillomavirus type distribution in 30,848 invasive cervical cancers worldwide: Variation by geographical region, histological type and year of publication. *International journal of cancer*, 128(4):927–935.

Lukes, D. L. (1982). *Differential equations: classical to controlled*. Elsevier.

Malik, T., Imran, M., and Jayaraman, R. (2016). Optimal control with multiple human papillomavirus vaccines. *Journal of theoretical biology*, 393:179–193.

Malik, T., Reimer, J., Gumel, A., Elbasha, E. H., and Mahmud, S. (2013). The impact of an imperfect vaccine and pap cytology screening on the transmission of human papillomavirus and occurrence of associated cervical dysplasia and cancer. *Mathematical Biosciences & Engineering*, 10(4):1173–1205.

Markowitz, L. E., Dunne, E. F., Saraiya, M., Chesson, H. W., Curtis, C. R., Gee, J., Bocchini Jr, J. A., and Unger, E. R. (2014). Human papillomavirus vaccination: recommendations of the advisory committee on immunization practices (acip). *Morbidity and Mortality Weekly Report: Recommendations and Reports*, 63(5):1–30.

Martcheva, M. (2015). *An introduction to mathematical epidemiology*, volume 61. Springer.

Martcheva, M., Bolker, B. M., and Holt, R. D. (2008). Vaccine-induced pathogen strain replacement: what are the mechanisms? *Journal of the Royal Society Interface*, 5(18):3–13.

McLaughlin-Drubin, M. E. and Meyers, C. (2004). Evidence for the coexistence of two genital hpv types within the same host cell in vitro. *Virology*, 321(2):173–180.

Mesher, D., Soldan, K., Lehtinen, M., Beddows, S., Brisson, M., Brotherton, J. M., Chow, E. P., Cummings, T., Drolet, M., Fairley, C. K., et al. (2016). Population-level effects of human papillomavirus vaccination programs on infections with nonvaccine genotypes. *Emerging infectious diseases*, 22(10):1732.

Molano, M., van den Brule, A., Plummer, M., Weiderpass, E., Posso, H., Arslan, A., Meijer, C. J., Muñoz, N., and Franceschi, S. (2003). Determinants of clearance of human papillomavirus infections in colombian women with normal cytology: a population-based, 5-year follow-up study. *American journal of epidemiology*, 158(5):486–494.

Mollers, M., Vriend, H. J., van der Sande, M. A., van Bergen, J. E., King, A. J., Lenselink, C. H., Bekkers, R. L., Meijer, C. J., de Melker, H. E., and Bogaards, J. A. (2014). Population-and type-specific clustering of multiple hpv types across diverse risk populations in the netherlands. *American journal of epidemiology*, 179(10):1236–1246.

Moody, C. A. and Laimins, L. A. (2010). Human papillomavirus oncoproteins: pathways to transformation. *Nature Reviews Cancer*, 10(8):550.

Muller, H. and Bauch, C. (2010). When do sexual partnerships need to be accounted for in transmission models of human papillomavirus? *International journal of environmental research and public health*, 7(2):635–650.

Muñoz, N., Méndez, F., Posso, H., Molano, M., Van Den Brule, A. J., Ronderos, M., Meijer, C., Muñoz, Á., and de Cancerologia HPV Study Group, I. N. (2004). Incidence, duration, and determinants of cervical human papillomavirus infection in a cohort of colombian women with normal cytological results. *The Journal of infectious diseases*, 190(12):2077–2087.

Murall, C. L., Bauch, C. T., and Day, T. (2015). Could the human papillomavirus vaccines drive virulence evolution? *Proceedings of the Royal Society B: Biological Sciences*, 282(1798):20141069.

Murall, C. L., McCann, K. S., and Bauch, C. T. (2014). Revising ecological assumptions about human papillomavirus interactions and type replacement. *Journal of theoretical biology*, 350:98–109.

Newall, A. T., Beutels, P., Wood, J. G., Edmunds, W. J., and MacIntyre, C. R. (2007). Cost-effectiveness analyses of human papillomavirus vaccination. *The Lancet infectious diseases*, 7(4):289–296.

Nishiura, H. and Chowell, G. (2009). The effective reproduction number as a prelude to statistical estimation of time-dependent epidemic trends. In *Mathematical and statistical estimation approaches in epidemiology*, pages 103–121. Springer.

Okosun, K. O., Ouifki, R., and Marcus, N. (2011). Optimal control analysis of a malaria disease transmission model that includes treatment and vaccination with waning immunity. *Biosystems*, 106(2-3):136–145.

Okosun, K. O., Rachid, O., and Marcus, N. (2013). Optimal control strategies and cost-effectiveness analysis of a malaria model. *BioSystems*, 111(2):83–101.

Olmos, D., Barradas, I., and Baca-Carrasco, D. (2015). On the calculation of r0 using submodels. *Differential Equations and Dynamical Systems*, pages 1–17.

Orlando, P. A., Brown, J. S., Gatenby, R. A., and Guliano, A. R. (2013). The ecology of human papillomavirus–induced epithelial lesions and the role of somatic evolution in their progression. *The Journal of infectious diseases*, 208(3):394–402.

Peralta, R., Vargas-De-León, C., Cabrera, A., and Miramontes, P. (2014). Dynamics of high-risk nonvaccine human papillomavirus types after actual vaccination scheme. *Computational and mathematical methods in medicine*, 2014.

Pontryagin, L. S. (2018). *Mathematical theory of optimal processes*. Routledge.

Prinja, S., Bahuguna, P., Faujdar, D. S., Jyani, G., Srinivasan, R., Ghoshal, S., Suri, V., Singh, M. P., and Kumar, R. (2017). Cost-effectiveness of human papillomavirus vaccination for adolescent girls in punjab state: Implications for india's universal immunization program. *Cancer*, 123(17):3253–3260.

Prüss-Üstün, A. and Corvalán, C. (2006). Preventing disease through healthy environments. *Geneva: World Health Organization*.

Roberts, M. and Heesterbeek, J. (2003). A new method for estimating the effort required to control an infectious disease. *Proceedings of the Royal Society of London B: Biological Sciences*, 270(1522):1359–1364.

Saccucci, M., Franco, E. L., Ding, L., Bernstein, D. I., Brown, D., and Kahn, J. A. (2018). Non–vaccine-type human papillomavirus prevalence after vaccine introduction: No evidence for type replacement but evidence for cross-protection. *Sexually transmitted diseases*, 45(4):260–265.

Saldaña, F. and Barradas, I. (2018). Control strategies in multigroup models: The case of the star network topology. *Bulletin of mathematical biology*, 80(11):2978–3001.

Saldaña, F. and Barradas, I. (2019). The role of behavioral changes and prompt treatment in the control of stis. *Infectious Disease Modelling*, 4:1–10.

Saldaña, F. and Barradas, I. (2020). Evaluating the potential of vaccine-induced type replacement for high-risk human papillomaviruses. *Mathematical Methods in the Applied Sciences*, 43(3):1216–1229.

Saldaña, F., Korobeinikov, A., and Barradas, I. (2019). Optimal control against the human papillomavirus: Protection versus eradication of the infection. In *Abstract and Applied Analysis*, volume 2019. Hindawi.

Saltelli, A., Tarantola, S., Campolongo, F., and Ratto, M. (2004). Sensitivity analysis in practice: a guide to assessing scientific models. *Chichester, England*.

Saltelli, A., Tarantola, S., and Chan, K.-S. (1999). A quantitative model-independent method for global sensitivity analysis of model output. *Technometrics*, 41(1):39–56.

Schiller, J. T. and Lowy, D. R. (2012). Understanding and learning from the success of prophylactic human papillomavirus vaccines. *Nature Reviews Microbiology*, 10(10):681.

Seto, K., Marra, F., Raymakers, A., and Marra, C. A. (2012). The cost effectiveness of human papillomavirus vaccines. *Drugs*, 72(5):715–743.

Sharomi, O. and Malik, T. (2017). Optimal control in epidemiology. *Annals of Operations Research*, 251(1-2):55–71.

Shuai, Z., Heesterbeek, J., and van den Driessche, P. (2013). Extending the type reproduction number to infectious disease control targeting contacts between types. *Journal of mathematical biology*, 67(5):1067–1082.

Shuai, Z., Heesterbeek, J., and van den Driessche, P. (2015). Erratum to: Extending the type reproduction number to infectious disease control targeting contacts between types. *Journal of mathematical biology*, 71(1):255–257.

Smith, M. A., Lew, J.-B., Walker, R. J., Brotherton, J. M., Nickson, C., and Canfell, K. (2011). The predicted impact of hpv vaccination on male infections and male hpv-related cancers in australia. *Vaccine*, 29(48):9112–9122.

Smith, R. J., Li, J., Mao, J., and Sahai, B. (2015). Using within-host mathematical modelling to predict the long-term outcome of human papillomavirus vaccines. *Cannadian Applied Mathematics Quarterly*, 21(2).

Soe, N. N., Ong, J. J., Ma, X., Fairley, C. K., Latt, P. M., Jing, J., Cheng, F., and Zhang, L. (2018). Should human papillomavirus vaccination target women over age 26, heterosexual men and men who have sex with men? a targeted literature review of cost-effectiveness. *Human vaccines & immunotherapeutics*, 14(12):3010–3018.

Stanley, M. (2010). Hpv-immune response to infection and vaccination. *Infectious agents and cancer*, 5(1):19.

Terpstra, W. (2003). *Human leptospirosis: guidance for diagnosis, surveillance and control*. World Health Organization.

Tien, J. H. and Earn, D. J. (2010). Multiple transmission pathways and disease dynamics in a waterborne pathogen model. *Bulletin of mathematical biology*, 72(6):1506–1533.

Tota, J. E., Jiang, M., Ramanakumar, A. V., Walter, S. D., Kaufman, J. S., Coutlée, F., Richardson, H., Burchell, A. N., Koushik, A., Mayrand, M. H., et al. (2016). Epidemiologic evaluation of human papillomavirus type competition and the potential for type replacement post-vaccination. *PloS one*, 11(12):e0166329.

Tota, J. E., Ramanakumar, A. V., Jiang, M., Dillner, J., Walter, S. D., Kaufman, J. S., Coutlée, F., Villa, L. L., and Franco, E. L. (2013). Epidemiologic approaches to evaluating the potential for human papillomavirus type replacement postvaccination. *American journal of epidemiology*, 178(4):625–634.

Triampo, W., Baowan, D., Tang, I., Nuttavut, N., Wong-Ekkabut, J., and Doungchawee, G. (2007). A simple deterministic model for the spread of leptospirosis in thailand. *Int. J. Bio. Med. Sci*, 2:22–26.

Trottier, H. and Franco, E. L. (2006). The epidemiology of genital human papillomavirus infection. *Vaccine*, 24:S4–S15.

Tumban, E., Peabody, J., Peabody, D. S., and Chackerian, B. (2011). A pan-hpv vaccine based on bacteriophage pp7 vlps displaying broadly cross-neutralizing epitopes from the hpv minor capsid protein, l2. *PloS one*, 6(8):e23310.

Ullmann, L. and Langoni, H. (2011). Interactions between environment, wild animals and human leptospirosis. *Journal of Venomous Animals and Toxins including Tropical Diseases*, 17(2):119–129.

Van den Driessche, P. and Watmough, J. (2002). Reproduction numbers and sub-threshold endemic equilibria for compartmental models of disease transmission. *Mathematical biosciences*, 180(1):29–48.

Vargas-De-León, C. (2011). On the global stability of sis, sir and sirs epidemic models with standard incidence. *Chaos, Solitons & Fractals*, 44(12):1106–1110.

Verma, M., Erwin, S., Abedi, V., Hontecillas, R., Hoops, S., Leber, A., Bassaganya-Riera, J., and Ciupe, S. M. (2017). Modeling the mechanisms by which hiv-associated immunosuppression influences hpv persistence at the oral mucosa. *PloS one*, 12(1):e0168133.

Villavicencio Pulido, G., Barradas, I., and Luna, B. (2017). Backward bifurcation for some general recovery functions. *Mathematical Methods in the Applied Sciences*, 40(5):1505–1515.

Wang, J., Liu, S., Zheng, B., and Takeuchi, Y. (2012). Qualitative and bifurcation analysis using an sir model with a saturated treatment function. *Mathematical and computer modelling*, 55(3-4):710–722.

Wang, W. (2006). Backward bifurcation of an epidemic model with treatment. *Mathematical biosciences*, 201(1-2):58–71.

Zhang, X. and Liu, X. (2008). Backward bifurcation of an epidemic model with saturated treatment function. *Journal of mathematical analysis and applications*, 348(1):433–443.